

# Discovery and Optimization of Narrow Spectrum Inhibitors of Tousled Like Kinase 2 (TLK2) Using Quantitative Structure Activity Relationships

Christopher R. M. Asquith<sup>a,b,c,\*</sup>, Michael P. East<sup>a</sup>, Tuomo Laitinen<sup>b</sup>, Carla Alamillo-Ferrer<sup>c</sup>, Erkka Hartikainen<sup>b</sup>, Carrow I. Wells<sup>c</sup>, Alison D. Axtman<sup>c</sup>, David H. Drewry<sup>c,d</sup>, Graham J. Tizzard<sup>e</sup>, Antti Poso<sup>b</sup>, Timothy M. Willson<sup>c</sup>, Gary L. Johnson<sup>a,d,\*</sup>

<sup>a</sup> Department of Pharmacology, School of Medicine, University of North Carolina at Chapel Hill, NC 27599, USA

<sup>b</sup> School of Pharmacy, Faculty of Health Sciences, University of Eastern Finland, 70211, Kuopio, Finland

<sup>c</sup> Structural Genomics Consortium and Division of Chemical Biology and Medicinal Chemistry, UNC Eshelman School of Pharmacy, University of North Carolina at Chapel Hill, Chapel Hill, NC 27599, USA

<sup>d</sup> Lineberger Comprehensive Cancer Center, University of North Carolina at Chapel Hill, Chapel Hill, NC 27599, USA

<sup>e</sup> UK National Crystallography Service, School of Chemistry, University of Southampton, Highfield Campus, Southampton, SO17 1BJ, UK

## ARTICLE INFO

### Article history:

Received

Revised

Accepted

Available online

### Keywords:

Kinase Inhibitors

Oxindole

Kinase Chemical Tool

Tousled Like Kinase 2 (TLK2)

quantitative structure-activity relationship (QSAR)

## ABSTRACT

The oxindole scaffold has been the center of several kinase drug discovery programs, some of which have led to approved medicines. A series of two oxindole matched pairs from the literature were identified where TLK2 was a potent off-target kinase. The oxindole has long been considered a promiscuous inhibitor template, but across these 4 specific literature oxindoles TLK2 activity was consistent, while the kinome profile was radically different from narrow to broad spectrum coverage. We synthesized a large series of analogues and through quantitative structure-activity relationship (QSAR) analysis, water mapping of the kinase ATP binding sites, small-molecule x-ray structural analysis and kinome profiling, narrow spectrum, sub-family selective, chemical tool compounds were identified to enable elucidation of TLK2 biology.

## 1. Introduction

Tousled-like kinase 2 (TLK2) is a ubiquitously expressed, nuclear serine/threonine kinase. Kinase activity of TLK2 and its closest human paralog TLK1 is activated by autophosphorylation, hetero- and homo-dimerization, and oligomerization through conserved coiled-coiled domains.<sup>1</sup> TLK kinase activity is highest during S-phase where TLKs phosphorylate ASF1 histone chaperones.<sup>2</sup> DNA rapidly associates with histones during replication and ASF1 chaperones regulate the soluble pool of histones H3 and H4 during this process.<sup>3</sup> Phosphorylation of ASF1 chaperones by TLKs stabilizes ASF1 protein,<sup>4</sup> and promotes interactions between ASF1 and histones as well as histones with downstream chaperones CAF1 and HIRA1. TLK2, but not TLK1, was also shown to regulate G2/M checkpoint recovery after DNA damage through an ASF1A dependent mechanism.<sup>5</sup> TLKs have ASF1 independent functions during DNA replication through the regulation of replication forks.<sup>6</sup> Depletion of TLKs results in replication fork stalling, the accumulation of single-stranded DNA, and ultimately, DNA damage and cell cycle arrest in G1. These phenotypes were rescued by ectopic expression of WT

TLKs but not kinase dead TLKs. Analysis of chromatin accessibility using the Assay for Transposase-Accessible Chromatin using sequencing (ATAC-seq) following knockdown of TLK1 or TLK2 increased accessibility and transcription of heterochromatin. As a result, loss of TLKs induced alternate lengthening of telomeres thereby activating the cGAS-STING-TBK1 mediated immune response. Consistent with this function, high levels of TLK2 in patients were associated with poor innate and adaptive immune responses in tumors and, potentially, immune evasion.<sup>7</sup> Thus, TLKs, and more specifically their kinase activity, are essential for proper chromatin assembly, DNA replication, and maintenance of heterochromatin.

The cellular functions of TLK1 and TLK2 are predominantly overlapping but their clinical implications are more diverse which may suggest other distinct functions. In the present study, we focus on TLK2. TLK2 has been implicated in neurodevelopmental disease and intellectual deficiency.<sup>8-10</sup> Neurodevelopmental defects manifested with TLK2 haploinsufficiency and were more severe in a single, homozygous case. TLK2 mutations observed in these studies resulted in loss of TLK2 kinase activity.<sup>11</sup> In cellular models of latent gammaherpesvirus infections, knockdown of

TLK1 or TLK2 was sufficient to reactivate latent Epstein-Barr virus infection whereas only knockdown of TLK2 resulted in reactivation of latent Kaposi sarcoma-associated herpesvirus.<sup>12</sup> Latency allows viral infections to evade the immune system and antiviral therapies resulting in lifelong, incurable infection. Reactivation of virus in combination with antiviral therapy is a promising approach known as “shock and kill” that could potentially cure these latent viral infections.<sup>13</sup> TLK2 has also been implicated in breast cancer and glioblastoma where TLK2 is amplified or over-expressed in a high percentage of patients and where higher expression levels are associated with poor patient outcomes.<sup>14-16</sup> In cell lines from both cancer types, ectopic expression of TLK2 lead to enhanced aggressiveness and activated SRC signalling whereas knockdown or pharmacological inhibition of TLK2 slowed growth and inhibited invasion. Knockout of TLK2 in mice resulted in late embryonic lethality due to defective trophoblast differentiation and placental failure.<sup>17</sup> Conditional knockout of TLK2 to bypass the placental defect led to healthy mice suggesting that TLK2 was otherwise dispensable for development and viability. These findings suggest that inhibition of TLK2 may be tolerable in normal, healthy cells in patients. Thus, TLK2 is a very promising target for drug development in multiple cancer types and as a latency reversing agent in shock and kill approaches for latent viral infections.<sup>13-14</sup>

While some recent advances have been made around TLK2 chemical tools, with a recent advancement based on indirubin

based derivatives, these analogues still inhibit both TLK1 and TLK2 with limited selectivity information.<sup>18</sup> There are currently no potent and selective TLK2 inhibitors as chemical probes to investigate TLK2 biology.<sup>19</sup> This despite several concerted efforts to map and identify leads within existing ATP-competitive kinase inhibitors and to define inhibitor chemical space.<sup>19-28</sup>

## 2. Results

Currently the only small molecule inhibitors available to modulate TLK2 are compounds with very broad kinome coverage including staurosporine, Syk inhibitor R406 and RTK inhibitor sunitinib, all of which inhibit TLK2 as an undesired off-target with low relative potency (**Figure 1**). However, the sunitinib oxindole based scaffold has demonstrated tractability on TLK2 where small modifications to afford SU14813 still maintain potency on TLK2 even when coverage has been reduced from 187 to 149 kinases. This is further supported by additional results of an enzyme assay-based panel identifying two further oxindoles, GW506033X and SU9516 that had 84% and 57% inhibition of TLK2 at 0.5  $\mu$ M, respectively.<sup>23</sup> The narrower kinome profile of SU9516 provided an attractive starting point for progress towards the development of a selective chemical probe for TLK2. Herein we report the synthesis, modelling, and characterization of oxindole based inhibitors as potent narrow-spectrum TLK2 inhibitors.

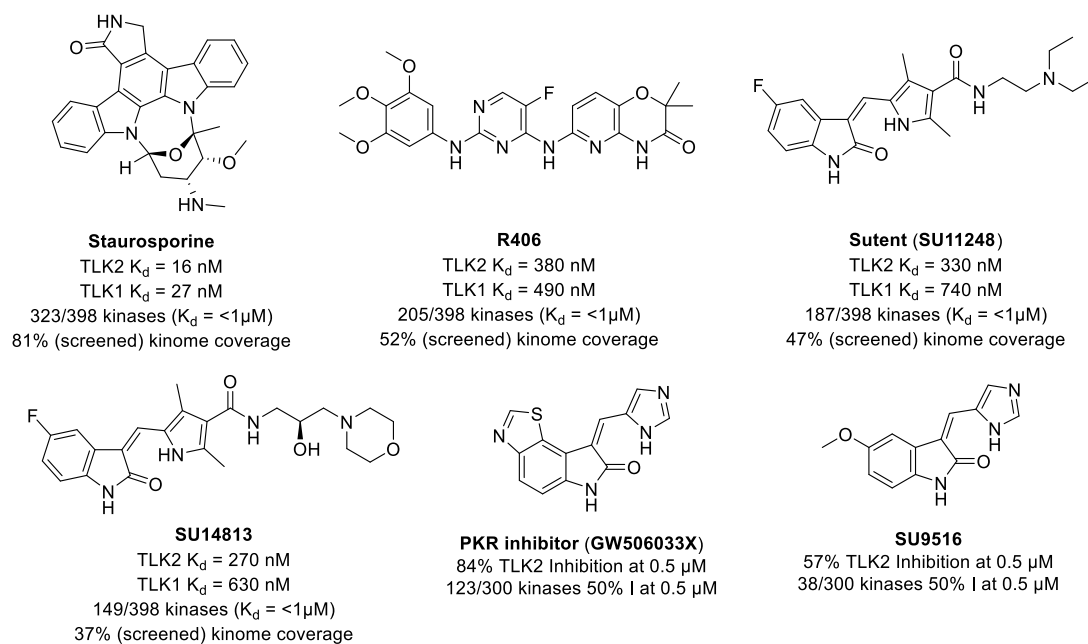


**Figure 1.** Previously reported kinase inhibitors with off-target of TLK2 inhibition, including two matched pair oxindoles.

Having identified the oxindole scaffold as a promising inhibitor chemotype, we first screened 21 commercially available oxindole based kinase inhibitors (**Figure 2**)<sup>29-35</sup> in a TLK2 enzyme assay (**Table S1-S2**).<sup>23</sup> This enabled us to quickly map the TLK2 vs the close kinome landscape and to prioritize our efforts around the smaller SU9516 and GW506033X oxindoles.

Several interchangeable matched pairs including sunitinib (SU11248), toceranib (SU11654), SU12662 and SU14813 all demonstrated consistent low single digit micromolar activity against TLK2. While all these compounds have promiscuous kinome profiles,<sup>20-22</sup> this data increased our confidence that the oxindole may provide a good starting point for TLK2 probe development. The two indirubin derivatives had the same activity against TLK2 ( $IC_{50} = 0.44 \mu M$ ) indicating that oxindoles were bound in the traditional binding mode, with space to grow the solvent exposed region of the molecule.<sup>29-35</sup> The only other two

oxindoles that showed activity below 1 micromolar were SU9516 and GW506033X, both containing an imidazole head group. The narrow kinome spectrum of SU9516 (10 kinases inhibited to 80% at 1  $\mu$ M) combined with the potency of GW506033X ( $IC_{50} = 0.061 \mu M$ ) afforded a promising indication that a potent narrow spectrum compound was possible.<sup>23</sup> We also noted that the same major kinase off-targets namely, fms-like tyrosine kinase 3 (FLT3) and tropomyosin receptor kinase C (TRKC) were recurring themes and likely a prognostic marker for further promiscuity across the kinome. In addition to screening for TLK2 potency, we screened these two off-targets as a micro-panel to check for selectivity between molecules before kinome-wide screening.<sup>36-38</sup>

Having decided to focus our attention on SU9516 (**1**) and related GW506033X, we first sought to explore the structural features required for TLK2 inhibition (**Scheme 1**). Initially we synthesized a series of direct SU9516 analogs (**1-35**) using

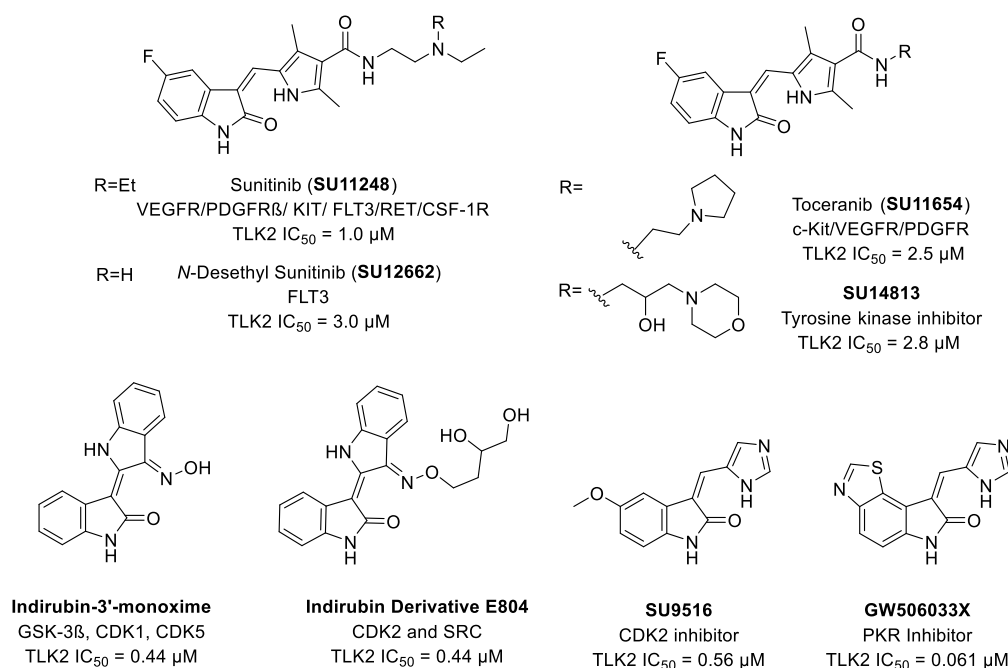


**Figure 2.** Screening of literature inhibitors with the oxindole scaffold with activities below 10 μM (see figure S1 for additional screening and structures). Format: Name, primary target, TLK2 IC<sub>50</sub>

commercially available 5- and/or 6-substituted oxindoles and the Knoevenagel condensation.<sup>39-41</sup> The oxindoles along with a corresponding aldehyde were suspended in ethanol and treated with piperidine under reflux to afford condensation products **1-35** in varying yields (15-85%). The products were isolated by direct crystallization from the crude reaction mixture or following chromatographic purification. A second set of analogues was synthesized in a two-step procedure: first using a Friedel Craft acylation by treatment of unsubstituted oxindole with aluminum (III) chloride and the corresponding acid chloride in dichloromethane to afford the 5-position ketone substituted products **36-39** in acceptable to good yields (30-74%).<sup>42-44</sup> Second, the ketone products (**36-39**) were then treated with the corresponding aldehyde, piperidine under reflux to afford condensation products **40-48** in acceptable to good yields (30-74%). To afford a series of sulphonamide analogs, we first treated the unsubstituted oxindole with neat chlorosulphonic acid at -10 °C, affording **49** in good yield (68%).<sup>45</sup> The sulfonyl chloride **49** was treated with the corresponding amine to afford the sulphonamide building blocks **50-51** in excellent yields, 78% and 85% respectively. The sulphonamides **50-51** were then treated with the previous Knoevenagel conditions with the respective aldehyde to afford the condensation products **52-55** in good yield (41-75%).

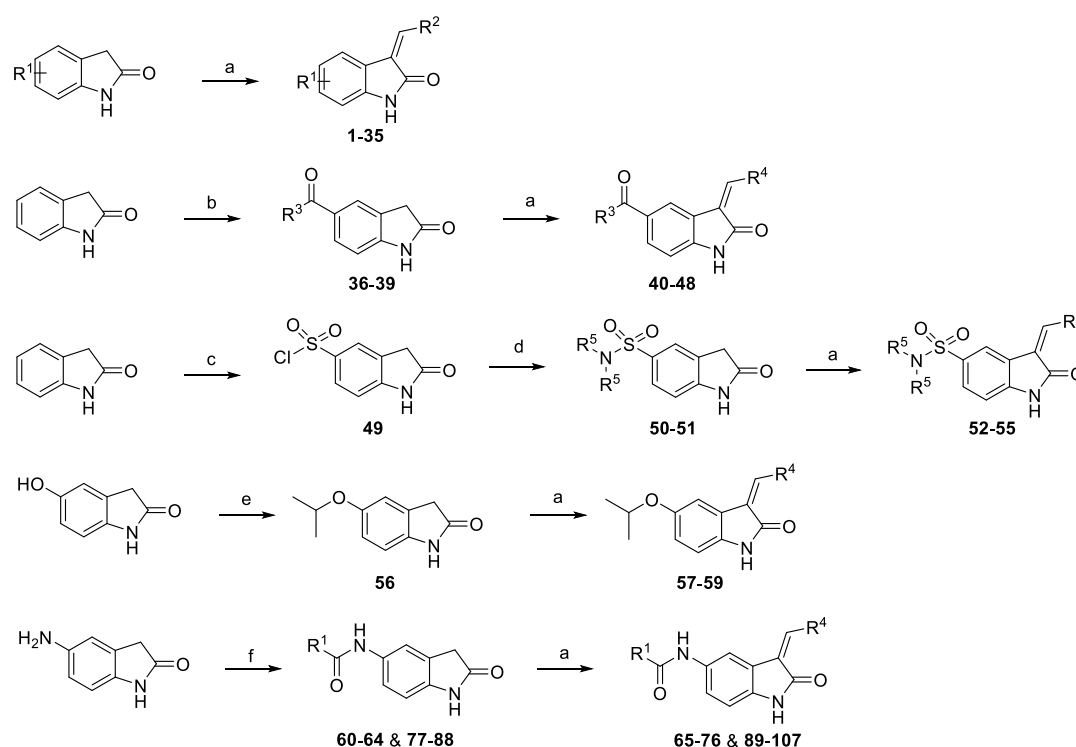
To access a novel 5-position *isopropyl* ether oxindole, a standard Mitsunobu reaction was performed on the 5-hydroxy oxindole with diethyl azadicarboxylate (DEAD), triphenylphosphine, *isopropyl* alcohol in THF at 0 °C to afford 5-*isopropoxy*indolin-2-one (**56**) in 30% yield.<sup>46-48</sup> The ether **56** was then subject to the Knoevenagel conditions with the corresponding aldehyde to afford the desired condensation products **57-59** in good yields (53-62%). Finally, we prepared a series of substituted oxindole amides, furnished with a standard HATU coupling,<sup>49</sup> in the presence of DIPEA and THF. The first set (**60-64**) was afforded in good yields (63-78 %), followed by a series of condensations under standard conditions to render a series of 5-position substituted amide final products (**65-76**) in a range of yields (15-71%). The second set of amide substitutions (**77-88**)

were also afforded in good to excellent yields (48-91%) followed by standard Knoevenagel conditions with the appropriate aldehyde to produce the condensation products (**89-107**) in a range of yields (11-71%).

Having prepared a series of oxindole analogues, these were screened in a TLK2 enzyme assay in a 10-point dose dependent format for TLK2 to determine an IC<sub>50</sub> value. The maximum concentration used was 20 μM with an ATP concentration of 10 μM. The corresponding collateral target evaluation was on FLT3 and TRKC which were screened at a 0.5 μM, consistent with previous reports.<sup>23</sup> The most advanced compounds were then subjected to a Kinase-Glo assay and additional TLK2 assay. The lead compounds were then screened in a DiscoverX kinome panel assay (>400 kinases) to assess their selectivity across the kinome.<sup>20-22</sup>

In the first series of analogues we followed up on the initial hit compound (Z)-3-((1*H*-imidazol-5-yl)methylene)-5-methoxyindolin-2-one (**1**) which when resynthesized produced a compound with consistent potency on TLK2 (IC<sub>50</sub> = 240 nM) (Table 1). The substitution of the imidazole with the pyrrole (**2**) resulted in a 6-fold drop in potency on TLK2. Introduction of the sterically hindered dimethyl group (**3**) afforded no activity on TLK2 at the maximum concentration tested but still showed activity on FLT3 and TRKC. The introduction of a pyrazole group (**4**) lead to a 36-fold reduction of TLK2 activity with respect to **1**. The 2-substituted imidazole (**5**) afforded a compound that was near equipotent with **1** against TLK2. However, none of the simple 5 membered analogues (**2-5**) improved activity on TLK2. A switch to a 6-member 2-pyridyl (**6**) and 3-pyridyl (**7**) head group ring system demonstrated no activity against TLK2 at the maximum concentration tested but also no activity against TRKC and FLT3. Removal of the 5-methoxy group to afford the unsubstituted oxindole (**8**) lead to a 2-fold drop in potency against TLK2. Interestingly the pyrrole substitution **9** shows the same potency as **8** unlike the corresponding drop observed between **1** and **2**.

The corresponding 3,5-dimethyl pyrrole substitution **10** was inactive against TLK2, while the pyrazole **11** showed a 13-fold drop compared with **8**. The 2-substituted imidazole analogue **12**



**Scheme 1.** Synthetic route to prepare the oxindole analogues - *reagents and conditions* a)  $R_2CHO$ , piperidine, EtOH, reflux, 4-24 h; b)  $R^1COCl$ ,  $AlCl_3$ ,  $CH_2Cl_2$ , rt, 48 h; c)  $ClSO_3H$ ,  $-5^\circ C$ , 2 h; d)  $(R^1)_2NH$ ,  $EtN(CH(CH_3)_2)_2$ , THF, rt, 12 h; e)  $R^1OH$ , diethyl azodicarboxylate (DEAD),  $PPh_3$ , rt,  $-5^\circ C$  to rt; f)  $R^1COCl$ , HATU,  $EtN(CH(CH_3)_2)_2$ , THF, rt, 12 h.

was equipotent with **8**, while the two pyridyl analogues **13** and **14** demonstrated no activity against TLK2 or TRKC/FLT3. Switching to the 6-methoxy oxindole substitution **15-20** lead to a net reduction of around 10-fold in activity on nearly all analogues with only the pyrrole maintaining TLK2 inhibition at the same level as **2**.

Given the decrease in inhibition of TLK2 activity at the 6-position, we decided to explore the 5,6-dimethoxyoxindole core **21-25** to assess potential synergistic effects of a double substitution pattern. The results of the 5 analogues were consistent with the mono-substituted 6-methoxy except for the pyrrole **22** that showed a 3-fold jump in potency against TLK2. However, **22** also showed a boost in TRKC and FLT3 inhibition, meaning it was also likely an overall increase in kinome inhibition rather than something solely related to TLK2. We decided to focus our attention on the 5-position as this seemed to be preferable for TLK2 inhibition. Switching the core to the 5-acetyloxindole **26-32** afforded our first compound **27** with more potency against TLK2 ( $IC_{50} = 150$  nM, than the original starting point (**1**) (TLK2  $IC_{50} = 240$  nM). The imidazole analogue was 3-fold less active against TLK2, but the pyrrole was 60% more potent against TLK2. The 3,5-dimethylpyrrole analogue (**28**) also demonstrated inhibition of TLK2 for the first time with an  $IC_{50} = 870$  nM. The pyrazole **29** was significantly weaker nearly 10-fold less potent than the imidazole parent **26**. The 2-substituted imidazole (**30**) is as active as the parent while the pyridyl analogues **31** and **32** showed no activity against TLK2 at the maximum concentration, but there was an increase in TRKC and FLT3 inhibition compared to the other pyridyl analogues synthesized.

There are clear trends observed between pyrrole, 5-position-imidazole, 4-position-imidazole, unsubstituted, 5-position-methoxy and acetyl group. The docking of **1**, **3**, **27** and **28** in the TLK2 protein crystal structure,<sup>11</sup> provided an insight into these trends (Figure 3). The differences between **1** and **3** can be simply explained by the steric clash between the 3,5-dimethylpyrrole on **3**. However, the reduced solvation by removal of the additional

nitrogen is also contributing to the reduced potency of **3** on TLK2 (Figure 3A-B). However, the acetyl substitution of **27** and **28** allowed for a shift in overall binding position that is able to compensate for this steric clash (Figure 3C-D) and enables a closing of the gap of potency from >40-fold between **1** and **3** to equipotent between **26** and **28**. We used this knowledge in the design of our next series of ketone-based substituted oxindole analogues.

The (Z)-3-((1H-pyrrol-2-yl)methylene)-5-acetyloxindolin-2-one (**27**) was the most potent analogue from the initial matrix array (Table 1). The acetyl showed a good trend towards TLK2 inhibition even enabling the 3,5-dimethyl pyrrole substitution **28** to have activity against TLK2 below 1  $\mu M$ . These two results together with a TLK2 inhibition preference for the pyrrole, unsubstituted 5-position and 4-position imidazole prompted us to focus on the acetyl derivatives (Table 2).

First, we looked at the simple carboxylic acid derivatives **33-35**. The direct replacement of the acetyl to form the carboxylic acid **33** demonstrated a 2-fold improvement in TLK2 inhibition, while the imidazole **34** was equipotent. However, the 2-substituted imidazole **35** showed a 6-fold boost in potency against TLK2 ( $IC_{50} = 26$  nM). Interestingly both imidazole substituted compounds also had good selectivity over the two off-targets FLT3 and TRKC. To pursue the aim of a TLK2 probe quality compound with single digit nanomolar activity against TLK2, we hence investigated larger substituents. The *n*-butyl substituent analogues **40-42** showed a slight decrease in inhibition compared to **27** with flat SAR across the three analogues. The larger phenyl analogues **43-44** showed no improvement with an overall 5-6-fold decrease compared with **27**. Introduction of a 4-fluoro substitution **45-46** mitigated some of the decrease in TLK2 inhibition to 2-3-fold compared with **27** with the same off-target FLT3/TRKC off-target profile. Switching from a phenyl to a furan afforded compounds **47-48** that were near equipotent with **27**. Despite decreased ligand efficiency compared with **27**, these furan analogues **47-48** presented a potential expansion point for further optimization.



**Table 1.** Matrix array of SU9516 derivatives with 5,6-oxindole substitutions and different heterocyclic head groups.

	Name	1	2	3	4	5	6	7 <sup>c</sup>
	TLK2 (IC <sub>50</sub> ) <sup>a</sup>	0.24 μM	1.5 μM	>20 μM	8.7 μM	0.38 μM	>20 μM	>20 μM
	FLT3 (% Inh.) <sup>b</sup>	6.9	19	1.8	57	9.6	93	91
	TRKC (% Inh.) <sup>b</sup>	3.7	20	3.3	39	6.7	85	80
	Name	8 <sup>c</sup>	9	10	11	12 <sup>c</sup>	13	14
	TLK2 (IC <sub>50</sub> ) <sup>a</sup>	0.44 μM	0.47 μM	>20 μM	5.9 μM	0.60 μM	>20 μM	>20 μM
	FLT3 (% Inh.) <sup>b</sup>	19	5.9	3.0	69	29	100	100
	TRKC (% Inh.) <sup>b</sup>	7.5	3.3	6.0	45	11	92	99
	Name		15	16	17	18	19	20 <sup>c</sup>
	TLK2 (IC <sub>50</sub> ) <sup>a</sup>		1.7 μM	>20 μM	>20 μM	2.2 μM	>20 μM	>20 μM
	FLT3 (% Inh.) <sup>b</sup>		13	24	89	33	100	87
	TRKC (% Inh.) <sup>b</sup>		19	36	75	37	95	77
	Name	21	22	23	24	25 <sup>c</sup>		
	TLK2 (IC <sub>50</sub> ) <sup>a</sup>	1.8 μM	0.63 μM	>20 μM	>20 μM	2.1 μM		
	FLT3 (% Inh.) <sup>b</sup>	13	5.3	18	65	20		
	TRKC (% Inh.) <sup>b</sup>	36	11	35	81	45		
	Name	26	27	28	29	30 <sup>c</sup>	31	32 <sup>c</sup>
	TLK2 (IC <sub>50</sub> ) <sup>a</sup>	0.77 μM	0.15 μM	0.87 μM	7.6 μM	0.62 μM	>20 μM	>20 μM
	FLT3 (% Inh.) <sup>b</sup>	6.4	3.0	1.9	25	11	77	85
	TRKC (% Inh.) <sup>b</sup>	9.0	3.1	1.1	38	18	67	79

<sup>a</sup>8-point dose response (n=1); <sup>b</sup>percentage inhibition at 0.5 μM (n=2); <sup>c</sup>E:Z ratio: **7** (50:50); **8** (33:67); **12** (40:60); **20** (28:72); **25** (44:56); **26** (32:68); **30** (47:53); **32** (48:52).<sup>39</sup>

The docking of **44**, **46** and **47** supported our initial observations with **27** (Figure 4). The aromatic groups that are able to interact with the catalytic lysine in **44**, **46** and **47** appeared to be preferable to a simple alkyl when attempting to drive potency on TLK2 below IC<sub>50</sub> = 100 nM (Figure 4). Comparing the unsubstituted **44** to the 4-fluoro substituted **46**, we observed a potential halogen bond between the fluorine and a backbone carbonyl which may explain the 3-fold boost in potency against TLK2 (Figure 4A-B).<sup>50-52</sup> However, further analysis of the binding and water network of **35**

**Table 2.** Investigation of derivatives of **27** with pyrrole and imidazole heterocyclic head groups.

Name	R <sup>1</sup>	X <sup>1</sup>	X <sup>2</sup>	TLK2 IC <sub>50</sub> (nM) <sup>a</sup>	FLT3 (%) <sup>b</sup>	TRKC (%) <sup>b</sup>
33		C-H	C-H	62	5.8	9.3
34 <sup>c</sup>	HO-	N	C-H	140	33	46
35		C-H	N	26	30	37
40		C-H	C-H	220	3.6	2.5
41		N	C-H	230	8.9	4.3
42		C-H	N	250	14	8.7
43		C-H	C-H	870	5.9	1.9
44		N	C-H	700	17	2.8
45		C-H	C-H	340	3.5	1.0
46	F	N	C-H	340	15	1.9
47		C-H	C-H	100	0.8	0.9
48		C-H	N	340	9.6	5.2

<sup>a</sup>8-point dose response (n=1); <sup>b</sup>percentage inhibition at 0.5 μM (n=2); <sup>c</sup>E:Z ratio: **33** (30:70).<sup>39</sup>

highlighted untapped potential within a network of interactions in the hydrophobic pocket (Figure 5). The carboxylic acid motif of **35** was able to align with the Thr612 which in-turn coordinated a main chain amide, which can be used in the next phase of development. The water network is not disrupted by this series of interactions, but this simulation highlights that the oxindole occupies an optimal binding position.

The relatively flat SAR of the ketone substitution towards TLK2 inhibition led us to expand our search to other 5-position substitution patterns including two different sulphonamides (**52-55**) and an isopropyl ether (**57-59**) (Table 3). Surprisingly, despite the relatively high potency of the acetyl (**27**), the sulphonamides (**60-65**) were inactive on TLK2 at the top concentration. The 5-isopropyl ether oxindole showed some potential. The pyrrole analog (**57**) was 3-fold more potent for TLK2 than the 5-methyl ether version (**2**). The imidazole (**58**) was 7-fold less potent on TLK2 than the corresponding 5-methyl ether (**1**). While the 2-substituted imidazole (**59**) was the only analog to show an improvement over the methyl counterpart with a 2-fold increase in potency against TLK2.

However, these limited improvements meant we switched to the 5-amide substituted oxindoles **65-76** in hope of driving down potency on TLK2 (Table 4). We first screened a direct *n*-propyl analog **65** that showed similar potency to **27** with a reduction in off-target potency of FLT3 and TRKC. The addition of a pendent ethyl group to form a pentan-3-yl substitution **66-68** dropped potency by around 10-fold against TLK2 compared to the corresponding *n*-propyl analog **65**. The cyclohexane substitution **69-71** was broadly similar in potency with **27** on TLK2, but with a significant improvement on the off-target profile with a reduction in off-target potency of FLT3 and TRKC compared to **27**. The unsubstituted phenyl **72-74** has an asymmetric structure activity relationship (SAR) for TLK2 with the pyrrole **72** 5-fold weaker than **27**. While the imidazole **73** is 4-fold more potent and both

improved off-target selectivity against FLT3 and TRKC. The 2-substituted imidazole **74**, is 3-fold less potent than **73** and equipotent to **27**. The furan substitution analogs **75** and **76** were equipotent with **27** on TLK2 but both demonstrated improved off-target selectivity against FLT3 and TRKC.

The unsubstituted phenyl **72**, is about an order of magnitude less active than close derivatives **73** and **74**. This is likely due to the water network coordination as the 5-membered 1,2-diazole, 1,3-diazole and pyrrole ring system are all pointing towards the solvent exposed region of the TLK2 ATP binding site. The interactions in the hydrophobic pocket region were identical for all three compounds, with the designed interaction of Thr612 and the cation- $\pi$  interaction between Lys491 and the phenyl ring observed in each of the docked examples (Figure 6A-C). However, we observed through WaterMap that analog **72** was not able to make a stable hydrogen bond network with first solvation shell waters (Figure 7), likely leading to weaker binding.<sup>53-56</sup> The lack of solvent coordination coupled with the ability of **74** to hydrophobically stack with Leu468 (Figure 7), which was not possible with **72** and **73**, provided a rational explanation for the results we observed.

**Table 3.** Investigation of sulphonamide and ether derivatives.

Name	R <sup>1</sup>	X <sup>1</sup> , X <sup>2</sup>		TLK2 IC <sub>50</sub> (nM) <sup>a</sup>	FLT3 (%) <sup>b</sup>	TRKC (%) <sup>b</sup>
		X <sup>1</sup>	X <sup>2</sup>			
<b>52</b>		C-H	C-H	> 20000	31	1.6
<b>53</b>		N	C-H	> 20000	55	12
<b>54</b>		C-H	C-H	> 20000	27	3.0
<b>55</b>		N	C-H	> 20000	62	27
<b>57</b>		C-H	C-H	560	8.3	2.8
<b>58</b>		N	C-H	1600	33	11
<b>59</b>		C-H	N	160	25	5.9

<sup>a</sup>8-point dose response (n=1); <sup>b</sup>percentage inhibition at 0.5  $\mu$ M (n=2)

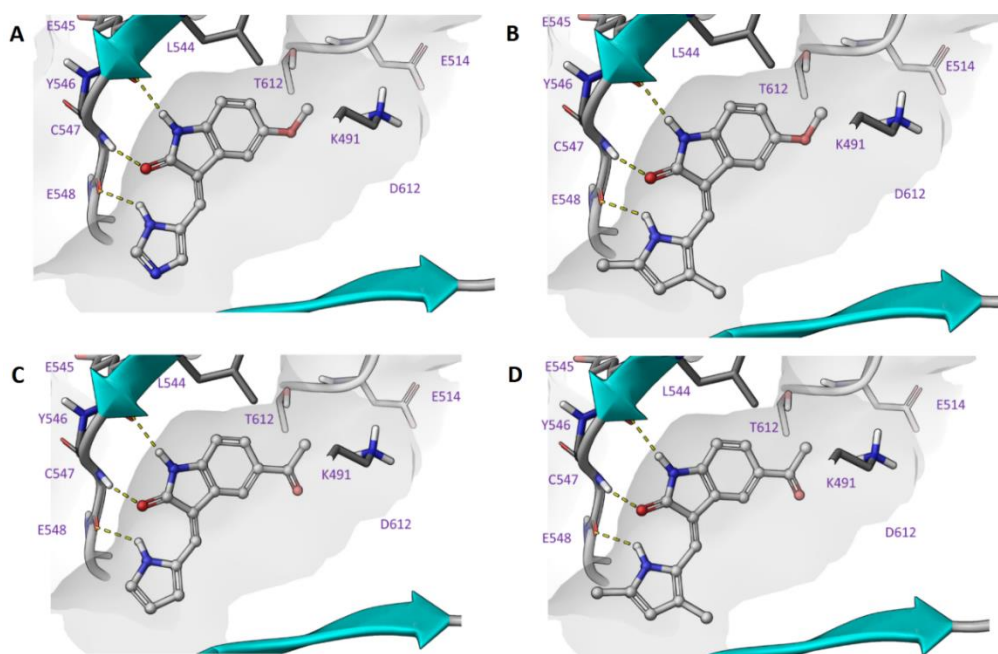


**Figure 3.** Inhibitor docking of A) **1**, B) **3**, C) **27**, D) **28** in TLK2 (PDB: 5O0Y), demonstrating key hinge binding interactions and space in the hydrophobic pocket.

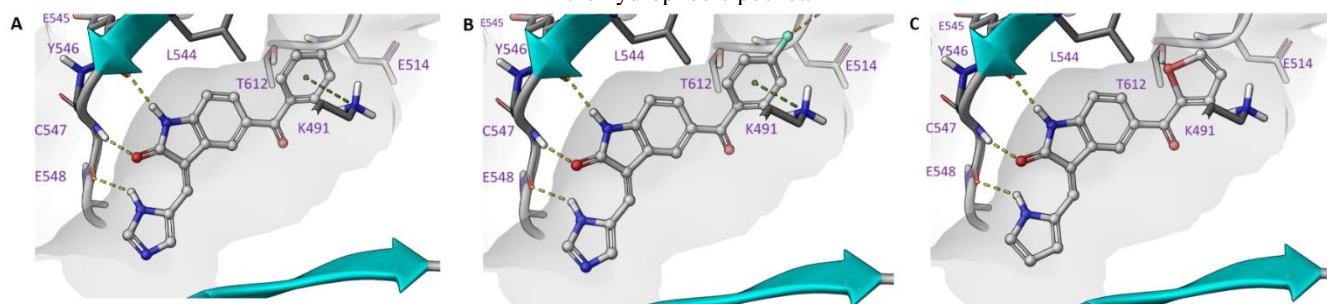


**Figure 4.** Inhibitor docking comparing of A) **44**, B) **46** and C) **47** in TLK2 (PDB: 5O0Y) all demonstrating key hinge binding interactions and an expansion in the hydrophobic pocket.

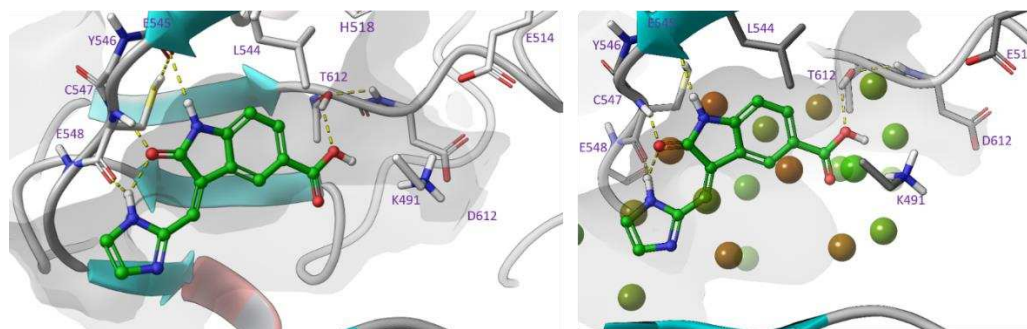
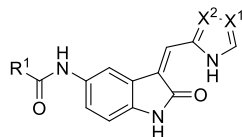


**Figure 5.** Left: favorable docking pose of compound **35**. Right: visualization of hydration sites from a WaterMap simulation close to docked compound **35**.

**Table 4.** Initial investigation of amide derivatives.



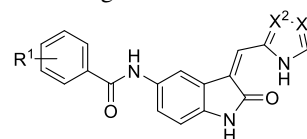
Name	R <sup>1</sup>	X <sup>1</sup>	X <sup>2</sup>	TLK2 IC <sub>50</sub> (nM) <sup>a</sup>	FLT3 (%) <sup>b</sup>	TRKC (%) <sup>b</sup>
<b>65</b>		C-H	C-H	170	11	4.9
<b>66</b>		C-H	C-H	2400	25	2.3
<b>67</b>		N	C-H	2300	61	6.0
<b>68</b>		C-H	N	2500	75	15
<b>69</b>		C-H	C-H	150	28	11
<b>70</b>		N	C-H	100	46	16
<b>71</b>		C-H	N	130	58	32
<b>72</b>		C-H	C-H	820	21	19
<b>73</b>		N	C-H	34	44	30
<b>74</b>		C-H	N	110	48	33
<b>75</b>		C-H	C-H	120	30	28
<b>76</b>		C-H	N	130	42	33

<sup>a</sup>8-point dose response (n=1); <sup>b</sup>percentage inhibition at 0.5  $\mu$ M (n=2)

To build on the encouraging results of **73** and **74**, we decided to explore the amide derivatives with a series of modifications to the phenyl ring system **88-106** and focused on the imidazole and 2-substituted imidazole head group (**Table 5**). First, we probed the 4-position of the phenyl ring, by introducing a nitrile group with an imidazole head group to afford the most potent compound **88** against TLK2 observed so far (IC<sub>50</sub> = 12 nM); 13-fold more potent than **27**, with good selectivity over FLT3/TRKC. The 3-position nitrile with the imidazole head group **89** afforded 8-fold less potency for TLK2 than **88**, but with slightly improved selectivity over FLT3/TRKC, however the 2-substituted imidazole **90** only had a 4-fold drop in potency for TLK2. The 2-position nitrile was not well tolerated with 2-substituted imidazole **91** having an IC<sub>50</sub> over 1  $\mu$ M on TLK2. The 4-methoxy substitution analogs **92-93** were 7-9-fold less potent on TLK2 than **89**. The 3-methoxy with the imidazole head group **94** was consistent with **92-93**, but the 2-substituted imidazole **95** was 28-fold less potent on TLK2 than **94**. In contrast to **91**, the 2-methoxy derivatives **96-97** were potent against TLK2 with the imidazole head group **96** being single digit nanomolar (IC<sub>50</sub> = 9.1 nM), the most potent compound to date. The 2-substituted imidazole derivative **97** was 7-fold less potent on TLK2 but had good selectivity over FLT3/TRKC. The fluorine substitutions around the phenyl ring system **98-102** had relatively flat SAR for TLK2. The 2-position fluoro imidazole **102** was the most potent against TLK2 (IC<sub>50</sub> = 110 nM) and all analogs **98-102** had good selectivity against FLT3 and TRKC. The larger trifluoromethyl substitution in the 4-position was partly tolerated with the imidazole head group **103** showing only a 3-fold drop with respect to **102**. However, the 2-substituted imidazole **104** showed limited to no activity against TLK2 at the highest

concentration tested, potentially due to the inactive geometric *E*-isomer contribution. The 2-position analogs **105-106** were consistent with **98-102**, with equipotency on TLK2 and good selectivity over FLT3. Interestingly, **105-106** both display reduced selectivity over TRKC compared with **103**.

**Table 5.** Advanced investigation of amide derivatives.



Name	R <sup>1</sup>	X <sup>1</sup>	X <sup>2</sup>	TLK2 IC <sub>50</sub> (nM) <sup>a</sup>	FLT3 (%) <sup>b</sup>	TRKC (%) <sup>b</sup>
<b>88<sup>c</sup></b>	4-CN	N	C-H	12	39	47
<b>89<sup>c</sup></b>	3-CN	N	C-H	95	56	52
<b>90</b>	3-CN	C-H	N	48	60	46
<b>91</b>	2-CN	C-H	N	4000	75	33
<b>92</b>	4-OMe	N	C-H	88	36	45
<b>93</b>	4-OMe	C-H	N	110	44	50
<b>94</b>	3-OMe	N	C-H	100	42	48
<b>95<sup>c</sup></b>	3-OMe	C-H	N	2800	84	80
<b>96</b>	2-OMe	N	C-H	9.1	25	43
<b>97</b>	2-OMe	C-H	N	67	40	34
<b>98</b>	4-F	N	C-H	190	41	39
<b>99</b>	4-F	C-H	N	140	46	53
<b>100</b>	3-F	N	C-H	200	34	33
<b>101<sup>c</sup></b>	3-F	C-H	N	490	70	60
<b>102</b>	2-F	C-H	N	110	26	24
<b>103</b>	4-CF <sub>3</sub>	N	C-H	330	58	57
<b>104<sup>c</sup></b>	4-CF <sub>3</sub>	C-H	N	6100	88	83
<b>105<sup>c</sup></b>	2-CF <sub>3</sub>	N	C-H	400	60	17
<b>106<sup>c</sup></b>	2-CF <sub>3</sub>	C-H	N	190	62	20

<sup>a</sup>8-point dose response (n=1); <sup>b</sup>percentage inhibition at 0.5  $\mu$ M (n=2); <sup>c</sup>*E*:*Z* ratio: **88** (50:50); **89** (43:57); **95** (37:63); **101** (35:65); **104** (34:66); **105** (38:62); **106** (34:66).<sup>39</sup>

The docking of **73**, **88** and **96** provided further evidence of the key interaction at the Thr612 residue with the amide bond carbonyl and the catalytic lysine (Lys491) and afford high potency low double and single digit nanomolar compounds against TLK2 (**Figure 8**). The high affinity was dependent on an aromatic ring system close to the active site but away from the hinge. We looked to exploit these traits to further optimize the analogs towards TLK2 inhibition and potentially increase kinome specificity in the process.

The recently released solved X-ray structures of TLK2 together with our molecular docking simulations, were also helpful in the design of more effective TLK2 inhibitors.<sup>10</sup> A 3D-QSAR model was constructed so that the main fields could be overlaid with co-crystallized ligands and verifiable favourable docking poses. We constructed a 3D-QSAR model for TLK2 using the field based QSAR functionality of Schrödinger Maestro (**Table 6** and **7**). The



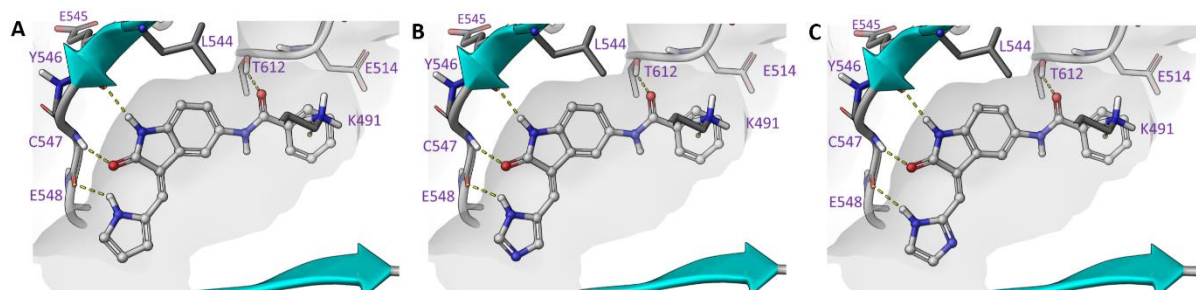


**Figure 6.** Inhibitor docking comparing A) **72**, B) **73**, C) **74** in TLK2 (PDB: 5O0Y) demonstrating key hinge binding interactions and an expansion in the hydrophobic pocket.

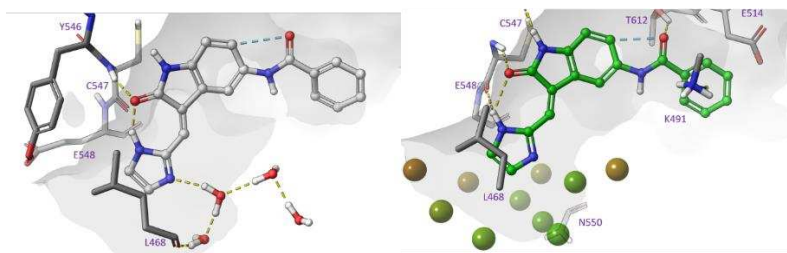


**Figure 7.** Snapshot of trajectory waters from WaterMap simulation illustrating favourable solvent interactions of **73**. For clarity, waters and hydration sites are shown only at the mouth of the pocket.

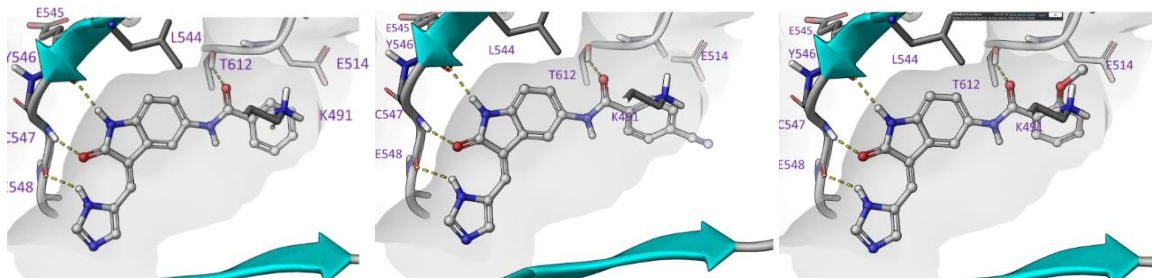


**Figure 8.** Inhibitor docking in TLK2 (PDB: 5O0Y) comparing A) **73**, B) **88** and C) **96**. All demonstrating key hinge binding interactions and a refined expansion in the hydrophobic pocket.

flexible ligand alignments were performed using a Bemis-Mucko method.<sup>52</sup> The 3D-QSAR model allowed recognition of the largest common scaffold and utilized a favorable docking pose of structurally representative derivatives as alignment templates. Torsion angles of larger substituents, including methoxy groups, were manually adjusted when required. The **Table 6** Validation of 3D-QSAR models for TLK2

models were constructed with 80% of compounds defined randomly as training sets with the rest of the compounds as a test set (**Figure 9**). The field values were calculated utilizing a grid spacing approach of 1.0 Å extended 3.0 Å beyond training set limits. Variables with  $|T\text{-value}| < 2$  were eliminated from final model building.

# Factors	SD	R <sup>2</sup>	R <sup>2</sup> CV	R <sup>2</sup> Scramble	Stability	F	P	RMSE	Q <sup>2</sup>	Pearsson-r
1	0.74	0.43	0.38	0.055	0.997	56.1	1.01E-10	0.85	0.15	0.54
2	0.50	0.74	0.63	0.18	0.96	105.0	2.48E-27	0.57	0.61	0.83
3	0.22	0.80	0.68	0.27	0.94	98.5	1.43E-29	0.54	0.65	0.82
4	0.28	0.85	0.70	0.36	0.92	104.2	3.60E-30	0.52	0.68	0.83
5	0.33	0.89	0.71	0.43	0.92	116.9	7.54E-34	0.46	0.75	0.86
6	0.30	0.91	0.71	0.48	0.88	122.9	3.73E-38	0.47	0.74	0.86

**Table 7.** Regression Statistics for TLK2 QSAR model

#Factors	gauss_s	gauss_e	gauss_h	gauss_a	gauss_d
1	0.53	0.062	0.13	0.19	0.09
2	0.27	0.070	0.32	0.26	0.09
3	0.28	0.069	0.31	0.24	0.10
4	0.29	0.067	0.28	0.25	0.12
5	0.30	0.068	0.25	0.25	0.14
6	0.31	0.068	0.23	0.27	0.13



The R-squared value of the TLK2 model with all four partial least squares regression (PLS) components were 0.75. The model had above average internal predictivities with a Q-square value of 0.75, which was determined by leave-one out (LOO) cross-validation. The stability of the model was 0.92 with four (PLS) components having demonstrated a robust predictivity of structure to activity output.

The shape of the oxindole series had a good alignment in the TLK2 ATP binding pocket with a strong interaction with hinge residues with semi-optimized back pocket QSAR fields (**Figure**

**10A-F**). The pyrrole/imidazole head group assisted the hinge interacting with an additional anchor point. The oxindole scaffold was able to form two direct hydrogen bond interactions *via* the oxindole amide functionality to the main chain amide of Tyr546 and Cys547. The N-H of the pyrrole/imidazole was then able to form an interaction with Glu548. The optimized amide derivatives were also able to interact *via* the carbonyl of the amide with Thr612 and had a cation- $\pi$  interaction with Lys491 forming with the pendent heterocycle. The internal conformational restriction of

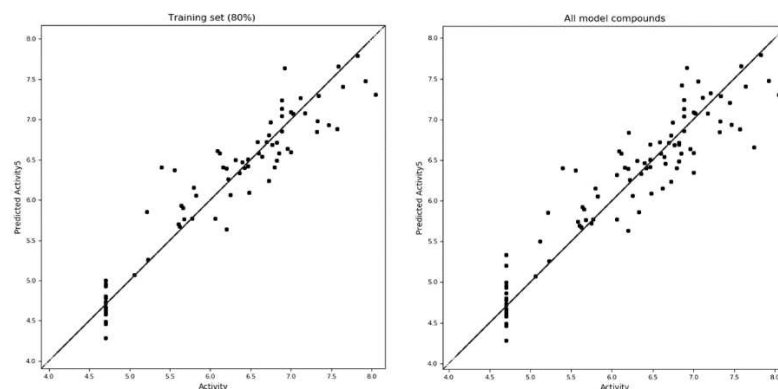


**Figure 9.** Scatter plots of field-based 3D-QSAR models showing predicted versus measured binding affinities (nM) of active compounds printed at logarithmic scale with the TLK2 training set (left) and TLK2 all compounds (right).

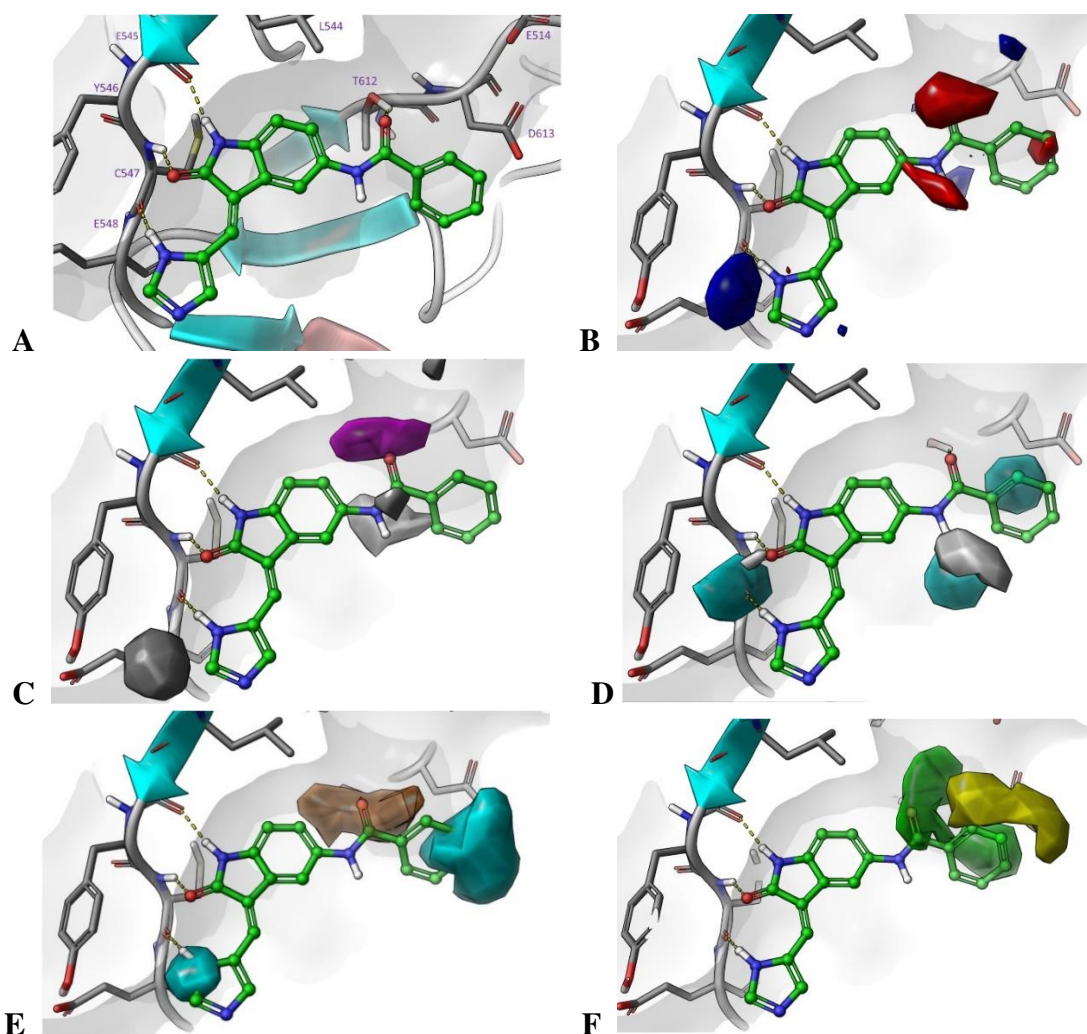


**Figure 10.** QSAR modelling on 73 template: A) Standard docking of 73 in TLK2 (PDB:5O0Y); B) Electrostatics (blue = positive and red = negative); C) hydrogen bonding acceptor fields (magenta = positive and grey = negative); D) hydrogen bonding donor fields (cyan = positive and grey = negative); E) hydrophobic fields (orange = positive and cyan = negative); F) Steric fields (green = positive and yellow = negative).

the oxindole scaffold between the carbonyl and amine of the pendant heterocycle was also assisting in the optimization of TLK2 binding, not only minimizing the entropic loss associated flexibility but also allowed the ligand to adopt a preferred conformation for binding.<sup>39,57-58</sup>

We further explored the rigidity within the oxindole core with the solving of a series of small molecule crystal structures **1**, **2**, **15**, **19**, **72**, and **74** (Figure 11, Table S3) and **4**, **9**, **11**, **13** and **16** (Figure S1, Table S3). Structures **1**, **2**, **16** and **19** were planar due to intramolecular hydrogen bonding between the pyrrole **15** and imidazole **1** and **2** ring and the oxindole carbonyl oxygen atom (Figure 11). The steric hindrance of the pyridine substituent of **19** and lack of hydrogen bond donor resulted in a deviation from planarity for this structure. Whilst the methylene pyrrole/imidazole rings were planar with the oxindole moiety, the benzamide substituents of **72** and **74** were not (Figure 11). The methylene imidazole substituted structures **1** and **15** included a hydrogen bonded dimer between the amine of the imidazole and the oxindole carbonyl instead except **74** which formed flat 1D tapes along the crystallographic *-ac* plane *via* oxindole amine, imidazole imine H-bonding. These tapes formed H-bonds to those above and below *via* hydrogen bonds between the amide

functionalities. The methylene pyrazole substituted structures showed no distinct packing motifs with **2** forming interleaved, corrugated tapes *via* oxindole amine, imidazole imine H-bonding and **16** forming a H-bonded, tetramer structure comprising two crystallographically independent molecules.

A series of oxindole derivatives were designed based on the quantitative structure-activity relationships (QSAR) QSAR model utilizing prior SAR knowledge and the small molecule crystal structure information. These were synthesized and tested using the same protocol as described above, with the addition of TLK1 screened at a 0.5  $\mu$ M concentration, consistent with previous reports.<sup>23</sup>

We synthesized the series of predicted analogs utilizing similar conditions as before (Scheme 1) with a few alterations in starting materials. The amide intermediates **107-129** were afforded by a routine HATU coupling to the respective 5-aminooxindole in good yields (57-84 %). The amide was then treated with the previous Knoevenagel conditions with the respective aldehyde to afford the condensation products **117-129** in a range of yields (21-71 %) (Scheme 2).

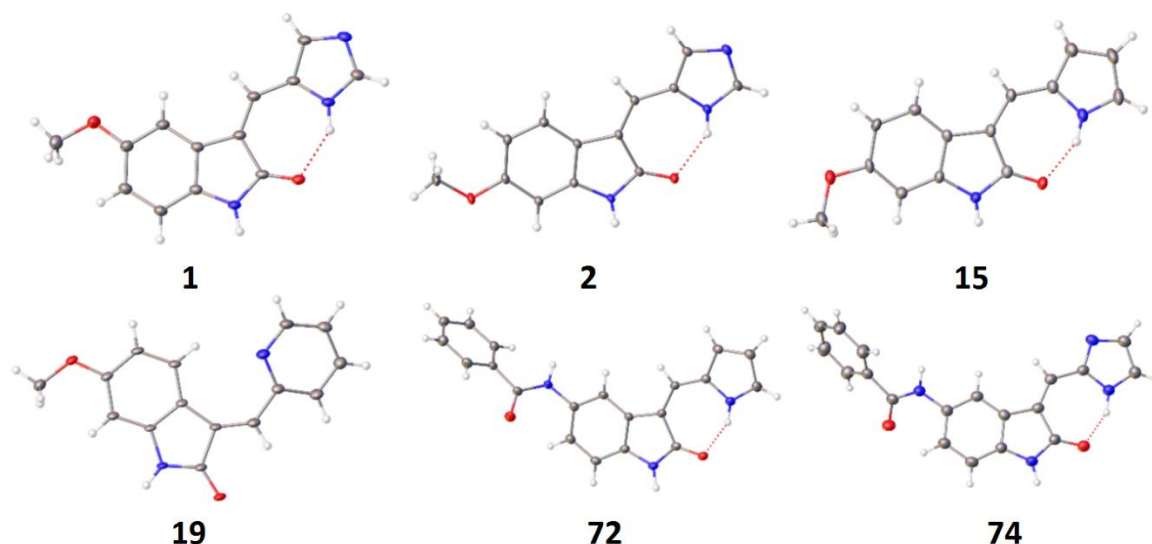
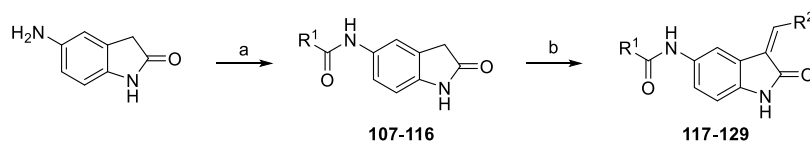


Figure 11. Small molecule crystal structures of **1**, **2**, **15**, **19**, **72** and **74**.

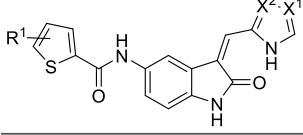


Scheme 2. Synthetic route to prepare predicted oxindole analogs - *reagents and conditions* a)  $R^1\text{COCl}$ ,  $\text{EtN}(\text{CH}(\text{CH}_3)_2)_2$ , THF, rt, 12 h; b)  $R^2\text{CHO}$ , piperidine, EtOH, reflux, 4-24 h.

The QSAR modelling suggested that the phenyl ring could be reduced to a 5-member ring and coupled with earlier knowledge of the furan **75** and **76**, so we synthesized the thiophenes **117-121** (Table 8). The activities observed were broadly in line with the QSAR model. The unsubstituted thiophene with the imidazole head group **117** was potent on TLK2 ( $\text{IC}_{50} = 23$  nM) but lacked selectivity over FLT3/TRKC, the 2-substituted imidazole **118** was equipotent but slightly more selective against FLT3/TRKC. The introduction of a 4-methoxy group onto the thiophene **119** reduced potency for TLK2 by 3-fold compared to **117**. However, the 4-ethoxy group **120** was equipotent with **117** with equivalent selectivity over FLT3/TRKC. Interestingly **120** was the only compound to show any significant activity on TLK1 in the initial screening (54% inhibition at 1  $\mu$ M). The final compound in this

series, the 4-fluoro **121** was 8-fold less potent against TLK2 compared to **117**.

Table 8. Results of initial set of QSAR predicted compounds.

Name	$R^1$	$X^1$	$X^2$				
				TLK2 $\text{IC}_{50}$ (nM) <sup>a</sup>	FLT3 (%) <sup>b</sup>	TRKC (%) <sup>b</sup>	TLK1 (%) <sup>b</sup>
<b>117</b>	H	N	C-H	23	12	16	89
<b>118<sup>c</sup></b>	H	C-H	N	36	20	26	80
<b>119</b>	4-OMe	N	C-H	77	20	22	87
<b>120<sup>c</sup></b>	4-OEt	N	C-H	27	9.4	8.0	54
<b>121</b>	4-F	N	C-H	180	23	12	100

<sup>a</sup>8-point dose response (n=1); <sup>b</sup>percentage inhibition at 0.5  $\mu$ M (n=2); <sup>c</sup>E:Z ratio: **112** (34:66); **114** (28:72).<sup>39</sup>

We then optimized these initial compounds to afford a series of more advanced amide derivatives **122-127** (Table 9). The fused thiophene, **122** was equipotent with **117**, with no difference in selectivity. This larger 5,5-system was tolerated, so an expansion of the phenyl substitution patterns was synthesized to include 3-trifluoromethyl, 5-fluoro **123** and the fused 2,3-catacol **124**, unfortunately these analogs both lost significant activities against TLK2 compared with **117**. We also looked at smaller 5-member rings, thiazole **125**, oxazole **126** and isothiazole **127** afforded potent compounds against TLK2 with the oxazole approaching towards single digit nanomolar against TLK2.

In a further effort to validate the model and test the limits of the two additional compounds **128** and **129** were synthesised (Table 10). These were based on the cores structure of **73** and tested the predictive power of the model. The addition of the 2-methyl (**128**) to the imidazole head group afforded an 8-fold increase in potency against TLK2 with no loss of selectivity against FLT3 and TRKC. The model was accurate for the pyrazole **129**, the introduction of the extra nitrogen led to an over 15-fold drop in TLK2 inhibition, consistent with previous SAR in this series.

**Table 9.** Optimization of compounds based on QSAR.

Name	R <sup>1</sup>	TLK2 IC <sub>50</sub> (nM) <sup>a</sup>	FLT3 (%) <sup>b</sup>	TRKC (%) <sup>b</sup>	TLK1 (%) <sup>b</sup>
<b>122</b>		47	15	24	88
<b>123</b>		630	55	30	99
<b>124</b>		260	45	25	86
<b>125</b>		120	18	11	97
<b>126</b>		15	8.0	12	89
<b>127<sup>c</sup></b>		46	14	3.8	90

<sup>a</sup>8-point dose response (n=1); <sup>b</sup>percentage inhibition at 0.5  $\mu$ M (n=2); <sup>c</sup>E:Z ratio: **127** (30:70).<sup>39</sup>

**Table 10.** Optimization of compounds based on QSAR.

Name	R	X <sup>1</sup>	X <sup>2</sup>	TLK2 IC <sub>50</sub> (nM)	FLT3 (%)	TRKC (%)	TLK1 (%)
<b>128</b>	Me	N	C-H	18	24	35	84
<b>129</b>	H	C-H	N	2600	87	86	92

<sup>a</sup>8-point dose response (n=1); <sup>b</sup>percentage inhibition at 0.5  $\mu$ M (n=2)

Aligning the results of the prediction with the experimental results, we found a good concordance (Table 11).

**Table 11.** Compound results based on QSAR prediction.

Compound	TLK2 Inhibition Activity (nM)			
	Predicted	Found	Log Predicted	log Actual
<b>117</b>	51	23	7.29	7.64
<b>118</b>	56	36	7.25	7.44
<b>119</b>	50	77	7.30	7.11
<b>120</b>	370	27	6.44	7.57
<b>121</b>	68	180	7.17	6.74
<b>122</b>	180	47	6.75	7.33
<b>123</b>	1800	630	5.76	6.20
<b>124</b>	40	260	7.40	6.59
<b>125</b>	8	120	8.08	6.92
<b>126</b>	8	15	8.12	7.82
<b>127</b>	37	46	7.44	7.34
<b>128</b>	180	18	6.74	7.74
<b>129</b>	960	2600	6.02	5.59

In addition to assessing the selectivity profile on the two near off-targets FLT3 and TRKC; we also investigated the wider kinome selectivity profile of ten of the most promising analogs using KinomeSCAN<sup>®</sup> at 1  $\mu$ M across over 400 kinases (Table 12, Figure 12).<sup>20-22</sup> The original starting point (**1**) was moderately selective across the kinome hitting 15 kinases over 90%. The 5-acetyl analog **27**, was the most promiscuous analog with 62 kinases over 90%, possibly due to the small flexible ketone orientated favourably to towards the common catalytic lysine motif (Figure 3D). Interestingly, **1**, **27** and **44** had similar hit kinases above 90%. Common kinases included MST2, CDKL2, ERK8, TRKA, JAK3(JH1domain-catalytic) and TNIK. The amide substitution in the 5-position not only increased selectivity across the kinome but also changed the kinases inhibited. Compounds **72-74** consistently hit MYLK4, BIKE, GRK4, SRPK3 above 90%, another four PRP4, AAK1, PIP5K1A, SRPK2 are revealed as consistent hits if the threshold is decreased to 80% inhibition, in addition to other kinases (see supporting information). The most narrow spectrum inhibitor across the kinome tested in the KinomeSCAN<sup>®</sup> assay was **97** which hit only 7 kinases above 90%; including BIKE, DRAK2, JAK1(JH2domain-pseudokinase), MAST1, PIP5K1A, GRK4, and TYK2 (JH2domain-pseudokinase). The selectivity of the designed thiophene amide **111** was moderate with 15 kinases inhibited. The addition of a methyl **128** onto the 5-position of the imidazole head group of **73** changed the kinome profile subtly at 90% inhibition, with inhibition reduced on TYK2(JH2domain-pseudokinase), AAK1 but also increased on DRAK2, PIP5K1A, RIOK1, MAST1, LKB1.

**Table 12.** Kinome selectivity profiling

Kinome profiling summary			TLK2 IC <sub>50</sub> (nM)
Name	>90	S(10)	
<b>1</b>	15	0.037	240
<b>27</b>	62	0.154	150
<b>44</b>	15	0.037	700
<b>72</b>	10	0.025	820
<b>73</b>	9	0.022	34
<b>74</b>	11	0.027	150
<b>97</b>	7	0.017	67
<b>111</b>	15	0.037	23
<b>128</b>	11	0.027	18

<sup>a</sup>number of kinases inhibited above 90%; <sup>b</sup>TLK2 enzyme assay result

Finally, we screened the most promising compounds **97**, **117**, **128**, the negative control compound **129**, along with the starting point compound **1** in an orthogonal assay measuring the

conversion of ATP to ADP.<sup>59-61</sup> The results were consistent with both the weak and potent TLK2 binding of the five compounds in

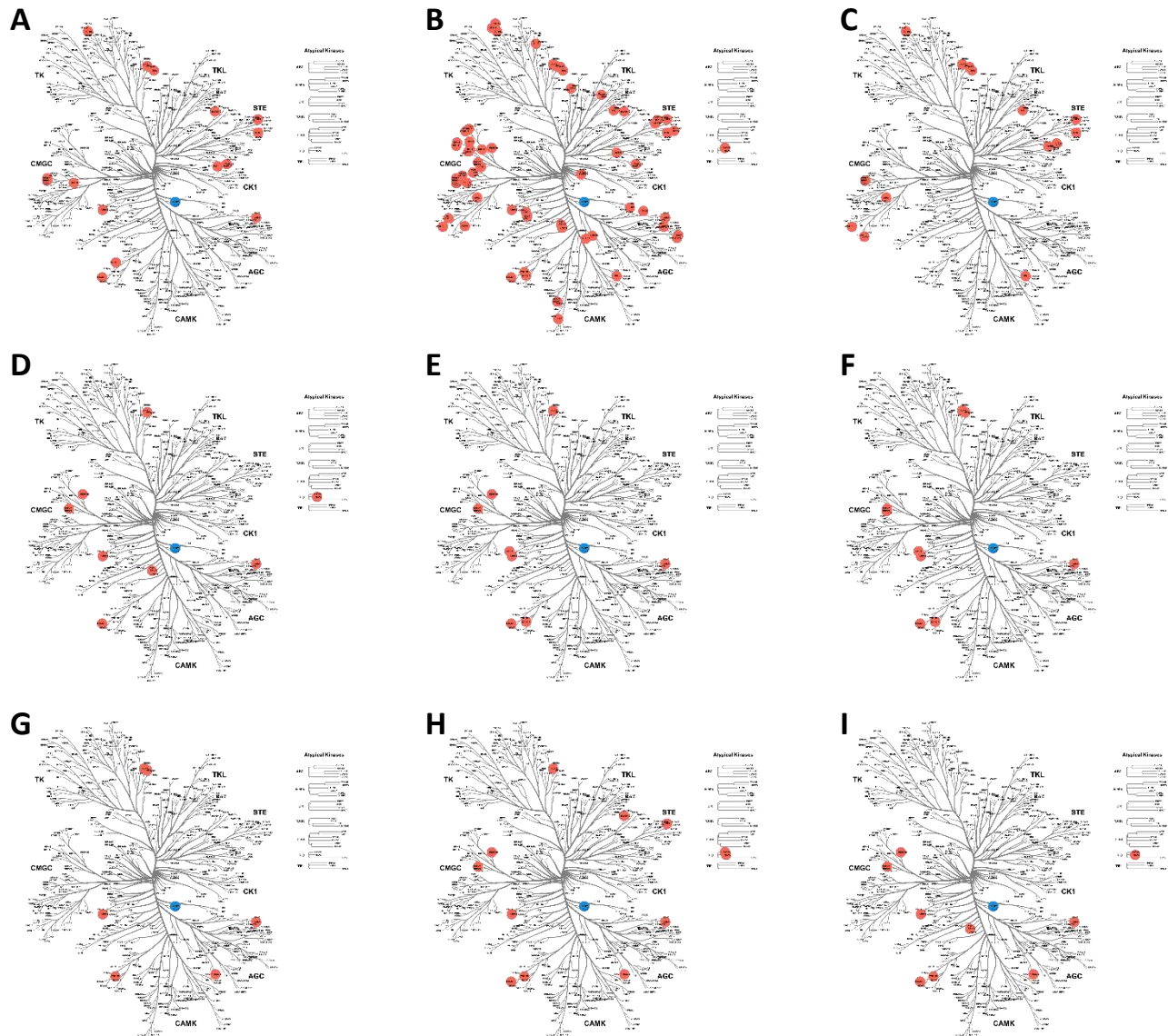


**Figure 12.** Kinome tree image of KinomeScan data for A) **1**, B) **27**, C) **44**, D) **72**, E) **73**, F) **74**, G) **97**, H) **111**, I) **128**

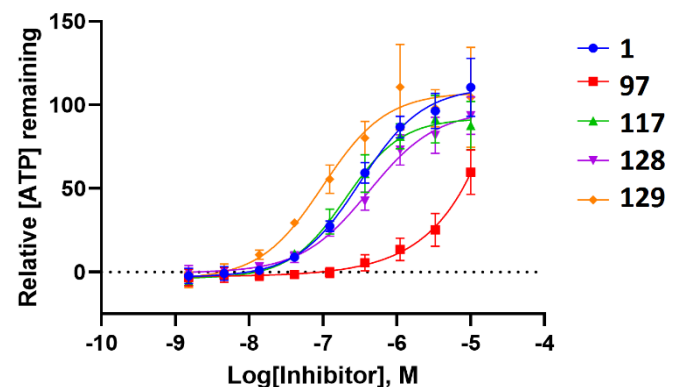
the enzyme assay (**Figure 13** and **Table 13**). The potent TLK2 activities of **97**, **117** and **128** in addition to their narrow spectrum

kinome selectivity makes them attractive starting points for further optimization.

**Table 13.** TLK2 Functional Inhibition Kinase-Glo Results

Name	TLK2 IC <sub>50</sub> (nM)	
	Enzyme	Kinase Glo
<b>1</b>	240	280
<b>97</b>	67	450
<b>117</b>	15	97
<b>128</b>	18	250
<b>129</b>	2700	7800

**Figure 13.** TLK2 Kinase-Glo curves (n=3) for **1**, **97**, **117**, **128**, **129**.





### 3. Discussion

TLK2 represents an attractive target for therapeutic development in a variety of cancer types and in “shock-and-kill” approaches for antiviral therapies. The published TLK2 inhibitors to date only offer compounds with moderate potency and poor kinome selectivity.<sup>18,62-63</sup> In the present study, we demonstrate optimization of a chemotype for increased potency and selectivity for the clinically important TLK2 kinase. Since we achieved selectivity over the closest human paralog, TLK1, this work also provides important tool compounds for better characterization of the specific cellular functions of TLK2.<sup>64-65</sup>

The original target for the oxindole scaffold was receptor tyrosine kinases namely VEGFR and PDGFR.<sup>66</sup> However, the scaffold demonstrated varying affinities for a large portion of the kinome.<sup>20-23</sup> There have been a number of priority cancer targets including TrkA,<sup>67</sup> CDK2,<sup>68-70</sup> PDK1,<sup>71</sup> and Src,<sup>72</sup> among others,<sup>73</sup> all inhibited by the oxindole scaffold. While the primary kinase targets were well defined, the oxindole chemotype has historically been considered as a broad-spectrum inhibitor chemotype. However, a LRRK2 program at Novartis by Troxler *et al.*,<sup>74</sup> suggested that the replacement of fluorine in the 5-position with a methoxy significantly improved kinome wide selectivity with the oxindole scaffold. This was supported by the narrow spectrum of the initial 5-methoxy substituted hit compound SU9516, when compared to the matched pair oxindoles GW5060033X and Sunitinib.<sup>20-23</sup>

The two oxindole matched pairs in the literature (**Figure 1**) demonstrated a tractable affinity to TLK2.<sup>20-23</sup> We found several key structural features that could be tuned within the scaffold including: 1) The electronics of the oxindole head group and the internal hydrogen bond; 2) the electronics and sterics of the amide substitution pattern and 3) formation of the key Lys491 interaction with the amide linker.

The use of conformational restriction has been an effective tool in drug discovery.<sup>75</sup> This methodology has been utilized to orient ATP competitive inhibitors in the preferred conformation. This can be used to not only increase potency, but also to enhance selectivity over other kinases/targets. There are several examples within kinase inhibitor design including Cyclin G-Associated Kinase (GAK),<sup>55,76</sup> Spleen tyrosine kinase (Syk)<sup>77</sup> and Cardiac troponin I-interacting kinase (TNIN3K)<sup>78-79</sup> where addition or removal of a single nitrogen to alter the inhibitor conformation resulted in an increase by 60-160-fold on target.<sup>80</sup> Another method employed in an EGFR inhibitor program involved fixing the pendent substituents with hydrogen bonds between an alcohol and a carbonyl.<sup>56</sup> There are a number of other non-kinase examples including the development of a human histamine H4 receptor (hH4R) inhibitor agonist,<sup>81</sup> and design of a selective CB2 cannabinoid receptor agonist.<sup>82</sup>

The adding or removing of a nitrogen has been proven to have a significant effect on activities across different systems, not only by altered conformation, but also in reduced de-solvation energy potential and as a hydrogen bond donor/acceptor.<sup>76</sup> The oxindole scaffold has multiple potential contact points within the TLK2 ATP binding site. However, we found that that the most crucial nitrogen was on the pendant head group contained within the pyrrole/imidazole and formed not only an interaction at the hinge with Glu548 but also, an internal hydrogen bond with the carbonyl of the oxindole. This internal hydrogen bond pre-organizes the orientation of the molecule as an optimal ATP memetic (**Figure 14**). The solvent exposed shell is a key modulator of activity, with differing profiles depending on the nitrogen location on the ‘head group’ 5-member ring. We can rationally explain these differences by modelling the first water network solvent shell.<sup>55,84-85</sup> Comparing **Figure 14D** to **Figure 14E-F** using WaterMap, both imidazoles are able to coordinate using the second nitrogen, while the pyrrole is not leading to a 10-20 fold drop in potency on TLK2.

**Table 8.** Toxicity profiling of different oxygen substituted anilines based on the scaffold of analogue **72** (**101-112**).<sup>a,b</sup>

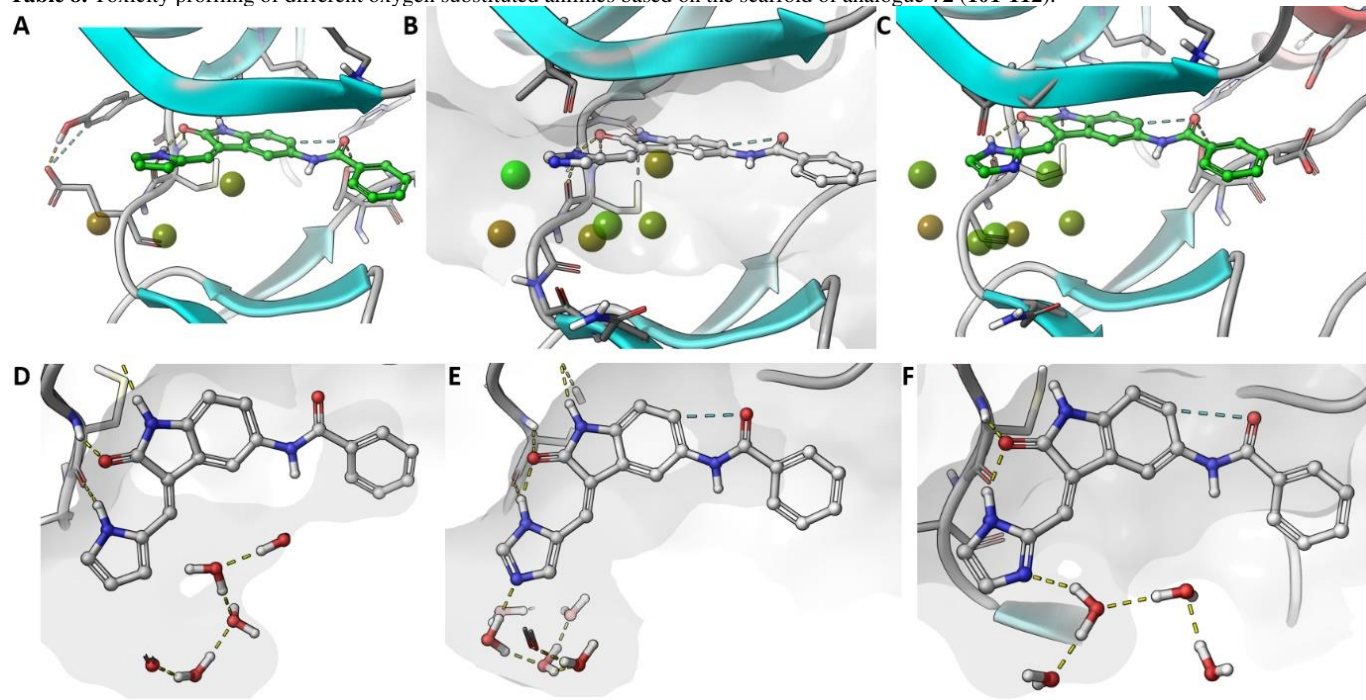


**Figure 14.** Representative oxindoles with three key head groups showing first shell solvent front interactions using WaterMap A) **72**, B) **73**, C) **74**, D) **72**, E) **73** and F) **74** in TLK2 (PDB: 5O0Y). Waters are presented with two different representations balls A-C (green - low energy and red - higher energy) and full formulae D-F.

In addition to the conformation and head group nitrogen and oxindole hinge interactions our modelling highlights that to

achieve a high affinity compound, a favourable fit into the hydrophobic back pocket is required. The key hydrogen bond

interaction to the catalytic lysine (Lys491) affords a considerable boost in potency. The challenge then is to maintain selectivity across the kinome, this is achieved in part by a series of cationic- $\pi$  interactions also donated by Lys491, but also favourable fine-tuned  $\pi$ - $\pi$  stacking interactions. This is demonstrated with a highlighted section of the 5-position substitution and the possibility to form a cationic- $\pi$  interaction with Lys491. The small molecule crystal structures (**Figure 4** & **Table S10**) support the theoretical observations with the TLK2 ATP binding site.

## Conclusions

Oxindole based inhibitors are often considered to be promiscuous across the kinome, this mainly derived from several well-known broad-spectrum inhibitors including sunitinib and GW506033X.<sup>86</sup> Here we demonstrate fine-tuning and optimisation to derive a narrow spectrum oxindole based TLK2 inhibitor, utilizing cutting edge modelling to prospectively design inhibitors. The result was compound **126** and **128** that were 10 to 15-fold more potent than the starting point **1** with maintenance of kinome selectivity and selectivity over the sub-family member TLK1. The QSAR and water network modelling provided new insights into the development of selective chemical probes for TLK2 and beyond. The comprehensive data sets also afford a more complete level of knowledge of the oxindole previously unavailable to the medicinal chemist's toolbox.

## Experimental

### Molecular Modelling

Ligand preparation: Structures of small molecules were parametrized and minimized using the LigPrep module of Schrodinger 2019-4 suite employing OPLS3e force field.

Protein preparation: The TLK2 kinase a crystal structure (PDB:5O0Y) co-crystallized with substrate analog (phosphothiothiophosphoric acid-adenylate ester) was downloaded from RCSB-databanks. The structure was H-bond optimized and minimized using standard protein preparation procedure of Schrödinger suite.

TLK2 Molecular docking: The ligand docking was performed using SP settings of Schrodinger docking protocol with softened vdW potential (scaling 0.6). The initial docking of resulted quite poor convergence, thus oxindole-indole scaffold can bind in several conformations. To ensure correct docking mode of the oxindole (2-indolone) scaffold to kinase folds was confirmed using LPDB module of the Schrödinger package and oxindole as a query. After visual inspection of PDB:2X2K, 2X2M, 4QMO and 1PF8. To further improve convergence of docking poses a hydrogen bond constraint to mainchain NH of hinge residue was required, as experimentally observed in the case of other oxindole containing scaffolds (NH of C507 in the case of TLK2). The grid box was centered using coordinate center of the core structure of corresponding x-ray ligand as template. Graphical illustrations were generated using Maestro software of Schrödinger. Flexible ligand alignments were performed using a Bemis-Mucko method, enabling recognition of the largest common scaffolds using a favorable docking pose of structurally representative derivative as alignment template (**73**). Torsion angles of larger substituents, such as methoxy groups, were manually adjusted to fit template structures when needed.

TLK2 3D-QSAR model: The model for the TLK2 kinase was constructed using the field based QSAR functionality of Schrödinger Maestro 2019-4. The models were constructed by

defining 80% of compounds randomly as training sets and rest of the compounds were considered as test set. Grid spacing of 1.0 Å extended 3.0 beyond training set limits was used to calculate field values. Subsequently, predicted versus measured affinities were plotted to identify outliers. The statistical metrics of models: R-square values with four PLS components were 0.79. The model shows acceptable internal predictivity (Q-square value 0.70), determined by leave-one-out (LOO) cross-validation. Stability value above 0.9 with four partial least squares regression (PLS) components let us to suggest that the quality and predictivity of the model inside the studied applicability domain was robust.

### Crystallography

Each compound had a suitable crystal was selected and mounted on a MITIGEN holder (MiTeGen, Ithaca, NY, USA) in perfluoroether oil on a Rigaku FRE+ diffractometer equipped with a Mo target, VHF Varimax confocal mirrors, an AFC12 goniometer and HyPix 6000 detector (**1**, **2**, **15**, **19**, **72** and **74**) or a Rigaku 007HF diffractometer equipped with a Cu target, HF Varimax confocal mirrors, an AFC11 goniometer and HyPix 6000 detector (**15**, **74**). The crystal was kept at a steady  $T = 100(2)$  K during data collection. CrysAlisPro<sup>87</sup> was used to record images, process all data and apply empirical absorption corrections. Unit cell parameters were refined against all data. The structures were solved by the ShelXT<sup>88</sup> structure solution program using the dual methods solution method and using Olex2<sup>89</sup> as the graphical interface. The models were refined with version 2018/3 of ShelXL<sup>88</sup> using full matrix least squares minimization on  $F^2$  minimization. All non-hydrogen atoms were refined anisotropically. Hydrogen atom positions were calculated geometrically and refined using the riding model, except for those bonded to N-atoms which were located in the difference map and refined with a riding model. Structure **72** crystallised as an ethanol solvate. The data for **72** were processed as a 2-component non-merohedral twin (rotation (UB1, UB2) = 179.9982° around [0.00 0.71 0.71] (reciprocal) or [-0.39 0.85 0.35] (direct) lattice vectors). CCDC deposit numbers: 2309069-2309077, see supporting information.

## Chemistry

### General chemistry

All reactions were performed using flame-dried round-bottomed flasks or reaction vessels. Where appropriate, reactions were carried out under an inert atmosphere of nitrogen with dry solvents, unless otherwise stated. Yields refer to chromatographically and spectroscopically pure isolated yields. Reagents were purchased at the highest commercial quality and used without further purification. Reactions were monitored by thin-layer chromatography carried out on 0.25-mm. Merck silica gel plates (60F<sub>254</sub>) using ultraviolet light as a visualizing agent. NMR spectra were recorded on a Varian Inova 400 (Varian, Palo Alto, CA, USA) or Inova 500 spectrometer (Varian, Palo Alto, CA, USA) and calibrated using residual undeuterated solvent as an internal reference (CDCl<sub>3</sub>: <sup>1</sup>H NMR = 7.26, <sup>13</sup>C NMR = 77.16). The following abbreviations or combinations thereof were used to explain the multiplicities observed: s = singlet, d = doublet, t = triplet, q = quartet, m = multiplet, br = broad. Liquid chromatography (LC) and high resolution mass spectra (HRMS) were recorded on a ThermoFisher hybrid LTQ FT (ICR 7T) (ThermoFisher, Waltham, MA USA). Compound spectra of **1-129** and mass spectrometry method are included in the Supplementary Materials. All compounds were >98% pure by <sup>1</sup>H/<sup>13</sup>C NMR and LCMS.

**3-[(3,5-Dimethyl-1H-pyrrol-2-yl)methylene]-1,3-dihydro-2H-indol-2-one** (SU5416/Semaxanib) (**10**) was consistent with commercial product and previous report.<sup>90</sup> **2-oxoindoline-5-sulfonyl chloride** (**49**) was prepared consistent with previous report.<sup>45</sup> **5-isopropoxyindolin-2-one** (**56**) was prepared consistent with previous report.<sup>74</sup>

## General Procedures

### Procedure A. Knoevenagel condensation

The oxindole (1.0 equiv), aldehyde (1.1 equiv), piperidine (2.4 equiv) were suspended in ethanol at reflux overnight. The solvent was removed and the resulting solid re-suspended DCM/EtOAc 1/1 and flushed through a plug of silica (DCM/EtOAc 1/1). The product was purified by silica gel flash column chromatography (hexane:EtOAc) to afford the title compound.

### Procedure B. Friedel-Crafts acylation

To a suspension of AlCl<sub>3</sub> (6.0 equiv) in CH<sub>2</sub>Cl<sub>2</sub> was added the appropriate acyl chloride (3.0 equiv) and the slurry was stirred at room temperature for 30 min, followed by the addition of oxindole (1.0 equiv) in CH<sub>2</sub>Cl<sub>2</sub>. The resulting mixture was stirred at room temperature for 2 days. Upon completion, the solution was cooled to 0 °C before quenching the reaction with ice/water, followed extraction of the organics with CH<sub>2</sub>Cl<sub>2</sub>. The combined organics were washed with saturated solution of NaHCO<sub>3</sub>, dried over Na<sub>2</sub>SO<sub>3</sub> and the solvent was removed by rotary evaporation before purification by silica gel flash column chromatography (cyclohexane:EtOAc 9:1 to 1:1) to afford the title compound.

### Procedure C. Friedel-Crafts acylation

The appropriate acyl chloride (3.0 equiv) was added to grinded AlCl<sub>3</sub> (5.0 equiv) and the slurry was heated to 150 °C, then oxindole (1.0 equiv) was added portionwise. The resulting mixture was heated at 185 °C for 5 min. Upon completion, the mixture was cooled to 0 °C and was quenched with ice/water. The acylated product precipitated and was collected by filtration. Purification by silica gel flash column chromatography (cyclohexane:EtOAc 9:1 to 1:1) afforded the title compound.

### General Procedure D. Sulphonamide coupling

To a solution of 2-oxoindoline-5-sulfonyl chloride (1.0 equiv) in THF the corresponding amine (1.1 equiv) and DIPEA (3.0 equiv) at room temperature, and the resulting mixture was stirred for 18 h at room temperature. Upon completion, the mixture was diluted with EtOAc and saturated solution of NaHCO<sub>3</sub> and layers were separated. The organics were further extracted from the aqueous with EtOAc and the combined organics were washed with brine, dried over Na<sub>2</sub>SO<sub>4</sub>, filtered and the solvent was removed by rotary evaporation. Purification by silica gel flash column chromatography (hexane:EtOAc or CH<sub>2</sub>Cl<sub>2</sub>:MeOH mixtures) afforded the desired compound.

### General Procedure E. Mitsunobu reaction

A dry three-neck flask was charged with 5-hydroxyindolin-2-one (1.0 equiv), PPh<sub>3</sub> (1.4 equiv) and the appropriate alcohol (1.4 equiv) in anhydrous THF (0.25M). The solution was cooled to 0 °C and diethyl azodicarboxylate (1.4 equiv) in PhMe was added dropwise. The resulting mixture was warmed to room temperature and stirred for 18 h. Upon completion, the solvent reduced *in vacuo*, before purification by silica gel flash column chromatography (hexane:EtOAc 8:2) to afford the title compound.

### General Procedure F. Amide HATU coupling

To a solution of amine (1.0 equiv) in THF, HATU (1.3 equiv), the corresponding carboxylic acid (1.1 equiv) and DIPEA (3.0 equiv) at room temperature, and the resulting mixture was stirred for 18 h at room temperature. Upon completion, the mixture was diluted with EtOAc and saturated solution of NaHCO<sub>3</sub> and layers were separated. The organics were further extracted from the aqueous with EtOAc and the combined organics were washed with brine, dried over Na<sub>2</sub>SO<sub>4</sub>, filtered and the solvent reduced *in vacuo*. Purification by silica gel flash column chromatography (hexane:EtOAc or CH<sub>2</sub>Cl<sub>2</sub>:MeOH mixtures) afforded the desired compound.

**(3Z)-3-[(1H-imidazol-5-yl)methylidene]-5-methoxy-2,3-dihydro-1H-indol-2-one** (**1**): Compound **1** was prepared by procedure A to afford a purple solid (177 mg, 0.734 mmol, 80%). MP 210-212 °C; <sup>1</sup>H NMR (400 MHz, DMSO-*d*<sub>6</sub>) δ 13.81 (s, 1H), 10.82 (s, 1H), 8.02 (s, 1H), 7.88 (s, 1H), 7.61 (s, 1H), 7.36 – 7.35 (m, 1H), 6.80 – 6.76 (m, 2H), 3.76 (s, 3H). HRMS *m/z* [M+H]<sup>+</sup> calcd for C<sub>13</sub>H<sub>12</sub>N<sub>3</sub>O<sub>2</sub>: 242.0930, found 242.0918, LC *t*<sub>R</sub> = 2.94 min, > 98% Purity. Consistent with previous report.<sup>85</sup>

**(3Z)-5-methoxy-3-(1H-pyrrol-2-ylmethylidene)-2,3-dihydro-1H-indol-2-one** (**2**): Compound **2** was prepared by procedure A to afford a dark orange solid (168 mg, 0.699 mmol, 76%). MP 220-222 °C; <sup>1</sup>H NMR (400 MHz, DMSO-*d*<sub>6</sub>) δ 13.16 (s, 1H), 10.84 (s, 1H), 7.56 (s, 1H), 7.52 (d, *J* = 8.4 Hz, 1H), 7.29 (q, *J* = 2.3 Hz, 1H), 6.75 (dt, *J* = 3.6, 1.7 Hz, 1H), 6.58 (dd, *J* = 8.4, 2.3 Hz, 1H), 6.45 (d, *J* = 2.3 Hz, 1H), 6.34 – 6.29 (m, 1H), 3.76 (s, 3H). <sup>13</sup>C NMR (100 MHz, DMSO-*d*<sub>6</sub>) δ 169.8, 159.3, 140.3, 129.6, 124.7, 124.2, 119.6, 119.1, 117.9, 117.1, 111.1, 107.0, 96.1, 55.3. HRMS *m/z* [M+H]<sup>+</sup> calcd for C<sub>14</sub>H<sub>13</sub>N<sub>2</sub>O<sub>2</sub>: 241.0977, found 241.0961, LC *t*<sub>R</sub> = 4.38 min, > 98% Purity.

**(3Z)-3-[(3,5-dimethyl-1H-pyrrol-2-yl)methylidene]-5-methoxy-2,3-dihydro-1H-indol-2-one** (**3**): Compound **3** was prepared by procedure A to afford a red solid (200 mg, 0.745 mmol, 81%). MP 231-233 °C; <sup>1</sup>H NMR (400 MHz, DMSO-*d*<sub>6</sub>) δ 13.45 (s, 1H), 10.57 (s, 1H), 7.58 (s, 1H), 7.40 (d, *J* = 2.4 Hz, 1H), 6.76 (d, *J* = 8.4 Hz, 1H), 6.67 (dd, *J* = 8.4, 2.4 Hz, 1H), 5.99 (d, *J* = 2.5 Hz, 1H), 3.77 (s, 3H), 2.31 (s, 6H). <sup>13</sup>C NMR (100 MHz, DMSO-*d*<sub>6</sub>) δ 169.5, 154.8, 135.6, 132.0, 131.6, 126.9, 126.6, 123.7, 113.3, 112.5, 111.9, 109.6, 104.1, 55.6, 13.5, 11.4. HRMS *m/z* [M+H]<sup>+</sup> calcd for C<sub>16</sub>H<sub>17</sub>N<sub>2</sub>O<sub>2</sub>: 269.1290, found 269.1282, LC *t*<sub>R</sub> = 4.79 min, > 98% Purity.

**(3Z)-5-methoxy-3-(1H-pyrazol-5-ylmethylidene)-2,3-dihydro-1H-indol-2-one** (**4**): Compound **4** was prepared by procedure A to afford a red solid (160 mg, 0.663 mmol, 72%). MP 192-194 °C; <sup>1</sup>H NMR (400 MHz, DMSO-*d*<sub>6</sub>) δ 10.93 (s, 1H), 7.87 (s, 2H), 7.73 (s, 1H), 7.40 (d, *J* = 2.2 Hz, 1H), 6.86 – 6.77 (m, 3H), 3.77 (s, 3H). <sup>13</sup>C NMR (100 MHz, DMSO-*d*<sub>6</sub>) δ 170.0, 154.8, 136.6, 134.5, 130.3, 126.0, 123.2, 114.9, 113.6, 111.0, 109.8, 106.3, 55.9. HRMS *m/z* [M+H]<sup>+</sup> calcd for C<sub>13</sub>H<sub>12</sub>N<sub>3</sub>O<sub>2</sub>: 242.0930, found 242.0920, LC *t*<sub>R</sub> = 3.85 min, > 98% Purity.

**(3Z)-3-(1H-imidazol-2-ylmethylidene)-5-methoxy-2,3-dihydro-1H-indol-2-one** (**5**): Compound **5** was prepared by procedure A to afford a red solid (164 mg, 0.680 mmol, 74%). MP >300 °C; <sup>1</sup>H NMR (400 MHz, DMSO-*d*<sub>6</sub>) δ 10.97 (s, 1H), 7.86 (s, 1H), 7.55 (t, *J* = 1.5 Hz, 2H), 7.34 (d, *J* = 1.2 Hz, 1H), 6.82 (d, *J* = 1.4 Hz, 2H), 3.77 (s, 3H). <sup>13</sup>C NMR (100 MHz, DMSO-*d*<sub>6</sub>) δ 168.9, 155.2, 143.7, 133.7, 132.6, 125.0, 124.7, 124.1, 120.6, 115.1, 110.5, 106.0, 55.6. HRMS *m/z* [M+H]<sup>+</sup> calcd for C<sub>13</sub>H<sub>12</sub>N<sub>3</sub>O<sub>2</sub>: 242.0930, found 242.0917, LC *t*<sub>R</sub> = 2.80 min, > 98% Purity.



**(3Z)-5-methoxy-3-(pyridin-2-ylmethylidene)-2,3-dihydro-1H-indol-2-one (6):** Compound **6** was prepared by procedure A to afford a dark red solid (176 mg, 0.698 mmol, 76%). MP 176-178 °C; <sup>1</sup>H NMR (400 MHz, DMSO-*d*<sub>6</sub>) δ 10.42 (s, 1H), 8.96 – 8.86 (m, 1H), 8.82 (d, *J* = 2.7 Hz, 1H), 7.96 (td, *J* = 7.6, 1.8 Hz, 1H), 7.88 (dt, *J* = 7.8, 1.1 Hz, 1H), 7.56 (s, 1H), 7.47 (ddd, *J* = 7.6, 4.7, 1.2 Hz, 1H), 6.88 (dd, *J* = 8.4, 2.7 Hz, 1H), 6.77 (d, *J* = 8.4 Hz, 1H), 3.77 (s, 3H). <sup>13</sup>C NMR (100 MHz, DMSO-*d*<sub>6</sub>) δ 169.3, 154.2, 153.2, 149.6, 137.3, 137.3, 133.7, 129.9, 128.6, 124.2, 122.3, 116.3, 114.0, 109.8, 55.3. HRMS *m/z* [M+H]<sup>+</sup> calcd for C<sub>15</sub>H<sub>13</sub>N<sub>2</sub>O<sub>2</sub>: 253.0977, found 253.0966, LC *t*<sub>R</sub> = 3.88 min, > 98% Purity.

**(3Z)-5-methoxy-3-(pyridin-3-ylmethylidene)-2,3-dihydro-1H-indol-2-one (7):** Compound **7** was prepared by procedure A to afford a red solid (104 mg, 0.412 mmol, 45%, ratio of E:Z - 50:50). MP 206-208 °C; (Z)-5-Methoxy-3-(pyridin-3-ylmethylene)indolin-2-one. <sup>1</sup>H NMR (500 MHz, DMSO-*d*<sub>6</sub>) δ 10.5 (d, *J* = 6.0 Hz, 1H), 9.19 (dd, *J* = 1.8, 1.1 Hz, 1H), 8.91 (dddd, *J* = 8.1, 2.3, 1.6, 0.6 Hz, 1H), 8.58 (dd, *J* = 4.8, 1.7 Hz, 1H), 7.84 (s, 1H), 7.49 (ddd, *J* = 8.0, 4.9, 0.9 Hz, 1H), 7.41 (d, *J* = 2.5 Hz, 1H), 6.82 (dd, *J* = 8.4, 2.5 Hz, 1H), 6.74 (dd, *J* = 8.4, 0.5 Hz, 1H), 3.77 (s, 3H). <sup>13</sup>C NMR (125 MHz, DMSO-*d*<sub>6</sub>) δ 167.1, 154.7, 152.4, 150.3, 137.9, 134.9, 133.0, 129.9, 129.3, 125.3, 123.2, 115.4, 110.1, 106.3, 55.6. (E)-5-Methoxy-3-(pyridin-3-ylmethylene)indolin-2-one. <sup>1</sup>H NMR (500 MHz, DMSO-*d*<sub>6</sub>) δ 10.5 (d, *J* = 6.0 Hz, 2H), 8.862 – 8.857 (m, 1H), 8.65 (ddd, *J* = 4.9, 1.7, 0.6 Hz, 1H), 8.12 (dddd, *J* = 7.9, 2.4, 1.7, 0.8 Hz, 1H), 7.62 (s, 1H), 7.56 (ddd, *J* = 7.9, 4.7, 0.5 Hz, 1H), 6.89 – 6.89 (m, 1H), 6.86 (dd, *J* = 8.4, 2.5 Hz, 1H), 6.80 (dd, *J* = 8.4, 0.5 Hz, 1H), 3.60 (s, 3H). <sup>13</sup>C NMR (125 MHz, DMSO-*d*<sub>6</sub>) δ 168.1, 154.0, 150.2, 149.7, 136.9, 136.3, 132.3, 130.5, 129.9, 123.6, 121.4, 115.6, 110.7, 108.9, 55.3. HRMS *m/z* [M+H]<sup>+</sup> calcd for C<sub>15</sub>H<sub>13</sub>N<sub>2</sub>O<sub>2</sub>: 253.0977, found 253.0966, LC *t*<sub>R</sub> = 3.10 min, > 98% Purity.

**(3Z)-3-(1H-pyrazol-5-ylmethylidene)-2,3-dihydro-1H-indol-2-one (8):** Compound **8** was prepared by procedure A to afford a bright yellow solid (156 mg, 0.739 mmol, 49%, ratio of E:Z - 33:67). MP 249-251 °C; (Z)-3-((1H-Pyrazol-5-yl)methylene)indolin-2-one. <sup>1</sup>H NMR (600 MHz, DMSO-*d*<sub>6</sub>) δ 10.39 (bs, 1H), 9.31 (d, *J* = 7.6 Hz, 1H), 8.00 (s, 1H), 7.90 (s, 1H), 7.47 (s, 1H), 7.16 (td, *J* = 7.6, 1.4 Hz, 1H), 6.96 (td, *J* = 7.6, 1.1 Hz, 1H), 6.82 (d, *J* = 8.5 Hz, 1H). <sup>13</sup>C NMR (125 MHz, DMSO-*d*<sub>6</sub>) δ 169.9, 141.5, 138.1, 137.0, 128.2, 126.9, 126.4, 126.1, 122.6, 121.28, 120.6, 108.7. (E)-3-((1H-Pyrazol-5-yl)methylene)indolin-2-one. <sup>1</sup>H NMR (600 MHz, DMSO-*d*<sub>6</sub>) δ 7.99 (s, 1H), 7.83 (s, 1H), 7.66 (d, *J* = 6.9 Hz, 1H), 7.21–7.15 (m, 1H), 7.01 (td, *J* = 7.6, 1.0 Hz, 1H), 6.89 (d, *J* = 7.7 Hz, 1H). <sup>13</sup>C NMR (125 MHz, DMSO-*d*<sub>6</sub>) δ 168.6, 139.8, 139.0, 138.1, 127.9, 124.3, 123.9, 121.3, 120.6, 120.2, 119.2, 109.5. HRMS *m/z* [M+H]<sup>+</sup> calcd for C<sub>12</sub>H<sub>10</sub>N<sub>3</sub>O: 212.0824, found 212.0814, LC *t*<sub>R</sub> = 2.82 min, > 98% Purity.

**(3Z)-3-(1H-pyrrol-2-ylmethylidene)-2,3-dihydro-1H-indol-2-one (9):** Compound **9** was prepared by procedure A to afford a dark orange solid (159 mg, 0.756 mmol, 67%). MP 218-220 °C; <sup>1</sup>H NMR (400 MHz, DMSO-*d*<sub>6</sub>) δ 13.34 (s, 1H), 10.89 (s, 1H), 7.74 (s, 1H), 7.63 (dt, *J* = 7.4, 0.9 Hz, 1H), 7.35 (td, *J* = 2.6, 1.4 Hz, 1H), 7.15 (td, *J* = 7.6, 1.2 Hz, 1H), 6.99 (td, *J* = 7.6, 1.1 Hz, 1H), 6.88 (dt, *J* = 7.8, 0.9 Hz, 1H), 6.83 (dt, *J* = 3.6, 1.7 Hz, 1H), 6.35 (dt, *J* = 3.7, 2.3 Hz, 1H). <sup>13</sup>C NMR (100 MHz, DMSO-*d*<sub>6</sub>) δ 169.2, 139.0, 129.6, 126.9, 126.3, 125.6, 125.2, 121.2, 120.3, 118.5, 116.8, 111.4, 109.5. HRMS *m/z* [M+H]<sup>+</sup> calcd for C<sub>13</sub>H<sub>11</sub>N<sub>2</sub>O: 211.0871, found 211.0865, LC *t*<sub>R</sub> = 4.47 min, > 98% Purity.

**(3Z)-3-(1H-pyrazol-5-ylmethylidene)-2,3-dihydro-1H-indol-2-one (11):** Compound **11** was prepared by procedure A to afford an orange solid (90 mg, 0.426 mmol, 38%). MP 190-192 °C; <sup>1</sup>H NMR (600 MHz, DMSO-*d*<sub>6</sub>) δ 13.56 (s, 1H), 10.52 (s, 1H), 7.94 (s, 1H), 7.72 (d, *J* = 7.5 Hz, 1H), 7.48 (s, 1H), 7.27 – 7.24 (m, 1H), 7.00 (td, *J* = 7.6, 1.1 Hz, 1H), 6.87 (d, *J* = 7.7 Hz, 1H), 6.85 – 6.80 (m, 1H). <sup>13</sup>C NMR (150 MHz, DMSO-*d*<sub>6</sub>) δ 169.5, 146.3, 142.5, 140.4, 129.7, 126.2, 125.8, 125.0, 121.9, 121.0, 110.6, 109.4. HRMS *m/z* [M+H]<sup>+</sup> calcd for C<sub>12</sub>H<sub>10</sub>N<sub>3</sub>O: 212.0824, found 212.0812, LC *t*<sub>R</sub> = 3.85 min, > 98% Purity.

**(3Z)-3-(1H-imidazol-2-ylmethylidene)-2,3-dihydro-1H-indol-2-one (12):** Compound **12** was prepared by procedure A to afford a bright yellow solid (195 mg, 0.923 mmol, 82% ratio of E:Z - 40:60 - not able to clearly distinguish E/Z isomers). MP >300 °C; Major diastereoisomer. 3-((1H-Imidazol-2-yl)methylene)indolin-2-one. <sup>1</sup>H NMR (600 MHz, DMSO-*d*<sub>6</sub>) δ 10.52 (s, 1H), 9.40 (dd, *J* = 7.7, 1.3 Hz, 1H), 7.45 (s, 2H), 7.39 (s, 1H), 7.24 – 7.22 (m, 1H), 7.00 (td, *J* = 7.6, 1.1 Hz, 1H), 6.85 (d, *J* = 7.7 Hz, 1H). <sup>13</sup>C NMR (150 MHz, DMSO-*d*<sub>6</sub>) δ 169.6, 143.4, 142.4, 129.6, 128.9, 127.1, 124.3, 121.8, 121.0, 120.9, 120.2, 109.1. Minor diastereoisomer. 3-((1H-Imidazol-2-yl)methylene)indolin-2-one. <sup>1</sup>H NMR (600 MHz, DMSO-*d*<sub>6</sub>) δ 14.10 (s, 1H), 7.83 (d, *J* = 7.4 Hz, 1H), 7.80 (s, 1H), 7.55 (bs, 1H), 7.34 (s, 1H), 7.26 – 7.23 (m, 1H), 7.03 (td, *J* = 7.6, 1.0 Hz, 1H), 6.92 (d, *J* = 7.8 Hz, 1H). <sup>13</sup>C NMR (150 MHz, DMSO-*d*<sub>6</sub>) δ 168.9, 143.7, 140.1, 132.5, 127.1, 124.4, 124.0, 123.7, 122.0, 121.0, 120.7, 110.0. HRMS *m/z* [M+H]<sup>+</sup> calcd for C<sub>12</sub>H<sub>10</sub>N<sub>3</sub>O: 212.0824, found 212.0813, LC *t*<sub>R</sub> = 2.60 min, > 98% Purity.

**(3Z)-3-(pyridin-2-ylmethylidene)-2,3-dihydro-1H-indol-2-one (13):** Compound **13** was prepared by procedure A to afford a dark orange solid (160 mg, 0.720 mmol, 64%). MP 191-193 °C; <sup>1</sup>H NMR (400 MHz, DMSO-*d*<sub>6</sub>) δ 10.62 (s, 1H), 9.03 – 8.97 (m, 1H), 8.88 (ddd, *J* = 4.8, 1.8, 0.8 Hz, 1H), 7.94 (td, *J* = 7.7, 1.8 Hz, 1H), 7.86 (dt, *J* = 7.9, 1.1 Hz, 1H), 7.57 (s, 1H), 7.46 (ddd, *J* = 7.5, 4.7, 1.2 Hz, 1H), 7.28 (td, *J* = 7.7, 1.3 Hz, 1H), 6.98 (td, *J* = 7.7, 1.1 Hz, 1H), 6.87 (dt, *J* = 7.7, 0.9 Hz, 1H). <sup>13</sup>C NMR (100 MHz, DMSO-*d*<sub>6</sub>) δ 169.3, 153.2, 149.7, 143.6, 137.2, 133.7, 130.8, 129.3, 128.4, 127.9, 124.1, 121.5, 121.2, 109.6. HRMS *m/z* [M+H]<sup>+</sup> calcd for C<sub>14</sub>H<sub>11</sub>N<sub>2</sub>O: 223.0871, found 223.0860, LC *t*<sub>R</sub> = 3.85 min, > 98% Purity.

**(3Z)-3-(pyridin-3-ylmethylidene)-2,3-dihydro-1H-indol-2-one (14):** Compound **14** was prepared by procedure A to afford a light yellow solid (45 mg, 0.203 mmol, 18%). MP 155-157 °C; <sup>1</sup>H NMR (400 MHz, DMSO-*d*<sub>6</sub>) δ 10.66 (s, 1H), 8.87 (dt, *J* = 1.9, 0.9 Hz, 1H), 8.65 (dd, *J* = 4.9, 1.6 Hz, 1H), 8.12 (dddd, *J* = 7.9, 2.4, 1.7, 0.8 Hz, 1H), 7.62 (s, 1H), 7.55 (ddd, *J* = 7.9, 4.8, 0.9 Hz, 1H), 7.37 (dd, *J* = 7.8, 1.1 Hz, 1H), 7.27 – 7.23 (m, 1H), 6.91 – 6.85 (m, 2H). <sup>13</sup>C NMR (100 MHz, DMSO-*d*<sub>6</sub>) δ 168.1, 150.1, 149.8, 143.2, 136.4, 132.1, 130.6, 130.6, 129.4, 123.7, 122.3, 121.3, 120.6, 110.3. HRMS *m/z* [M+H]<sup>+</sup> calcd for C<sub>14</sub>H<sub>11</sub>N<sub>2</sub>O: 223.0871, found 223.0861, LC *t*<sub>R</sub> = 2.60 min, > 98% Purity.

**(3Z)-6-methoxy-3-(1H-pyrrol-2-ylmethylidene)-2,3-dihydro-1H-indol-2-one (15):** Compound **15** was prepared by procedure A to afford an orange solid (137 mg, 0.570 mmol, 62%). MP 225-226 °C; <sup>1</sup>H NMR (400 MHz, DMSO-*d*<sub>6</sub>) δ 13.16 (s, 1H), 10.84 (s, 1H), 7.56 (s, 1H), 7.52 (d, *J* = 8.4 Hz, 1H), 7.29 (td, *J* = 2.6, 1.4 Hz, 1H), 6.75 (dt, *J* = 3.6, 1.7 Hz, 1H), 6.58 (dd, *J* = 8.4, 2.3 Hz, 1H), 6.45 (d, *J* = 2.3 Hz, 1H), 6.32 (dt, *J* = 3.7, 2.4 Hz, 1H), 3.76 (s, 3H). <sup>13</sup>C NMR (100 MHz, DMSO-*d*<sub>6</sub>) δ 169.8, 159.3, 140.3, 129.6, 124.7, 124.2, 119.6, 119.1, 117.9, 117.1, 111.1, 107.0, 96.1, 55.3. HRMS *m/z* [M+H]<sup>+</sup> calcd for C<sub>14</sub>H<sub>13</sub>N<sub>2</sub>O<sub>2</sub>: 241.0977, found 241.0962, LC *t*<sub>R</sub> = 4.41 min, > 98% Purity.



**(3Z)-3-[(3,5-dimethyl-1H-pyrrol-2-yl)methylidene]-6-methoxy-2,3-dihydro-1H-indol-2-one (16):** Compound **16** was prepared by procedure A to afford an orange solid (200 mg, 0.745 mmol, 81%). MP 231-233 °C; <sup>1</sup>H NMR (400 MHz, DMSO-*d*<sub>6</sub>) δ 13.14 (s, 1H), 10.72 (s, 1H), 7.60 (d, *J* = 8.4 Hz, 1H), 7.40 (s, 1H), 6.56 (dd, *J* = 8.4, 2.3 Hz, 1H), 6.45 (d, *J* = 2.3 Hz, 1H), 5.96 (d, *J* = 2.5 Hz, 1H), 3.75 (s, 3H), 2.30 (s, 3H), 2.27 (s, 3H). <sup>13</sup>C NMR (100 MHz, DMSO-*d*<sub>6</sub>) δ 169.9, 158.5, 139.4, 134.4, 130.1, 126.5, 121.6, 119.1, 118.6, 113.1, 112.0, 106.7, 95.8, 55.2, 13.5, 11.3. HRMS *m/z* [M+H]<sup>+</sup> calcd for C<sub>16</sub>H<sub>17</sub>N<sub>2</sub>O<sub>2</sub>: 269.1290, found 269.1272, LC *t*<sub>R</sub> = 4.67 min, > 98% Purity.

**(3Z)-6-methoxy-3-(1H-pyrazol-5-ylmethylidene)-2,3-dihydro-1H-indol-2-one (17):** Compound **17** was prepared by procedure A to afford an orange solid (189 mg, 0.783 mmol, 85%). MP 209-211 °C; <sup>1</sup>H NMR (400 MHz, DMSO-*d*<sub>6</sub>) δ 11.06 (s, 1H), 7.80 (s, 1H), 7.64 (dd, *J* = 19.1, 8.0 Hz, 3H), 6.85 (s, 1H), 6.62 (d, *J* = 8.4 Hz, 1H), 6.47 (s, 1H), 3.78 (s, 3H). <sup>13</sup>C NMR (100 MHz, DMSO-*d*<sub>6</sub>) δ 169.3, 160.8, 141.8, 140.2, 138.0, 125.0, 121.3, 118.6, 116.5, 110.7, 107.6, 96.5, 55.4. HRMS *m/z* [M+H]<sup>+</sup> calcd for C<sub>13</sub>H<sub>12</sub>N<sub>3</sub>O<sub>2</sub>: 242.0930, found 242.0917, LC *t*<sub>R</sub> = 3.54 min, > 98% Purity.

**(3Z)-3-(1H-imidazol-2-ylmethylidene)-6-methoxy-2,3-dihydro-1H-indol-2-one (18):** Compound **18** was prepared by procedure A to afford an orange solid (126 mg, 0.522 mmol, 57%). MP >300 °C; <sup>1</sup>H NMR (600 MHz, DMSO-*d*<sub>6</sub>) δ 13.94 (s, 1H), 11.33 (s, 1H), 7.73 (d, *J* = 8.4 Hz, 1H), 7.61 (s, 1H), 7.50 (s, 1H), 7.29 (s, 1H), 6.60 (dd, *J* = 8.4, 2.3 Hz, 1H), 6.48 (d, *J* = 2.3 Hz, 1H), 3.78 (s, 3H). <sup>13</sup>C NMR (150 MHz, DMSO-*d*<sub>6</sub>) δ 169.6, 160.6, 143.9, 141.7, 132.0, 123.8, 121.9, 121.5, 120.1, 116.7, 107.5, 96.4, 55.4. HRMS *m/z* [M+H]<sup>+</sup> calcd for C<sub>13</sub>H<sub>12</sub>N<sub>3</sub>O<sub>2</sub>: 242.0930, found 242.0916, LC *t*<sub>R</sub> = 2.82 min, > 98% Purity.

**(3Z)-6-methoxy-3-(pyridin-2-ylmethylidene)-2,3-dihydro-1H-indol-2-one (19):** Compound **19** was prepared by procedure A to afford a mustard solid (151 mg, 0.599 mmol, 65%). MP 182-184 °C; <sup>1</sup>H NMR (400 MHz, DMSO-*d*<sub>6</sub>) δ 10.57 (s, 1H), 8.98 (d, *J* = 8.6 Hz, 1H), 8.89 – 8.78 (m, 1H), 7.92 (td, *J* = 7.7, 1.9 Hz, 1H), 7.81 (dt, *J* = 8.0, 1.1 Hz, 1H), 7.42 (ddd, *J* = 7.6, 4.7, 1.2 Hz, 1H), 7.39 (s, 1H), 6.55 (dd, *J* = 8.7, 2.5 Hz, 1H), 6.42 (d, *J* = 2.4 Hz, 1H), 3.79 (s, 3H). <sup>13</sup>C NMR (100 MHz, DMSO-*d*<sub>6</sub>) δ 170.0, 161.7, 153.6, 149.5, 145.5, 137.1, 130.4, 129.6, 128.9, 128.0, 123.7, 114.6, 106.5, 96.0, 55.3. HRMS *m/z* [M+H]<sup>+</sup> calcd for C<sub>15</sub>H<sub>13</sub>N<sub>2</sub>O<sub>2</sub>: 253.0977, found 253.0970, LC *t*<sub>R</sub> = 3.85 min, > 98% Purity.

**(Z)-6-methoxy-3-(pyridin-3-ylmethylene)indolin-2-one (20)** Compound **20** was prepared by procedure A to afford a mustard solid (93 mg, 0.369 mmol, 40%, ratio of E:Z - 28:72). MP 177-179 °C; (Z)-6-Methoxy-3-(pyridin-3-ylmethylene)indolin-2-one. <sup>1</sup>H NMR (600 MHz, DMSO-*d*<sub>6</sub>) δ 10.73 (bs, 1H), 8.84 (d, *J* = 2.3 Hz, 1H), 8.62 (dd, *J* = 4.9, 1.6 Hz, 1H), 8.08 (dt, *J* = 7.9, 2.1 Hz, 1H), 7.53 (dd, *J* = 7.9, 4.8 Hz, 1H), 7.43 (s, 1H), 7.32 (d, *J* = 8.5 Hz, 1H), 6.45 – 6.42 (m, 2H), 3.75 (s, 3H). <sup>13</sup>C NMR (150 MHz, DMSO-*d*<sub>6</sub>) δ 168.9, 161.5, 149.77, 149.75, 145.1, 136.2, 130.9, 129.0, 128.6, 123.7, 123.1, 113.4, 106.8, 96.7, 55.4. (E)-6-Methoxy-3-(pyridin-3-ylmethylene)indolin-2-one. <sup>1</sup>H NMR (600 MHz, DMSO-*d*<sub>6</sub>) δ 9.13 (d, *J* = 2.2 Hz, 1H), 8.82 (dt, *J* = 8.1, 2.0 Hz, 1H), 8.54 (dd, *J* = 4.8, 1.7 Hz, 1H), 7.62 (s, 1H), 7.62 (d, *J* = 8.1 Hz, 1H), 7.46 (dd, *J* = 8.1, 4.8 Hz, 1H), 6.57 (dd, *J* = 8.4, 2.4 Hz, 1H), 6.40 (d, *J* = 2.3 Hz, 1H), 3.78 (s, 3H). <sup>13</sup>C NMR (150 MHz, DMSO-*d*<sub>6</sub>) δ 167.7, 161.0, 152.1, 149.7, 142.7, 137.5, 130.2, 129.9, 128.6, 123.5, 121.5, 117.1, 106.9, 96.0, 55.4. HRMS *m/z* [M+H]<sup>+</sup> calcd for C<sub>15</sub>H<sub>13</sub>N<sub>2</sub>O<sub>2</sub>: 253.0977, found 253.0965, LC *t*<sub>R</sub> = 2.70 min, > 98% Purity.

**(Z)-3-(1H-imidazol-5-ylmethylidene)-5,6-dimethoxy-2,3-dihydro-1H-indol-2-one (21):** Compound **21** was prepared by procedure A to afford a bright red solid (160 mg, 0.590 mmol, 76%, ratio of E:Z - 50:50). MP 222-224 °C; (Z)-3-((1H-Imidazol-5-yl)methylene)-5,6-dimethoxyindolin-2-one. <sup>1</sup>H NMR (600 MHz, DMSO-*d*<sub>6</sub>) δ 13.71 (bs, 1H), 7.94 (s, 1H), 7.68 (s, 1H), 7.56 (s, 1H), 7.38 (s, 1H), 6.53 (s, 1H), 3.77 (s, 3H), 3.77 (s, 3H). (E)-3-((1H-Imidazol-5-yl)methylene)-5,6-dimethoxyindolin-2-one. <sup>1</sup>H NMR (600 MHz, DMSO-*d*<sub>6</sub>) δ 10.14 (s, 1H), 9.20 (s, 1H), 7.97 (s, 1H), 7.81 (d, *J* = 1.1 Hz, 1H), 7.30 (s, 1H), 6.47 (s, 1H), 3.78 (s, 3H), 3.76 (s, 3H). <sup>13</sup>C NMR (150 MHz, DMSO-*d*<sub>6</sub>) δ 170.6, 150.0, 143.1, 137.9, 136.7, 125.1, 124.3, 122.2, 114.1, 113.1, 104.8, 94.6, 56.5, 55.6. HRMS *m/z* [M+H]<sup>+</sup> calcd for C<sub>14</sub>H<sub>14</sub>N<sub>3</sub>O<sub>3</sub>: 272.1035, found 272.1023, LC *t*<sub>R</sub> = 2.76 min, > 98% Purity.

**(3Z)-5,6-dimethoxy-3-(1H-pyrrol-2-ylmethylidene)-2,3-dihydro-1H-indol-2-one (22):** Compound **22** was prepared by procedure A to afford a bright red solid (93 mg, 0.369 mmol, 40%). MP 167-169 °C; <sup>1</sup>H NMR (400 MHz, DMSO-*d*<sub>6</sub>) δ 13.27 (s, 1H), 10.65 (s, 1H), 7.61 (s, 1H), 7.35 (s, 1H), 7.29 (q, *J* = 2.2 Hz, 1H), 6.73 (dt, *J* = 3.6, 1.7 Hz, 1H), 6.52 (s, 1H), 6.32 (dt, *J* = 4.0, 2.4 Hz, 1H), 3.77 (d, *J* = 2.2 Hz, 6H). <sup>13</sup>C NMR (100 MHz, DMSO-*d*<sub>6</sub>) δ 169.6, 149.1, 144.4, 133.2, 129.7, 124.6, 124.4, 118.9, 117.9, 116.3, 111.1, 104.3, 95.4, 56.3, 55.8. HRMS *m/z* [M+H]<sup>+</sup> calcd for C<sub>15</sub>H<sub>15</sub>N<sub>2</sub>O<sub>3</sub>: 271.1083, found 271.1072, LC *t*<sub>R</sub> = 4.29 min, > 98% Purity.

**(3Z)-3-[(3,5-dimethyl-1H-pyrrol-2-yl)methylidene]-5,6-dimethoxy-2,3-dihydro-1H-indol-2-one (23):** Compound **23** was prepared by procedure A to afford a dark red solid (167 mg, 0.560 mmol, 72%). MP 282-285 °C; <sup>1</sup>H NMR (400 MHz, DMSO-*d*<sub>6</sub>) δ 13.28 (s, 1H), 10.53 (s, 1H), 7.45 (s, 1H), 7.42 (s, 1H), 6.51 (s, 1H), 5.96 (d, *J* = 2.5 Hz, 1H), 3.78 (s, 3H), 3.75 (s, 3H), 2.30 (s, 6H). <sup>13</sup>C NMR (100 MHz, DMSO-*d*<sub>6</sub>) δ 169.7, 148.4, 144.3, 134.3, 132.3, 130.1, 126.6, 121.9, 117.2, 114.0, 112.0, 104.3, 95.3, 56.6, 55.8, 13.5, 11.4. HRMS *m/z* [M+H]<sup>+</sup> calcd for C<sub>22</sub>H<sub>13</sub>N<sub>4</sub>O: 349.1089, found 349.1088, LC *t*<sub>R</sub> = 4.61 min, > 98% Purity.

**(3Z)-5,6-dimethoxy-3-(1H-pyrazol-5-ylmethylidene)-2,3-dihydro-1H-indol-2-one (24):** Compound **24** was prepared by procedure A to afford a dark red solid (160 mg, 0.590 mmol, 76%). MP 230-232 °C; <sup>1</sup>H NMR (400 MHz, DMSO-*d*<sub>6</sub>) δ 13.49 (s, 1H), 10.26 (s, 1H), 8.85 (s, 1H), 7.89 (d, *J* = 2.3 Hz, 1H), 7.29 (s, 1H), 6.75 (d, *J* = 2.3 Hz, 1H), 6.51 (s, 1H), 3.80 (s, 3H), 3.77 (s, 3H). <sup>13</sup>C NMR (100 MHz, DMSO-*d*<sub>6</sub>) δ 170.2, 150.9, 146.6, 143.2, 137.8, 129.7, 125.7, 122.6, 113.2, 112.6, 109.9, 94.9, 56.5, 55.6. HRMS *m/z* [M+H]<sup>+</sup> calcd for C<sub>14</sub>H<sub>14</sub>N<sub>3</sub>O<sub>3</sub>: 272.1035, found 272.1028, LC *t*<sub>R</sub> = 3.21 min, > 98% Purity.

**(Z)-3-(1H-imidazol-2-ylmethylidene)-5,6-dimethoxy-2,3-dihydro-1H-indol-2-one (25):** Compound **25** was prepared by procedure A to afford a dark red solid (95 mg, 0.350 mmol, 45%, ratio of E:Z - 44:56). MP >300 °C; (E)-3-((1H-Imidazol-2-yl)methylene)-5,6-dimethoxyindolin-2-one. <sup>1</sup>H NMR (500 MHz, DMSO-*d*<sub>6</sub>) δ 10.28 (bs, 1H), 9.26 (s, 1H), 7.41 (s, 2H), 7.21 (s, 1H), 6.50 (s, 1H), 3.80 (s, 3H), 3.77 (s, 3H). <sup>13</sup>C NMR (125 MHz, DMSO-*d*<sub>6</sub>) δ 170.2, 151.1, 143.5, 143.2, 137.8, 132.1, 125.6, 117.5, 113.28, 113.26, 94.8, 56.5, 55.6. (Z)-3-((1H-Imidazol-2-yl)methylene)-5,6-dimethoxyindolin-2-one. <sup>1</sup>H NMR (500 MHz, DMSO-*d*<sub>6</sub>) δ 14.01 (bs, 1H), 7.69 (s, 1H), 7.56 (s, 1H), 7.50 (bs, 1H), 7.30 (bs, 1H), 6.54 (s, 1H), 3.78 (s, 3H), 3.77 (s, 3H). <sup>13</sup>C NMR (125 MHz, DMSO-*d*<sub>6</sub>) δ 169.4, 150.6, 144.7, 144.0, 134.5, 124.5, 122.2, 120.0, 115.1, 105.5, 95.5, 56.3, 55.8. HRMS *m/z*

[M+H]<sup>+</sup> calcd for C<sub>14</sub>H<sub>14</sub>N<sub>3</sub>O<sub>3</sub>: 272.1035, found 272.1022, LC t<sub>R</sub> = 2.74 min, > 98% Purity.

**(Z)-5-acetyl-3-(1H-pyrazol-5-ylmethylidene)-2,3-dihydro-1H-indol-2-one (26):** Compound **26** was prepared by procedure A to afford a bright orange solid (154 mg, 0.608 mmol, 71%, *E/Z* ratio 32:68). MP 262–265 °C; (Z)-3-((1H-Pyrazol-5-yl)methylene)-5-acetylin-dolin-2-one. <sup>1</sup>H NMR (500 MHz, DMSO-*d*<sub>6</sub>) δ 10.80 (s, 1H), 10.12 (d, *J* = 1.8 Hz, 1H), 8.02 (s, 1H), 7.94 (d, *J* = 1.1 Hz, 1H), 7.82 (dd, *J* = 8.1, 1.9 Hz, 1H), 7.56 (s, 1H), 6.92 (d, *J* = 8.2 Hz, 1H), 2.57 (s, 3H). <sup>13</sup>C NMR (150 MHz, DMSO-*d*<sub>6</sub>) δ 196.8, 170.5, 145.4, 139.7, 137.0, 130.4, 128.9, 127.5, 122.7, 119.7, 119.4, 108.6, 26.5. (*E*)-3-((1H-Pyrazol-5-yl)methylene)-5-acetylin-dolin-2-one. <sup>1</sup>H NMR (600 MHz, DMSO-*d*<sub>6</sub>) δ 10.80 (s, 1H), 8.33 (d, *J* = 1.7 Hz, 1H), 8.06 (s, 1H), 8.01 (s, 1H), 7.85 (dd, *J* = 8.2, 1.7 Hz, 1H), 6.99 (d, *J* = 8.2 Hz, 1H), 2.58 (s, 3H). HRMS *m/z* [M+H]<sup>+</sup> calcd for C<sub>14</sub>H<sub>12</sub>N<sub>3</sub>O<sub>2</sub>: 254.0930, found 254.0918, LC t<sub>R</sub> = 2.74 min, > 98% Purity.

**(3Z)-5-acetyl-3-(1H-pyrrol-2-ylmethylidene)-2,3-dihydro-1H-indol-2-one (27):** Compound **27** was prepared by procedure A to afford a dark orange solid (117 mg, 0.467 mmol, 54%). MP 218–220 °C; <sup>1</sup>H NMR (400 MHz, DMSO-*d*<sub>6</sub>) δ 10.58 (s, 1H), 9.08 – 8.92 (m, 1H), 8.85 (ddd, *J* = 4.8, 1.9, 0.8 Hz, 1H), 7.92 (td, *J* = 7.7, 1.8 Hz, 1H), 7.84 (dt, *J* = 7.9, 1.1 Hz, 1H), 7.43 (ddd, *J* = 7.6, 4.7, 1.2 Hz, 1H), 7.25 (td, *J* = 7.6, 1.3 Hz, 1H), 6.95 (td, *J* = 7.7, 1.1 Hz, 1H), 6.84 (dt, *J* = 7.7, 0.8 Hz, 1H), 3.31 (s, 3H). <sup>13</sup>C NMR (100 MHz, DMSO-*d*<sub>6</sub>) δ 169.3, 153.2, 149.7, 143.6, 137.3, 133.7, 130.8, 129.3, 128.4, 127.9, 124.1, 121.5, 121.2, 109.6, 39.3. HRMS *m/z* [M+H]<sup>+</sup> calcd for C<sub>15</sub>H<sub>13</sub>N<sub>2</sub>O<sub>2</sub>: 253.0977, found 253.0963, LC t<sub>R</sub> = 3.99 min, > 98% Purity.

**(3Z)-5-acetyl-3-[(3,5-dimethyl-1H-pyrrol-2-yl)methylidene]-2,3-dihydro-1H-indol-2-one (28):** Compound **28** was prepared by procedure A to afford a dark orange solid (149 mg, 0.532 mmol, 62%). MP >300 °C; <sup>1</sup>H NMR (400 MHz, DMSO-*d*<sub>6</sub>) δ 13.33 (s, 1H), 11.14 (s, 1H), 8.35 (d, *J* = 1.6 Hz, 1H), 7.82 – 7.68 (m, 2H), 6.96 (d, *J* = 8.2 Hz, 1H), 6.05 (d, *J* = 2.5 Hz, 1H), 2.59 (s, 3H), 2.35 (s, 3H), 2.33 (s, 3H). <sup>13</sup>C NMR (100 MHz, DMSO-*d*<sub>6</sub>) δ 197.0, 169.8, 141.8, 136.8, 133.1, 130.5, 126.9, 126.6, 125.9, 124.7, 118.5, 113.0, 111.3, 108.9, 26.7, 13.6, 11.5. HRMS *m/z* [M+H]<sup>+</sup> calcd for C<sub>17</sub>H<sub>17</sub>N<sub>2</sub>O<sub>2</sub>: 281.1290, found 281.1278, LC t<sub>R</sub> = 4.62 min, > 98% Purity.

**(3Z)-5-acetyl-3-(1H-pyrazol-5-ylmethylidene)-2,3-dihydro-1H-indol-2-one (29):** Compound **29** was prepared by procedure A to afford a mustard solid (33 mg, 0.130 mmol, 15%). MP 240–242 °C; <sup>1</sup>H NMR (600 MHz, DMSO-*d*<sub>6</sub>) δ 13.76 (s, 1H), 10.94 (s, 1H), 9.75 (s, 1H), 7.96 (s, 1H), 7.92 (dd, *J* = 8.2, 1.8 Hz, 1H), 7.56 (s, 1H), 6.97 (d, *J* = 8.1 Hz, 1H), 6.86 (s, 1H), 2.58 (s, 3H). <sup>13</sup>C NMR (150 MHz, DMSO-*d*<sub>6</sub>) δ 196.6, 170.0, 146.5, 146.2, 130.7, 130.1, 127.2, 127.0, 124.0, 121.8, 120.4, 111.0, 109.1, 26.5. HRMS *m/z* [M+H]<sup>+</sup> calcd for C<sub>14</sub>H<sub>12</sub>N<sub>3</sub>O<sub>2</sub>: 254.0930, found 254.0920, LC t<sub>R</sub> = 3.30 min, > 98% Purity.

**(Z)-5-acetyl-3-(1H-imidazol-2-ylmethylidene)-2,3-dihydro-1H-indol-2-one (30):** Compound **30** was prepared by procedure A to afford a bright yellow solid (134 mg, 0.529 mmol, 62%, *E/Z* ratio 47:53 - not able to distinguish *E/Z* isomers). MP >300 °C; Major diastereoisomer. 3-((1H-Imidazol-2-yl)methylene)-5-acetylin-dolin-2-one. <sup>1</sup>H NMR (600 MHz, DMSO-*d*<sub>6</sub>) δ 10.94 (bs, 1H), 10.14 (d, *J* = 1.8 Hz, 1H), 7.91 (dd, *J* = 8.2, 1.9 Hz, 1H), 7.56 (bs, 1H), 7.48 (bs, 1H), 7.46 (s, 1H), 6.96 (d, *J* = 8.2 Hz, 1H), 2.58 (s, 3H). Minor diastereoisomer. 3-((1H-Imidazol-2-yl)methylene)-5-acetylin-dolin-2-one. <sup>1</sup>H NMR (600 MHz, DMSO-*d*<sub>6</sub>) δ 13.97 (bs, 1H), 10.95 (bs, 1H), 8.54 (d, *J* = 1.6 Hz, 1H), 8.06 (s, 1H),

7.88 (dd, *J* = 8.2, 1.7 Hz, 1H), 7.59 (d, *J* = 2.1 Hz, 1H), 7.39 (d, *J* = 1.3 Hz, 1H), 7.03 (d, *J* = 8.1 Hz, 1H), 2.60 (s, 3H). HRMS *m/z* [M+H]<sup>+</sup> calcd for C<sub>14</sub>H<sub>12</sub>N<sub>3</sub>O<sub>2</sub>: 254.0930, found 254.0917, LC t<sub>R</sub> = 2.86 min, > 98% Purity.

**(3Z)-5-acetyl-3-(pyridin-2-ylmethylidene)-2,3-dihydro-1H-indol-2-one (31):** Compound **31** was prepared by procedure A to afford a mustard solid (190 mg, 0.719 mmol, 63%). MP 250–252 °C; <sup>1</sup>H NMR (400 MHz, DMSO-*d*<sub>6</sub>) δ 11.00 (s, 1H), 9.77 (d, *J* = 1.8 Hz, 1H), 8.88 (dt, *J* = 4.8, 1.2 Hz, 1H), 7.96 (td, *J* = 7.6, 1.8 Hz, 1H), 7.93 – 7.80 (m, 2H), 7.62 (s, 1H), 7.49 (ddd, *J* = 7.5, 4.7, 1.3 Hz, 1H), 6.94 (d, *J* = 8.2 Hz, 1H), 2.55 (s, 3H). <sup>13</sup>C NMR (100 MHz, DMSO-*d*<sub>6</sub>) δ 196.4, 169.7, 152.9, 149.7, 147.6, 137.5, 134.9, 131.5, 130.6, 128.9, 128.9, 128.4, 124.6, 121.3, 109.5, 26.4. HRMS *m/z* [M+H]<sup>+</sup> calcd for C<sub>16</sub>H<sub>13</sub>N<sub>2</sub>O<sub>2</sub>: 265.0977, found 265.0966, LC t<sub>R</sub> = 3.72 min, > 98% Purity.

**(3Z)-5-acetyl-3-(pyridin-3-ylmethylidene)-2,3-dihydro-1H-indol-2-one (32):** Compound **32** was prepared by procedure A to afford a yellow solid (88 mg, 0.333 mmol, 39%, *E/Z* ratio 48:52 - not able to distinguish *E/Z* isomers). MP 209–211 °C; Major diastereoisomer. 5-Acetyl-3-(pyridin-3-ylmethylene)indolin-2-one. <sup>1</sup>H NMR (600 MHz, DMSO-*d*<sub>6</sub>) δ 11.10 (bs, 1H), 9.24 (d, *J* = 2.2 Hz, 1H), 8.93 – 8.91 (m, 2H), 8.61 (dd, *J* = 4.8, 1.7 Hz, 1H), 8.08 (s, 1H), 7.94 – 7.91 (m, 1H), 7.51 (dd, *J* = 8.1, 4.8 Hz, 1H), 6.94 (d, *J* = 8.2 Hz, 1H), 2.58 (s, 3H). Minor diastereoisomer. 5-Acetyl-3-(pyridin-3-ylmethylene)indolin-2-one. <sup>1</sup>H NMR (600 MHz, DMSO-*d*<sub>6</sub>) δ 11.08 (bs, 1H), 8.69 (dd, *J* = 4.8, 1.6 Hz, 1H), 8.38 (d, *J* = 1.6 Hz, 1H), 8.23 – 8.15 (m, 1H), 7.99 (d, *J* = 1.7 Hz, 1H), 7.94 – 7.91 (m, 1H), 7.73 (s, 1H), 7.59 (dd, *J* = 7.7, 5.0 Hz, 1H), 6.99 (d, *J* = 8.2 Hz, 1H), 2.42 (s, 3H). HRMS *m/z* [M+H]<sup>+</sup> calcd for C<sub>16</sub>H<sub>13</sub>N<sub>2</sub>O<sub>2</sub>: 265.0977, found 265.0967, LC t<sub>R</sub> = 2.46 min, > 98% Purity.

**(3Z)-2-oxo-3-(1H-pyrrol-2-ylmethylidene)-2,3-dihydro-1H-indole-5-carboxylic acid (33):** Compound **33** was prepared by procedure A to afford a dark orange solid (90 mg, 0.354 mmol, 42%, *E/Z* ratio 30:70). MP >220 °C (decomp.); (Z)-3-((1H-pyrrol-2-yl)methylene)-2-oxoindoline-5-carboxylic acid. <sup>1</sup>H NMR (600 MHz, DMSO-*d*<sub>6</sub>) δ 13.28 (bs, 1H), 11.07 (bs, 1H), 8.18 (d, *J* = 1.5 Hz, 1H), 7.77 (dd, *J* = 8.0, 1.4 Hz, 1H), 7.77 (s, 1H), 7.34 – 7.33 (m, 1H), 6.88 – 6.85 (m, 1H), 6.83 (d, *J* = 8.0 Hz, 1H), 6.34 (dt, *J* = 3.7, 2.3 Hz, 1H). <sup>13</sup>C NMR (125 MHz, DMSO-*d*<sub>6</sub>) δ 170.3, 169.7, 140.1, 129.7 (s, 2C), 128.6, 126.1, 125.4, 124.1, 120.3, 119.5, 117.1, 111.3, 108.3. (*E*)-3-((1H-pyrrol-2-yl)methylene)-2-oxoindoline-5-carboxylic acid. <sup>1</sup>H NMR (600 MHz, DMSO-*d*<sub>6</sub>) δ 11.91 (bs, 1H), 10.58 (bs, 1H), 8.59 (d, *J* = 1.5 Hz, 1H), 7.81 (dd, *J* = 8.0, 1.4 Hz, 1H), 7.52 (s, 1H), 7.21 – 7.20 (m, 1H), 7.15 – 7.05 (m, 1H), 6.80 (d, *J* = 8.0 Hz, 1H), 6.42 – 6.41 (m, 1H). <sup>13</sup>C NMR (125 MHz, DMSO-*d*<sub>6</sub>) δ 170.3, 169.7, 142.6, 132.2, 129.8 (s, 2C), 127.6, 124.8, 124.0, 123.1, 120.9, 113.5, 111.5, 108.2. HRMS *m/z* [M+H]<sup>+</sup> calcd for C<sub>14</sub>H<sub>11</sub>N<sub>2</sub>O<sub>3</sub>: 255.0770, found 255.0762, LC t<sub>R</sub> = 3.79 min, > 98% Purity.

**(3Z)-3-(1H-imidazol-5-ylmethylidene)-2-oxo-2,3-dihydro-1H-indole-5-carboxylic acid (34):** Compound **34** was prepared by procedure A to afford a yellow solid (104 mg, 0.408 mmol, 48%). MP >300 °C; <sup>1</sup>H NMR (600 MHz, DMSO-*d*<sub>6</sub>) δ 10.75 (s, 1H), 9.90 (s, 1H), 8.25 (s, 1H), 8.07 (s, 1H), 7.96 (s, 1H), 7.83 (dd, *J* = 8.1, 1.7 Hz, 1H), 7.54 (s, 1H), 6.89 (d, *J* = 8.1 Hz, 1H). <sup>13</sup>C NMR (150 MHz, DMSO-*d*<sub>6</sub>) δ 170.3, 167.9, 145.3, 138.3, 130.6, 129.8, 128.2, 126.6, 124.4, 123.9, 122.4, 120.6, 108.6. HRMS *m/z* [M+H]<sup>+</sup> calcd for C<sub>13</sub>H<sub>10</sub>N<sub>3</sub>O<sub>3</sub>: 256.0722, found 256.0716, LC t<sub>R</sub> = 2.46 min, > 98% Purity.

**(3Z)-3-(1H-imidazol-2-ylmethylidene)-2-oxo-2,3-dihydro-1H-indole-5-carboxylic acid (35):** Compound **35** was prepared by procedure A to afford a yellow solid (113 mg, 0.443 mmol, 52%). MP >260 °C (decomp.); <sup>1</sup>H NMR (600 MHz, DMSO-*d*<sub>6</sub>) δ 14.34 (s, 1H), 8.15 (d, *J* = 1.4 Hz, 1H), 7.83 (dd, *J* = 8.0, 1.4 Hz, 1H), 7.57 (s, 1H), 7.53 (s, 1H), 7.36 – 7.25 (m, 1H), 6.81 (d, *J* = 7.9 Hz, 1H). <sup>13</sup>C NMR (150 MHz, DMSO-*d*<sub>6</sub>) δ 174.4, 169.3, 143.9, 137.0, 134.7, 132.2, 130.5, 128.2, 125.0, 123.0, 122.8, 120.5, 108.8. HRMS *m/z* [M+H]<sup>+</sup> calcd for C<sub>13</sub>H<sub>10</sub>N<sub>3</sub>O<sub>3</sub>: 256.0722, found 256.0714, LC *t*<sub>R</sub> = 2.46 min, > 98% Purity.

**5-butyrylindolin-2-one (36):** Compound **36** was prepared by procedure B to afford a colourless solid (901 mg, 4.431 mmol, 59%). MP 130–132 °C; <sup>1</sup>H NMR (400 MHz, DMSO-*d*<sub>6</sub>) δ 10.73 (s, 1H), 7.89 – 7.82 (m, 1H), 7.82 – 7.76 (m, 1H), 6.89 (d, *J* = 8.1 Hz, 1H), 3.54 (s, 2H), 2.90 (t, *J* = 7.2 Hz, 2H), 1.61 (h, *J* = 7.3 Hz, 2H), 0.91 (t, *J* = 7.4 Hz, 3H). <sup>13</sup>C NMR (100 MHz, DMSO-*d*<sub>6</sub>) δ 198.5, 176.8, 148.2, 130.4, 129.0, 126.1, 124.1, 108.7, 39.4, 35.5, 17.6, 13.7. HRMS *m/z* [M+H]<sup>+</sup> calcd for C<sub>12</sub>H<sub>14</sub>N<sub>2</sub>O<sub>2</sub>: 204.1025, found 204.1017, LC *t*<sub>R</sub> = 3.18 min, > 98% Purity.

**5-benzoylindolin-2-one (37):** Compound **37** was prepared by procedure C to afford a colourless solid (1.319 g, 5.555 mmol, 74%). MP 186–188 °C; <sup>1</sup>H NMR (400 MHz, DMSO-*d*<sub>6</sub>) δ 10.81 (s, 1H), 7.73 – 7.59 (m, 5H), 7.57 – 7.51 (m, 2H), 6.95 (d, *J* = 8.6 Hz, 1H), 3.57 (s, 2H). <sup>13</sup>C NMR (100 MHz, DMSO-*d*<sub>6</sub>) δ 194.7, 176.7, 148.3, 138.0, 131.9, 131.3, 130.0, 129.2 (s, 2C), 128.4 (s, 2C), 126.2, 126.0, 108.7, 35.6. HRMS *m/z* [M+H]<sup>+</sup> calcd for C<sub>15</sub>H<sub>12</sub>N<sub>2</sub>O<sub>2</sub>: 238.0868, found 238.0858, LC *t*<sub>R</sub> = 3.36 min, > 98% Purity.

**5-(4-fluorobenzoyl)indolin-2-one (38):** Compound **38** was prepared by procedure B to afford a colourless/light green solid (571 mg, 2.237 mmol, 30%). MP 155–157 °C; <sup>1</sup>H NMR (400 MHz, DMSO-*d*<sub>6</sub>) δ 10.86 (s, 1H), 7.76 – 7.55 (m, 3H), 7.51 (td, *J* = 7.4, 1.7 Hz, 1H), 7.40 – 7.31 (m, 2H), 6.95 (d, *J* = 8.6 Hz, 1H), 3.57 (s, 2H). <sup>13</sup>C NMR (100 MHz, DMSO-*d*<sub>6</sub>) δ 191.4, 176.8, 158.8 (d, *J* = 247.6 Hz), 149.3, 132.8 (d, *J* = 8.2 Hz), 131.2, 130.0 (d, *J* = 14.9 Hz), 129.9, 127.20 (d, *J* = 16.1 Hz), 126.5, 125.5, 124.7 (d, *J* = 3.4 Hz), 116.1 (d, *J* = 21.4 Hz), 109.0, 35.5. HRMS *m/z* [M+H]<sup>+</sup> calcd for C<sub>15</sub>H<sub>11</sub>FN<sub>2</sub>O<sub>2</sub>: 256.0774, found 256.0763, LC *t*<sub>R</sub> = 3.40 min, > 98% Purity.

**5-(furan-2-carbonyl)indolin-2-one (39):** Compound **39** was prepared by procedure B to afford a beige solid (836 mg, 3.579 mmol, 49%). Consistent with previous report.<sup>86</sup>

**(3Z)-5-butanoyl-3-(1H-pyrrol-2-ylmethylidene)-2,3-dihydro-1H-indol-2-one (40):** Compound **40** was prepared by procedure A to afford a mustard solid (43 mg, 0.153 mmol, 31%). MP 153–155 °C; <sup>1</sup>H NMR (400 MHz, DMSO-*d*<sub>6</sub>) δ 13.22 (s, 1H), 11.23 (s, 1H), 8.30 (d, *J* = 1.6 Hz, 1H), 7.99 (s, 1H), 7.82 (dd, *J* = 8.2, 1.7 Hz, 1H), 7.40 (q, *J* = 1.8, 1.3 Hz, 1H), 6.97 (d, *J* = 8.2 Hz, 1H), 6.92 (dt, *J* = 3.6, 1.7 Hz, 1H), 6.39 (dt, *J* = 3.7, 2.3 Hz, 1H), 2.99 (t, *J* = 7.2 Hz, 2H), 1.66 (h, *J* = 7.3 Hz, 2H), 0.95 (t, *J* = 7.4 Hz, 3H). <sup>13</sup>C NMR (100 MHz, DMSO-*d*<sub>6</sub>) δ 198.8, 169.6, 142.6, 130.6, 129.6, 127.8, 127.5, 126.5, 125.3, 121.3, 118.6, 115.6, 111.8, 109.2, 17.6 (s, 2C), 13.8. HRMS *m/z* [M+H]<sup>+</sup> calcd for C<sub>17</sub>H<sub>17</sub>N<sub>2</sub>O<sub>2</sub>: 281.1290, found 281.1286, LC *t*<sub>R</sub> = 4.85 min, > 98% Purity.

**(3Z)-5-butanoyl-3-(1H-imidazol-5-ylmethylidene)-2,3-dihydro-1H-indol-2-one (41):** Compound **41** was prepared by procedure A to afford a bright yellow solid (58 mg, 0.207 mmol, 42%). MP >300 °C; <sup>1</sup>H NMR (600 MHz, DMSO-*d*<sub>6</sub>) δ 10.52 (s, 1H), 10.36 (d, *J* = 1.9 Hz, 1H), 8.53 (s, 1H), 7.75 – 7.61 (m, 3H), 7.51 (s, 1H), 6.85 (d, *J* = 8.1 Hz, 1H), 2.96 (t, *J* = 7.3 Hz, 2H), 1.74

– 1.68 (m, 2H), 0.99 (t, *J* = 7.4 Hz, 3H). <sup>13</sup>C NMR (150 MHz, DMSO-*d*<sub>6</sub>) δ 174.3, 170.5, 165.8, 156.3, 148.0, 145.3, 130.8, 124.3, 122.2, 121.8, 114.0, 111.9, 108.1, 48.6, 25.6, 14.0. HRMS *m/z* [M+H]<sup>+</sup> calcd for C<sub>16</sub>H<sub>16</sub>N<sub>3</sub>O<sub>2</sub>: 282.1243, found 282.1233, LC *t*<sub>R</sub> = 3.36 min, > 98% Purity.

**(3Z)-5-butanoyl-3-(1H-imidazol-2-ylmethylidene)-2,3-dihydro-1H-indol-2-one (42):** Compound **42** was prepared by procedure A to afford a bright yellow solid (77 mg, 0.274 mmol, 56%). MP >300 °C; <sup>1</sup>H NMR (600 MHz, DMSO-*d*<sub>6</sub>) δ 13.98 (s, 1H), 11.48 (s, 1H), 8.56 (d, *J* = 1.6 Hz, 1H), 8.08 (s, 1H), 7.89 (dd, *J* = 8.2, 1.7 Hz, 1H), 7.59 (d, *J* = 2.1 Hz, 1H), 7.39 (d, *J* = 1.1 Hz, 1H), 7.02 (d, *J* = 8.2 Hz, 1H), 3.03 (t, *J* = 7.2 Hz, 2H), 1.65 (q, *J* = 7.3 Hz, 2H), 0.96 (t, *J* = 7.4 Hz, 3H). <sup>13</sup>C NMR (150 MHz, DMSO-*d*<sub>6</sub>) δ 199.0, 169.4, 143.6, 143.5, 132.9, 131.1, 129.2, 125.9, 124.1, 122.6, 121.2, 120.8, 109.9, 40.1, 17.6, 13.8. HRMS *m/z* [M+H]<sup>+</sup> calcd for C<sub>16</sub>H<sub>16</sub>N<sub>3</sub>O<sub>2</sub>: 282.1243, found 282.1236, LC *t*<sub>R</sub> = 3.29 min, > 98% Purity.

**(3Z)-5-benzoyl-3-(1H-pyrrol-2-ylmethylidene)-2,3-dihydro-1H-indol-2-one (43):** Compound **43** was prepared by procedure A to afford a red solid (29 mg, 0.092 mmol, 22%). MP 232–234 °C; <sup>1</sup>H NMR (400 MHz, DMSO-*d*<sub>6</sub>) δ 13.21 (s, 1H), 11.29 (s, 1H), 8.10 (d, *J* = 1.6 Hz, 1H), 7.97 (s, 1H), 7.78 – 7.70 (m, 2H), 7.69 – 7.64 (m, 1H), 7.61 – 7.53 (m, 3H), 7.41 (q, *J* = 1.8, 1.2 Hz, 1H), 7.03 (d, *J* = 8.1 Hz, 1H), 6.93 (dt, *J* = 3.6, 1.7 Hz, 1H), 6.38 (dt, *J* = 3.7, 2.3 Hz, 1H). <sup>13</sup>C NMR (100 MHz, DMSO-*d*<sub>6</sub>) δ 195.1, 169.6, 142.6, 138.0, 132.1, 130.4, 130.0, 129.6, 129.4 (s, 2C), 128.5 (s, 2C), 128.1, 126.6, 125.4, 121.6, 119.9, 115.2, 111.8, 109.1. HRMS *m/z* [M+H]<sup>+</sup> calcd for C<sub>20</sub>H<sub>15</sub>N<sub>2</sub>O<sub>2</sub>: 315.1134, found 315.1120, LC *t*<sub>R</sub> = 4.90 min, > 98% Purity.

**(3Z)-5-benzoyl-3-(1H-imidazol-5-ylmethylidene)-2,3-dihydro-1H-indol-2-one (44):** Compound **44** was prepared by procedure A to afford a dark orange solid (24 mg, 0.076 mmol, 24%). MP 255–257 °C; <sup>1</sup>H NMR (400 MHz, DMSO-*d*<sub>6</sub>) δ 10.86 (s, 1H), 9.96 (s, 1H), 7.95 (d, *J* = 1.0 Hz, 1H), 7.78 – 7.71 (m, 4H), 7.69 – 7.55 (m, 5H), 6.99 (d, *J* = 8.1 Hz, 1H). <sup>13</sup>C NMR (100 MHz, DMSO-*d*<sub>6</sub>) δ 194.9, 170.3, 145.6, 138.3, 137.8, 136.9, 131.7, 131.3, 129.9, 129.5, 129.3 (s, 2C), 128.6, 128.2 (s, 2C), 126.6, 122.34, 120.6, 108.9. HRMS *m/z* [M+H]<sup>+</sup> calcd for C<sub>19</sub>H<sub>14</sub>N<sub>3</sub>O<sub>2</sub>: 316.1086, found 316.1076, LC *t*<sub>R</sub> = 3.51 min, > 98% Purity.

**(3Z)-5-[(4-fluorophenyl)carbonyl]-3-(1H-pyrrol-2-ylmethylidene)-2,3-dihydro-1H-indol-2-one (45):** Compound **45** was prepared by procedure A to afford a dark orange solid (37 mg, 0.111 mmol, 28%). MP 242–244 °C; <sup>1</sup>H NMR (400 MHz, DMSO-*d*<sub>6</sub>) δ 13.19 (s, 1H), 11.35 (s, 1H), 8.14 (d, *J* = 1.6 Hz, 1H), 7.98 (s, 1H), 7.65 (ddd, *J* = 13.9, 5.5, 2.7 Hz, 1H), 7.62 – 7.51 (m, 2H), 7.46 – 7.30 (m, 3H), 7.02 (d, *J* = 8.1 Hz, 1H), 6.94 (dt, *J* = 3.7, 1.7 Hz, 1H), 6.39 (dt, *J* = 4.1, 2.3 Hz, 1H). <sup>13</sup>C NMR (100 MHz, DMSO-*d*<sub>6</sub>) δ 191.7, 169.6, 159.0 (d, *J* = 248.1 Hz), 143.5, 132.9 (d, *J* = 8.2 Hz), 130.4, 130.2 (d, *J* = 3.0 Hz), 130.0, 129.6, 128.3, 127.3 (d, *J* = 15.7 Hz), 126.8, 125.7, 124.7 (d, *J* = 3.4 Hz), 121.8, 119.3, 116.2 (d, *J* = 21.4 Hz), 114.9, 111.8, 109.3. HRMS *m/z* [M+H]<sup>+</sup> calcd for C<sub>20</sub>H<sub>14</sub>N<sub>2</sub>O<sub>2</sub>F: 333.1039, found 333.1035, LC *t*<sub>R</sub> = 4.88 min, > 98% Purity.

**(3Z)-5-[(4-fluorophenyl)carbonyl]-3-(1H-imidazol-5-ylmethylidene)-2,3-dihydro-1H-indol-2-one (46):** Compound **46** was prepared by procedure A to afford a bright yellow solid (51 mg, 0.153 mmol, 39%). MP >300 °C; <sup>1</sup>H NMR (600 MHz, DMSO-*d*<sub>6</sub>) δ 10.04 (d, *J* = 1.6 Hz, 1H), 7.98 (d, *J* = 39.4 Hz, 1H), 7.75 (s, 1H), 7.70 (dd, *J* = 8.2, 1.9 Hz, 1H), 7.66 (tdd, *J* = 7.5, 5.3, 1.8 Hz, 1H), 7.53 (dd, *J* = 7.2, 1.9 Hz, 1H), 7.50 (d, *J* = 5.3 Hz, 1H), 7.42 (s, 1H), 7.39 (d, *J* = 3.9 Hz, 1H), 7.37 (d, *J* = 7.5 Hz,



1H), 6.94 (d,  $J = 8.2$  Hz, 1H).  $^{13}\text{C}$  NMR (150 MHz, DMSO- $d_6$ )  $\delta$  192.1, 173.7, 170.8, 158.9 (d,  $J = 246.5$  Hz), 145.3, 137.1, 132.1 (d,  $J = 8.5$  Hz), 129.9, 129.8 (d,  $J = 3.6$  Hz, 2C), 129.6, 129.6, 128.2 (d,  $J = 16.6$  Hz, 2C), 128.1, 124.5 (d,  $J = 3.5$  Hz), 123.6, 115.9 (d,  $J = 21.5$  Hz), 108.6. HRMS  $m/z$   $[\text{M}+\text{H}]^+$  calcd for  $\text{C}_{19}\text{H}_{13}\text{N}_3\text{O}_2\text{F}$ : 334.0992, found 334.0979, LC  $t_R = 3.57$  min, > 98% Purity.

**(Z)-3-((1H-pyrrol-2-yl)methylene)-5-(furan-2-carbonyl)indolin-2-one (47):** Compound **47** was prepared by procedure A to afford a yellow solid (19 mg, 0.062 mmol, 14%). MP >220 °C (decomp.);  $^1\text{H}$  NMR (600 MHz, DMSO- $d_6$ )  $\delta$  13.82 (s, 1H), 8.53 (s, 1H), 8.13 (s, 1H), 8.08 (d,  $J = 1.6$  Hz, 1H), 7.83 (s, 1H), 7.78 (dd,  $J = 8.2, 1.7$  Hz, 1H), 7.37 (d,  $J = 3.5$  Hz, 1H), 7.33 (s, 1H), 6.95 (d,  $J = 8.1$  Hz, 1H), 6.91 – 6.80 (m, 1H), 6.78 (dd,  $J = 3.6, 1.7$  Hz, 1H), 6.34 (d,  $J = 3.0$  Hz, 1H).  $^{13}\text{C}$  NMR (150 MHz, DMSO- $d_6$ )  $\delta$  180.6, 174.2, 165.6, 151.9, 147.6, 133.6, 130.0, 129.2, 126.6, 125.4, 119.8, 118.9, 116.2, 115.5, 114.1, 112.4, 111.3, 109.9. HRMS  $m/z$   $[\text{M}+\text{H}]^+$  calcd for  $\text{C}_{18}\text{H}_{13}\text{N}_2\text{O}_3$ : 305.0926, found 305.0920, LC  $t_R = 4.44$  min, > 98% Purity.

**(3Z)-5-[(furan-2-yl)carbonyl]-3-(1H-imidazol-2-ylmethylidene)-2,3-dihydro-1H-indol-2-one (48):** Compound **48** was prepared by procedure A to afford a yellow solid (23 mg, 0.075 mmol, 17%). MP >270 °C (decomp.);  $^1\text{H}$  NMR (600 MHz, DMSO- $d_6$ )  $\delta$  10.73 (s, 2H), 10.55 (s, 1H), 8.53 (s, 1H), 8.09 (d,  $J = 1.6$  Hz, 1H), 7.81 (dd,  $J = 8.1, 2.0$  Hz, 1H), 7.73 (d,  $J = 3.6$  Hz, 1H), 7.53 (s, 1H), 7.36 (s, 1H), 6.96 (d,  $J = 8.1$  Hz, 1H), 6.85 (dd,  $J = 3.5, 1.7$  Hz, 1H).  $^{13}\text{C}$  NMR (150 MHz, DMSO- $d_6$ )  $\delta$  180.4, 173.9, 165.5, 151.6, 147.5, 131.8, 129.7, 129.2, 127.6, 122.5, 120.1, 117.3, 114.9, 114.0, 112.4, 111.2, 108.6. HRMS  $m/z$   $[\text{M}+\text{H}]^+$  calcd for  $\text{C}_{17}\text{H}_{12}\text{N}_3\text{O}_3$ : 306.0879, found 306.0867, LC  $t_R = 2.96$  min, > 98% Purity.

***N,N*-dimethyl-2-oxoindoline-5-sulfonamide (50):** Compound **50** was prepared by procedure D to afford a beige solid (447 mg, 1.985 mmol, 55%). MP 198-200 °C;  $^1\text{H}$  NMR (400 MHz, DMSO- $d_6$ )  $\delta$  10.82 (s, 1H), 7.67 – 7.46 (m, 2H), 7.04 – 6.96 (m, 1H), 3.60 (s, 2H), 2.57 (s, 6H).  $^{13}\text{C}$  NMR (100 MHz, DMSO- $d_6$ )  $\delta$  176.4, 148.0, 128.4, 126.9, 126.9, 123.7, 109.1, 37.6 (s, 2C), 35.7. HRMS  $m/z$   $[\text{M}+\text{H}]^+$  calcd for  $\text{C}_{10}\text{H}_{13}\text{N}_2\text{O}_3\text{S}$ : 241.0649, found 241.0633.

**5-((4-methylpiperazin-1-yl)sulfonyl)indolin-2-one (51):** Compound **51** was prepared by procedure D to afford a beige/brown solid (496 mg, 1.679 mmol, 39%). MP 170-172 °C; HRMS  $m/z$   $[\text{M}+\text{H}]^+$  calcd for  $\text{C}_{13}\text{H}_{18}\text{N}_3\text{O}_3\text{S}$ : 296.1069, found 296.1054. Consistent with previous report.<sup>88</sup>

**(3Z)-*N,N*-dimethyl-2-oxo-3-(1H-pyrrol-2-ylmethylidene)-2,3-dihydro-1H-indole-5-sulfonamide (52):** Compound **52** was prepared by procedure A to afford an orange solid (54 mg, 0.170 mmol, 41%). MP 258-260 °C;  $^1\text{H}$  NMR (400 MHz, DMSO- $d_6$ )  $\delta$  13.23 (s, 1H), 11.33 (s, 1H), 8.11 (s, 1H), 8.05 (d,  $J = 1.7$  Hz, 1H), 7.53 (dd,  $J = 8.2, 1.8$  Hz, 1H), 7.44 (q,  $J = 2.3$  Hz, 1H), 7.09 (d,  $J = 8.2$  Hz, 1H), 6.94 (dt,  $J = 3.7, 1.7$  Hz, 1H), 6.41 (dt,  $J = 4.1, 2.3$  Hz, 1H), 2.61 (s, 6H).  $^{13}\text{C}$  NMR (100 MHz, DMSO- $d_6$ )  $\delta$  169.3, 142.1, 129.6, 128.9, 127.1, 127.1, 126.6, 125.9, 122.0, 117.9, 114.7, 112.0, 109.5, 37.7 (2C, s). HRMS  $m/z$   $[\text{M}+\text{H}]^+$  calcd for  $\text{C}_{15}\text{H}_{16}\text{N}_3\text{O}_3\text{S}$ : 318.0912, found 318.0897, LC  $t_R = 4.10$  min, > 98% Purity.

**(3Z)-3-(1H-imidazol-5-ylmethylidene)-*N,N*-dimethyl-2-oxo-2,3-dihydro-1H-indole-5-sulfonamide (53):** Compound **53** was prepared by procedure A to afford an orange solid (52 mg, 0.217 mmol, 52%). MP 275-277 °C;  $^1\text{H}$  NMR (400 MHz, DMSO- $d_6$ )  $\delta$  12.81 (s, 1H), 10.87 (s, 1H), 9.92 (d,  $J = 1.9$  Hz, 1H), 8.07 (t,  $J =$

0.9 Hz, 1H), 8.02 (d,  $J = 1.1$  Hz, 1H), 7.62 (d,  $J = 0.7$  Hz, 1H), 7.58 (dd,  $J = 8.2, 2.0$  Hz, 1H), 7.04 – 6.99 (m, 1H), 2.65 (s, 6H).  $^{13}\text{C}$  NMR (100 MHz, DMSO- $d_6$ )  $\delta$  170.0, 145.1, 138.3, 136.9, 129.4, 128.4, 127.14, 127.09, 125.9, 123.0, 120.1, 108.9, 37.8. HRMS  $m/z$   $[\text{M}+\text{H}]^+$  calcd for  $\text{C}_{14}\text{H}_{15}\text{N}_4\text{O}_3\text{S}$ : 319.0865, found 319.0850, LC  $t_R = 2.54$  min, > 98% Purity.

**(3Z)-5-[(4-methylpiperazin-1-yl)sulfonyl]-3-(1H-pyrrol-2-ylmethylidene)-2,3-dihydro-1H-indol-2-one (54):** Compound **54** was prepared by procedure A to afford a bright yellow solid (82 mg, 0.220 mmol, 65%). MP >260 °C (decomp.);  $^1\text{H}$  NMR (400 MHz, DMSO- $d_6$ )  $\delta$  13.23 (s, 1H), 11.35 (s, 1H), 8.09 (s, 1H), 8.02 (d,  $J = 1.7$  Hz, 1H), 7.51 (dd,  $J = 8.2, 1.8$  Hz, 1H), 7.44 (q,  $J = 2.2$  Hz, 1H), 7.09 (d,  $J = 8.1$  Hz, 1H), 6.95 (dt,  $J = 3.6, 1.7$  Hz, 1H), 6.41 (dt,  $J = 4.0, 2.3$  Hz, 1H), 2.89 (t,  $J = 4.7$  Hz, 4H), 2.36 (t,  $J = 4.9$  Hz, 4H), 2.13 (s, 3H).  $^{13}\text{C}$  NMR (100 MHz, DMSO- $d_6$ )  $\delta$  169.3, 142.2, 129.6, 129.0, 127.2, 127.2, 126.6, 125.9, 122.1, 117.8, 114.6, 112.0, 109.5, 53.5, 45.8 (s, 2C), 45.3 (s, 2C). HRMS  $m/z$   $[\text{M}+\text{H}]^+$  calcd for  $\text{C}_{18}\text{H}_{21}\text{N}_4\text{O}_3\text{S}$ : 373.1334, found 373.1326, LC  $t_R = 3.10$  min, > 98% Purity.

**(3Z)-3-(1H-imidazol-5-ylmethylidene)-5-[(4-methylpiperazin-1-yl)sulfonyl]-2,3-dihydro-1H-indol-2-one (55):** Compound **55** was prepared by procedure A to afford a bright yellow solid (67 mg, 0.228 mmol, 67%). MP >260 °C (decomp.);  $^1\text{H}$  NMR (600 MHz, DMSO- $d_6$ )  $\delta$  10.85 (s, 1H), 9.96 (d,  $J = 1.9$  Hz, 1H), 7.97 (s, 1H), 7.94 (s, 1H), 7.59 (s, 1H), 7.52 (dd,  $J = 8.1, 2.0$  Hz, 1H), 6.99 (d,  $J = 8.1$  Hz, 1H), 2.95 (s, 4H), 2.36 (d,  $J = 5.2$  Hz, 4H), 2.12 (s, 3H).  $^{13}\text{C}$  NMR (150 MHz, DMSO- $d_6$ )  $\delta$  170.2, 144.7, 140.9, 137.0, 129.9, 127.8, 127.7, 127.0, 125.6, 123.4, 118.5, 108.6, 53.7 (s, 2C), 45.9 (s, 2C), 45.3. HRMS  $m/z$   $[\text{M}+\text{H}]^+$  calcd for  $\text{C}_{17}\text{H}_{20}\text{N}_5\text{O}_3\text{S}$ : 374.1287, found 374.1276, LC  $t_R = 2.29$  min, > 98% Purity.

**(Z)-3-((1H-pyrrol-2-yl)methylene)-5-isopropoxyindolin-2-one (57):** Compound **57** was prepared by procedure A to afford a red solid (48 mg, 0.179 mmol, 68%). MP 149-151 °C;  $^1\text{H}$  NMR (400 MHz, DMSO- $d_6$ )  $\delta$  13.39 (s, 1H), 10.68 (s, 1H), 7.76 (s, 1H), 7.34 (td,  $J = 2.6, 1.3$  Hz, 1H), 7.31 (d,  $J = 2.3$  Hz, 1H), 6.79 (dt,  $J = 3.6, 1.7$  Hz, 1H), 6.75 (d,  $J = 8.3$  Hz, 1H), 6.70 (dd,  $J = 8.4, 2.3$  Hz, 1H), 6.35 (dt,  $J = 3.6, 2.3$  Hz, 1H), 4.54 (p,  $J = 6.0$  Hz, 1H), 1.26 (s, 3H), 1.25 (s, 3H).  $^{13}\text{C}$  NMR (100 MHz, DMSO- $d_6$ )  $\delta$  169.3, 152.8, 132.9, 129.5, 126.6, 126.2, 125.5, 120.1, 117.4, 115.4, 111.4, 110.0, 107.0, 70.1, 22.0 (s, 2C). HRMS  $m/z$   $[\text{M}+\text{H}]^+$  calcd for  $\text{C}_{16}\text{H}_{17}\text{N}_2\text{O}_2$ : 269.1290, found 269.1283, LC  $t_R = 4.97$  min, > 98% Purity.

**(3Z)-3-(1H-imidazol-5-ylmethylidene)-5-(propan-2-yloxy)-2,3-dihydro-1H-indol-2-one (58):** Compound **58** was prepared by procedure A to afford an orange solid (37 mg, 0.137 mmol, 53%). MP 211-213 °C;  $^1\text{H}$  NMR (400 MHz, DMSO- $d_6$ )  $\delta$  13.79 (s, 1H), 10.81 (s, 1H), 8.01 (s, 1H), 7.87 (s, 1H), 7.59 (s, 1H), 7.36 – 7.34 (m, 1H), 6.76 (d,  $J = 3.0$  Hz, 2H), 4.57 – 4.51 (m, 1H), 1.27 (s, 3H), 1.25 (s, 3H).  $^{13}\text{C}$  NMR (100 MHz, DMSO- $d_6$ )  $\delta$  13C NMR (100 MHz, DMSO- $d_6$ )  $\delta$  169.1, 153.0, 139.5, 138.1, 133.6, 128.1, 125.4, 123.1, 120.6, 116.5, 110.3, 107.7, 70.1, 22.0. HRMS  $m/z$   $[\text{M}+\text{H}]^+$  calcd for  $\text{C}_{15}\text{H}_{16}\text{N}_3\text{O}_2$ : 270.1243, found 270.1230, LC  $t_R = 3.42$  min, > 98% Purity.

**(3Z)-3-(1H-imidazol-2-ylmethylidene)-5-(propan-2-yloxy)-2,3-dihydro-1H-indol-2-one (59):** Compound **59** was prepared by procedure A to afford a bright orange solid (44 mg, 0.163 mmol, 62%). MP 256-258 °C;  $^1\text{H}$  NMR (400 MHz, DMSO- $d_6$ )  $\delta$  10.30 (s, 1H), 9.17 (d,  $J = 2.6$  Hz, 1H), 7.85 (s, 1H), 7.55 – 7.34 (m, 3H), 6.79 (d,  $J = 1.4$  Hz, 2H), 4.59 (p,  $J = 6.0$  Hz, 1H), 1.30 – 1.25 (m, 6H).  $^{13}\text{C}$  NMR (100 MHz, DMSO- $d_6$ )  $\delta$  169.0, 153.2, 143.7, 133.7, 132.5, 125.0, 124.7, 124.2, 120.6, 117.4, 110.6, 108.3, 69.9, 22.0



(s, 2C). HRMS  $m/z$   $[M+H]^+$  calcd for  $C_{15}H_{16}N_3O_2$ : 270.1243, found 270.1230, LC  $t_R$  = 3.29 min, > 98% Purity.

***N*-(2-oxoindolin-5-yl)butyramide (60)**: Compound **60** was prepared by procedure F to afford a colourless solid (552 mg, 2.531 mmol, 75%). MP 165–167 °C;  $^1H$  NMR (600 MHz, DMSO- $d_6$ )  $\delta$  10.26 (s, 1H), 9.70 (s, 1H), 7.55 – 7.47 (m, 1H), 7.32 (dd,  $J$  = 8.3, 2.0 Hz, 1H), 6.71 (d,  $J$  = 8.3 Hz, 1H), 3.44 (s, 2H), 2.23 (t,  $J$  = 7.3 Hz, 2H), 1.59 (h,  $J$  = 7.4 Hz, 2H), 0.90 (t,  $J$  = 7.4 Hz, 3H).  $^{13}C$  NMR (150 MHz, DMSO- $d_6$ )  $\delta$  176.3, 170.6, 139.1, 133.5, 126.0, 118.4, 116.5, 108.8, 38.3, 36.1, 18.7, 13.6. HRMS  $m/z$   $[M+H]^+$  calcd for  $C_{12}H_{15}N_2O_2$ : 219.1134, found 219.1125, LC  $t_R$  = 2.51 min, > 98% Purity.

**2-ethyl-*N*-(2-oxoindolin-5-yl)butanamide (61)**: Compound **61** was prepared by procedure F to afford a colourless solid (590 mg, 2.395 mmol, 71%). MP 228–230 °C;  $^1H$  NMR (400 MHz, DMSO- $d_6$ )  $\delta$  10.26 (s, 1H), 9.68 (s, 1H), 7.54 (d,  $J$  = 2.0 Hz, 1H), 7.33 (dd,  $J$  = 8.4, 2.1 Hz, 1H), 6.72 (d,  $J$  = 8.3 Hz, 1H), 3.45 (s, 2H), 2.16 (tt,  $J$  = 9.4, 5.1 Hz, 1H), 1.59 – 1.48 (m, 2H), 1.47 – 1.36 (m, 2H), 0.84 (t,  $J$  = 7.4 Hz, 6H).  $^{13}C$  NMR (100 MHz, DMSO- $d_6$ )  $\delta$  176.3, 173.4, 139.2, 133.3, 126.0, 118.69, 116.8, 108.8, 49.8, 36.0, 25.3 (s, 2C), 11.9 (s, 2C). HRMS  $m/z$   $[M+H]^+$  calcd for  $C_{14}H_{19}N_2O_2$ : 247.1447, found 247.1436, LC  $t_R$  = 3.06 min, > 98% Purity.

***N*-(2-oxoindolin-5-yl)cyclohexanecarboxamide (62)**: Compound **62** was prepared by procedure F to afford a colourless solid (780 mg, 2.632 mmol, 78%). MP 223–225 °C;  $^1H$  NMR (600 MHz, DMSO- $d_6$ )  $\delta$  10.25 (s, 1H), 9.62 (s, 1H), 7.57 – 7.45 (m, 1H), 7.33 (dd,  $J$  = 8.4, 2.1 Hz, 1H), 6.70 (d,  $J$  = 8.3 Hz, 1H), 3.44 (s, 2H), 2.27 (tt,  $J$  = 11.7, 3.3 Hz, 1H), 2.03 – 1.67 (m, 4H), 1.68 – 1.60 (m, 1H), 1.39 (qd,  $J$  = 13.4, 12.9, 3.7 Hz, 2H), 1.29 – 1.13 (m, 3H).  $^{13}C$  NMR (150 MHz, DMSO- $d_6$ )  $\delta$  176.3, 173.8, 139.0, 133.6, 125.9, 118.4, 116.5, 108.8, 44.8, 36.0, 29.2 (s, 2C), 25.42, 25.26 (s, 2C). HRMS  $m/z$   $[M+H]^+$  calcd for  $C_{15}H_{19}N_2O_2$ : 259.1447, found 259.1435, LC  $t_R$  = 3.25 min, > 98% Purity.

***N*-(2-oxoindolin-5-yl)benzamide (63)**: Compound **63** was prepared by procedure F to afford a colourless solid (647 mg, 2.565 mmol, 76%). MP 115–117 °C;  $^1H$  NMR (600 MHz, DMSO- $d_6$ )  $\delta$  10.37 (s, 1H), 10.14 (s, 1H), 7.99 – 7.90 (m, 2H), 7.67 (d,  $J$  = 2.0 Hz, 1H), 7.59 – 7.55 (m, 1H), 7.55 – 7.44 (m, 3H), 6.79 (d,  $J$  = 8.3 Hz, 1H), 3.49 (s, 2H).  $^{13}C$  NMR (150 MHz, DMSO- $d_6$ )  $\delta$  176.4, 165.2, 139.8, 135.1, 133.2, 131.4, 128.4 (s, 2C), 127.6 (s, 2C), 125.9, 119.9, 117.8, 108.8, 36.1. HRMS  $m/z$   $[M+H]^+$  calcd for  $C_{15}H_{13}N_2O_2$ : 253.0977, found 253.0967, LC  $t_R$  = 2.93 min, > 98% Purity.

***N*-(2-oxoindolin-5-yl)furan-2-carboxamide (64)**: Compound **55** was prepared by procedure F to afford a beige solid (605 mg, 2.498 mmol, 74%).  $^1H$  NMR (600 MHz, DMSO- $d_6$ )  $\delta$  10.35 (s, 1H), 10.07 (s, 1H), 7.90 (d,  $J$  = 1.6 Hz, 1H), 7.64 (d,  $J$  = 2.2 Hz, 1H), 7.49 (dd,  $J$  = 8.4, 2.1 Hz, 1H), 7.29 (d,  $J$  = 3.4 Hz, 1H), 6.78 (d,  $J$  = 8.3 Hz, 1H), 6.68 (dd,  $J$  = 3.5, 1.7 Hz, 1H), 3.49 (s, 2H).  $^{13}C$  NMR (150 MHz, DMSO- $d_6$ )  $\delta$  176.4, 156.0, 147.7, 145.5, 139.9, 132.4, 126.0, 120.0, 117.8, 114.3, 112.1, 108.8, 36.1. HRMS  $m/z$   $[M+H]^+$  calcd for  $C_{13}H_{11}N_2O_3$ : 243.0770, found 243.0759, LC  $t_R$  = 2.51 min, > 98% Purity.

***N*-[(3*Z*)-2-oxo-3-(1*H*-pyrrol-2-ylmethylidene)-2,3-dihydro-1*H*-indol-5-yl]butanamide (65)**: Compound **65** was prepared by procedure A to afford a bright yellow solid (85 mg, 0.288 mmol, 63%). MP 260–262 °C;  $^1H$  NMR (400 MHz, DMSO- $d_6$ )  $\delta$  13.34 (s, 1H), 10.80 (s, 1H), 9.74 (s, 1H), 7.95 (d,  $J$  = 2.0 Hz, 1H), 7.59 (s, 1H), 7.35 (q,  $J$  = 2.2 Hz, 1H), 7.17 (dd,  $J$  = 8.3, 2.0 Hz, 1H),

6.92 (dt,  $J$  = 3.5, 1.6 Hz, 1H), 6.80 (d,  $J$  = 8.3 Hz, 1H), 6.35 (dt,  $J$  = 3.7, 2.3 Hz, 1H), 2.27 (t,  $J$  = 7.3 Hz, 2H), 1.62 (h,  $J$  = 7.4 Hz, 2H), 0.93 (t,  $J$  = 7.4 Hz, 3H).  $^{13}C$  NMR (100 MHz, DMSO- $d_6$ )  $\delta$  170.7, 169.3, 134.8, 133.5, 129.5, 126.1, 125.7, 125.1, 120.7, 118.8, 117.0, 111.4, 110.5, 109.4, 38.2, 18.7, 13.7. HRMS  $m/z$   $[M+H]^+$  calcd for  $C_{17}H_{18}N_3O_2$ : 296.1399, found 296.1392, LC  $t_R$  = 4.14 min, > 98% Purity.

**2-ethyl-*N*-[(3*Z*)-2-oxo-3-(1*H*-pyrrol-2-ylmethylidene)-2,3-dihydro-1*H*-indol-5-yl]butanamide (66)**: Compound **66** was prepared by procedure A to afford a yellow solid (86 mg, 0.266 mmol, 66%). MP >300 °C;  $^1H$  NMR (400 MHz, DMSO- $d_6$ )  $\delta$  13.32 (s, 1H), 10.79 (s, 1H), 9.72 (s, 1H), 8.02 – 7.92 (m, 1H), 7.60 (s, 1H), 7.33 (td,  $J$  = 2.6, 1.4 Hz, 1H), 7.16 (dd,  $J$  = 8.3, 2.0 Hz, 1H), 6.90 (dt,  $J$  = 3.6, 1.7 Hz, 1H), 6.83 – 6.73 (m, 1H), 6.33 (dt,  $J$  = 3.7, 2.3 Hz, 1H), 2.18 (tt,  $J$  = 9.4, 5.1 Hz, 1H), 1.55 (ddq,  $J$  = 13.2, 9.0, 7.4 Hz, 2H), 1.48 – 1.35 (m, 2H), 0.86 (t,  $J$  = 7.4 Hz, 6H).  $^{13}C$  NMR (100 MHz, DMSO- $d_6$ )  $\delta$  173.5, 169.3, 134.9, 133.3, 129.5, 126.2, 125.7, 125.1, 120.7, 119.1, 117.0, 111.4, 110.8, 109.4, 49.8, 25.3 (2C, s), 11.9 (2C, s). HRMS  $m/z$   $[M+H]^+$  calcd for  $C_{19}H_{22}N_3O_2$ : 324.1712, found 324.1702, LC  $t_R$  = 4.56 min, > 98% Purity.

**2-ethyl-*N*-[(3*Z*)-3-(1*H*-imidazol-5-ylmethylidene)-2-oxo-2,3-dihydro-1*H*-indol-5-yl]butanamide (67)**: Compound **67** was prepared by procedure A to afford a yellow solid (70 mg, 0.216 mmol, 53%). MP 285–287 °C;  $^1H$  NMR (600 MHz, DMSO- $d_6$ )  $\delta$  13.74 (s, 1H), 9.84 (s, 1H), 8.02 (s, 1H), 7.98 (s, 1H), 7.85 (d,  $J$  = 22.8 Hz, 1H), 7.71 (s, 1H), 7.24 (dd,  $J$  = 8.2, 2.0 Hz, 1H), 6.82 (d,  $J$  = 8.2 Hz, 1H), 2.21 (tt,  $J$  = 9.5, 5.0 Hz, 1H), 1.56 (dddd,  $J$  = 13.5, 7.3, 5.8, 1.9 Hz, 2H), 1.44 (ddd,  $J$  = 13.0, 7.3, 5.2 Hz, 2H), 0.87 (t,  $J$  = 7.4 Hz, 6H).  $^{13}C$  NMR (150 MHz, DMSO- $d_6$ )  $\delta$  174.4, 173.6, 140.3, 135.8, 133.5, 132.5, 124.4, 121.2, 120.4, 120.0, 111.5, 109.6, 108.2, 49.7, 25.3 (s, 2C), 11.9 (s, 2C). HRMS  $m/z$   $[M+H]^+$  calcd for  $C_{18}H_{21}N_4O_2$ : 325.1665, found 325.1660, LC  $t_R$  = 3.29 min, > 98% Purity.

**2-ethyl-*N*-[(3*Z*)-3-(1*H*-imidazol-2-ylmethylidene)-2-oxo-2,3-dihydro-1*H*-indol-5-yl]butanamide (68)**: Compound **68** was prepared by procedure A to afford a yellow solid (74 mg, 0.228 mmol, 56%). MP >300 °C;  $^1H$  NMR (600 MHz, DMSO- $d_6$ )  $\delta$  14.06 (s, 1H), 11.08 (s, 1H), 9.80 (s, 1H), 7.99 (s, 1H), 7.56 (d,  $J$  = 4.2 Hz, 2H), 7.46 – 7.27 (m, 2H), 6.86 (d,  $J$  = 8.2 Hz, 1H), 2.20 (tt,  $J$  = 9.8, 5.0 Hz, 1H), 1.56 (dq,  $J$  = 15.5, 7.6 Hz, 2H), 1.45 (dq,  $J$  = 13.2, 6.7, 6.0 Hz, 2H), 0.87 (t,  $J$  = 7.5 Hz, 6H).  $^{13}C$  NMR (150 MHz, DMSO- $d_6$ )  $\delta$  173.7, 169.0, 143.4, 135.9, 133.8, 132.6, 124.0, 123.8, 123.7, 121.1, 120.9, 112.0, 110.0, 49.8, 25.3, 11.9. HRMS  $m/z$   $[M+H]^+$  calcd for  $C_{18}H_{21}N_4O_2$ : 325.1665, found 325.1656, LC  $t_R$  = 3.24 min, > 98% Purity.

***N*-[(3*Z*)-2-oxo-3-(1*H*-pyrrol-2-ylmethylidene)-2,3-dihydro-1*H*-indol-5-yl]cyclohexanecarboxamide (69)**: Compound **69** was prepared by procedure A to afford a yellow solid (71 mg, 0.274 mmol, 71%). MP >300 °C;  $^1H$  NMR (400 MHz, DMSO- $d_6$ )  $\delta$  13.37 – 13.27 (m, 1H), 10.78 (s, 1H), 9.66 (s, 1H), 7.96 (d,  $J$  = 1.9 Hz, 1H), 7.57 (s, 1H), 7.33 (td,  $J$  = 2.6, 1.3 Hz, 1H), 7.14 (dd,  $J$  = 8.3, 2.0 Hz, 1H), 6.89 (dt,  $J$  = 3.7, 1.7 Hz, 1H), 6.78 (d,  $J$  = 8.3 Hz, 1H), 6.33 (dt,  $J$  = 3.7, 2.3 Hz, 1H), 2.33 – 2.25 (m, 1H), 1.76 (td,  $J$  = 13.9, 3.4 Hz, 4H), 1.64 (d,  $J$  = 11.3 Hz, 1H), 1.41 (qd,  $J$  = 13.6, 13.1, 3.5 Hz, 2H), 1.31 – 1.14 (m, 3H).  $^{13}C$  NMR (100 MHz, DMSO- $d_6$ )  $\delta$  173.9, 169.3, 134.8, 133.6, 129.5, 126.1, 125.7, 125.0, 120.6, 118.8, 117.0, 111.4, 110.6, 109.4, 44.7, 29.2 (2C, s), 25.4, 25.3 (2C, s). HRMS  $m/z$   $[M+H]^+$  calcd for  $C_{20}H_{22}N_3O_2$ : 336.1712, found 336.1703, LC  $t_R$  = 4.71 min, > 98% Purity.

***N*-[**(3Z)**-3-(1H-imidazol-5-ylmethylidene)-2-oxo-2,3-dihydro-1H-indol-5-yl]cyclohexanecarboxamide (70):** Compound **70** was prepared by procedure A to afford a yellow solid (89 mg, 0.265 mmol, 68%). >300 °C; <sup>1</sup>H NMR (400 MHz, DMSO-*d*<sub>6</sub>) δ 13.70 (s, 1H), 10.89 (s, 1H), 9.71 (s, 1H), 8.00 (d, *J* = 8.4 Hz, 2H), 7.70 (s, 2H), 7.21 (d, *J* = 8.3 Hz, 1H), 6.81 (d, *J* = 8.3 Hz, 1H), 2.31 (tt, *J* = 11.7, 3.4 Hz, 1H), 2.08 – 1.67 (m, 4H), 1.65 (dd, *J* = 10.5, 4.0 Hz, 1H), 1.42 (qd, *J* = 13.7, 13.1, 3.5 Hz, 2H), 1.35 – 1.06 (m, 3H). <sup>13</sup>C NMR (100 MHz, DMSO-*d*<sub>6</sub>) δ 173.9, 168.9, 146.2, 139.5, 138.6, 135.5, 133.8, 128.0, 124.3, 123.7, 119.8, 111.2, 109.7, 44.7, 29.2 (2C, s), 25.4, 25.3 (2C, s). HRMS *m/z* [M+H]<sup>+</sup> calcd for C<sub>19</sub>H<sub>21</sub>N<sub>4</sub>O<sub>2</sub>: 337.1665, found 337.1657, LC *t*<sub>R</sub> = 3.47 min, > 98% Purity.

***N*-[**(3Z)**-3-(1H-imidazol-2-ylmethylidene)-2-oxo-2,3-dihydro-1H-indol-5-yl]cyclohexanecarboxamide (71):** Compound **71** was prepared by procedure A to afford a yellow solid (81 mg, 0.241 mmol, 62%). MP >300 °C; <sup>1</sup>H NMR (600 MHz, DMSO-*d*<sub>6</sub>) δ 14.05 (s, 1H), 11.07 (s, 1H), 9.74 (s, 1H), 7.98 (d, *J* = 2.0 Hz, 1H), 7.56 (d, *J* = 2.1 Hz, 1H), 7.51 (s, 1H), 7.38 (dd, *J* = 8.4, 2.0 Hz, 1H), 7.34 (t, *J* = 1.2 Hz, 1H), 6.85 (d, *J* = 8.3 Hz, 1H), 2.31 (tt, *J* = 11.7, 3.5 Hz, 1H), 1.78 (ddt, *J* = 23.2, 12.4, 3.3 Hz, 4H), 1.68 – 1.63 (m, 1H), 1.42 (qd, *J* = 12.5, 3.2 Hz, 2H), 1.27 (qt, *J* = 12.4, 3.1 Hz, 2H), 1.20 (tt, *J* = 12.5, 3.2 Hz, 1H). <sup>13</sup>C NMR (150 MHz, DMSO-*d*<sub>6</sub>) δ 174.0, 168.9, 143.4, 135.7, 134.1, 132.6, 123.8, 123.8, 123.8, 120.9, 120.8, 111.6, 110.0, 44.8, 29.2 (2C, s), 25.4, 25.3 (2C, s). HRMS *m/z* [M+H]<sup>+</sup> calcd for C<sub>19</sub>H<sub>21</sub>N<sub>4</sub>O<sub>2</sub>: 337.1665, found 337.1652, LC *t*<sub>R</sub> = 2.88 min, > 98% Purity.

***N*-[**(3Z)**-2-oxo-3-(1H-pyrrol-2-ylmethylidene)-2,3-dihydro-1H-indol-5-yl]benzamide (72):** Compound **55** was prepared by procedure A to afford a mustard solid (60 mg, 0.182 mmol, 46%). MP 254–256 °C; <sup>1</sup>H NMR (400 MHz, DMSO-*d*<sub>6</sub>) δ 13.34 (s, 1H), 10.87 (s, 1H), 10.17 (s, 1H), 8.08 (d, *J* = 1.9 Hz, 1H), 8.03 – 7.94 (m, 2H), 7.65 (s, 1H), 7.62 – 7.50 (m, 3H), 7.43 – 7.33 (m, 2H), 6.92 (dt, *J* = 3.6, 1.7 Hz, 1H), 6.87 (d, *J* = 8.3 Hz, 1H), 6.36 (dt, *J* = 3.7, 2.3 Hz, 1H). <sup>13</sup>C NMR (100 MHz, DMSO-*d*<sub>6</sub>) δ 169.3, 165.1, 135.4, 135.0, 133.1, 131.4, 129.5, 128.4 (s, 2C), 127.5 (s, 2C), 126.2, 125.8, 125.1, 120.7, 120.3, 116.9, 112.0, 111.5, 109.4. HRMS *m/z* [M+H]<sup>+</sup> calcd for C<sub>20</sub>H<sub>16</sub>N<sub>3</sub>O<sub>2</sub>: 330.1242, found 330.1234, LC *t*<sub>R</sub> = 4.45 min, > 98% Purity.

***N*-[**(3Z)**-3-(1H-imidazol-5-ylmethylidene)-2-oxo-2,3-dihydro-1H-indol-5-yl]benzamide (73):** Compound **73** was prepared by procedure A to afford an orange solid (78 mg, 0.236 mmol, 60%, *E*:*Z* ratio 43:57 - not able to distinguish *E*/*Z* isomers). MP >300 °C; Major diastereoisomer. *N*-(3-((1H-imidazol-5-yl)methylene)-2-oxoindolin-5-yl)benzamide. <sup>1</sup>H NMR (600 MHz, DMSO-*d*<sub>6</sub>) δ 10.25 (bs, 1H), 10.19 (bs, 1H), 8.11 (d, *J* = 2.1 Hz, 1H), 8.01 – 7.95 (m, 3H), 7.84 (s, 1H), 7.74 (s, 1H), 7.55 – 7.49 (m, 3H), 7.45 (dd, *J* = 8.3, 2.0 Hz, 1H), 6.89 (d, *J* = 8.3 Hz, 1H). Minor diastereoisomer. *N*-(3-((1H-imidazol-5-yl)methylene)-2-oxoindolin-5-yl)benzamide. <sup>1</sup>H NMR (600 MHz, DMSO-*d*<sub>6</sub>) δ 10.32 (bs, 1H), 9.31 (bs, 1H), 8.00 – 7.98 (m, 1H), 7.81 (s, 1H), 7.59 – 7.55 (m, 2H), 7.53 – 7.50 (m, 3H), 7.49 (s, 1H), 7.40 (dd, *J* = 8.2, 2.2 Hz, 1H), 6.79 (d, *J* = 8.2 Hz, 1H). HRMS *m/z* [M+H]<sup>+</sup> calcd for C<sub>19</sub>H<sub>15</sub>N<sub>4</sub>O<sub>2</sub>: 331.1195, found 331.1181, LC *t*<sub>R</sub> = 3.20 min, > 98% Purity.

***N*-[**(3Z)**-3-(1H-imidazol-2-ylmethylidene)-2-oxo-2,3-dihydro-1H-indol-5-yl]benzamide (74):** Compound **74** was prepared by procedure A to afford an orange solid (89 mg, 0.269 mmol, 68%). MP >300 °C; <sup>1</sup>H NMR (400 MHz, DMSO-*d*<sub>6</sub>) δ 11.14 (s, 1H), 10.22 (s, 1H), 8.11 (d, *J* = 2.0 Hz, 1H), 7.98 (dd, *J* = 7.0, 1.9 Hz, 2H), 7.62 – 7.51 (m, 6H), 7.35 (d, *J* = 1.4 Hz, 1H), 6.93 (d, *J* = 8.4 Hz, 1H). <sup>13</sup>C NMR (100 MHz, DMSO-*d*<sub>6</sub>) δ 169.0, 165.3, 143.4,

136.4, 134.9, 133.6, 132.6, 131.5, 128.4 (s, 2C), 127.6 (s, 2C), 124.0, 123.8, 123.7, 122.3, 120.9, 113.3, 109.9. HRMS *m/z* [M+H]<sup>+</sup> calcd for C<sub>19</sub>H<sub>15</sub>N<sub>4</sub>O<sub>2</sub>: 331.1195, found 331.1186, LC *t*<sub>R</sub> = 3.23 min, > 98% Purity.

***N*-[**(3Z)**-2-oxo-3-(1H-pyrrol-2-ylmethylidene)-2,3-dihydro-1H-indol-5-yl]furan-2-carboxamide (75):** Compound **75** was prepared by procedure A to afford an orange solid (74 mg, 0.232 mmol, 56%). MP 226–228 °C; <sup>1</sup>H NMR (600 MHz, DMSO-*d*<sub>6</sub>) δ 13.38 (s, 1H), 10.94 (s, 1H), 10.13 (s, 1H), 8.01 (d, *J* = 2.0 Hz, 1H), 7.94 (d, *J* = 1.7 Hz, 1H), 7.64 (s, 1H), 7.39 (dd, *J* = 8.3, 2.0 Hz, 1H), 7.37 (t, *J* = 1.9 Hz, 1H), 7.33 (d, *J* = 3.5 Hz, 1H), 6.91 (dd, *J* = 3.6, 1.4 Hz, 1H), 6.87 (d, *J* = 8.3 Hz, 1H), 6.71 (dd, *J* = 3.5, 1.8 Hz, 1H), 6.36 (dd, *J* = 3.7, 2.4 Hz, 1H). <sup>13</sup>C NMR (150 MHz, DMSO-*d*<sub>6</sub>) δ 174.0, 169.4, 156.1, 147.7, 145.5, 135.8, 132.3, 129.5, 126.2, 125.8, 125.2, 120.6, 120.3, 117.0, 114.2, 112.1, 111.5, 109.5. HRMS *m/z* [M+H]<sup>+</sup> calcd for C<sub>18</sub>H<sub>14</sub>N<sub>3</sub>O<sub>3</sub>: 320.1035, found 320.1018, LC *t*<sub>R</sub> = 3.90 min, > 98% Purity.

***N*-[**(3Z)**-3-(1H-imidazol-2-ylmethylidene)-2-oxo-2,3-dihydro-1H-indol-5-yl]furan-2-carboxamide (76):** Compound **76** was prepared by procedure A to afford an orange solid (72 mg, 0.225 mmol, 54%). MP >300 °C; <sup>1</sup>H NMR (600 MHz, DMSO-*d*<sub>6</sub>) δ 14.06 (s, 1H), 11.14 (s, 1H), 10.14 (s, 1H), 8.06 (d, *J* = 2.0 Hz, 1H), 7.94 (dd, *J* = 1.7, 0.8 Hz, 1H), 7.59 (s, 1H), 7.58 – 7.52 (m, 2H), 7.35 (t, *J* = 1.1 Hz, 1H), 7.31 (dd, *J* = 3.5, 0.8 Hz, 1H), 6.91 (d, *J* = 8.3 Hz, 1H), 6.71 (dd, *J* = 3.5, 1.7 Hz, 1H). <sup>13</sup>C NMR (150 MHz, DMSO-*d*<sub>6</sub>) δ 169.0, 156.2, 147.6, 145.6, 143.4, 136.5, 132.9, 132.6, 124.1, 123.9, 123.6, 122.3, 121.0, 114.4, 113.3, 112.1, 110.0. HRMS *m/z* [M+H]<sup>+</sup> calcd for C<sub>17</sub>H<sub>13</sub>N<sub>4</sub>O<sub>3</sub>: 321.0988, found 321.0979, LC *t*<sub>R</sub> = 2.35 min, > 98% Purity.

**4-cyano-*N*-(2-oxoindolin-5-yl)benzamide (77):** Compound **77** was prepared by procedure F to afford a colourless solid (786 mg, 2.835 mmol, 84%). MP >240 °C (decomp.); <sup>1</sup>H NMR (600 MHz, DMSO-*d*<sub>6</sub>) δ 10.36 (s, 1H), 10.35 (s, 1H), 8.08 (d, *J* = 8.1 Hz, 2H), 8.01 (d, *J* = 8.3 Hz, 2H), 7.66 (d, *J* = 2.1 Hz, 1H), 7.52 (dd, *J* = 8.3, 2.1 Hz, 1H), 6.80 (d, *J* = 8.3 Hz, 1H), 3.50 (s, 2H). <sup>13</sup>C NMR (150 MHz, DMSO-*d*<sub>6</sub>) δ 176.3, 163.7, 140.1, 139.1, 132.7, 132.4 (s, 2C), 128.4 (s, 2C), 126.0, 120.0, 118.4, 117.8, 113.7, 108.9, 36.1. HRMS *m/z* [M+H]<sup>+</sup> calcd for C<sub>16</sub>H<sub>12</sub>N<sub>3</sub>O<sub>2</sub>: 278.0929, found 278.0920, LC *t*<sub>R</sub> = 2.90 min, > 98% Purity.

**3-cyano-*N*-(2-oxoindolin-5-yl)benzamide (78):** Compound **78** was prepared by procedure F to afford a colourless solid (814 mg, 2.936 mmol, 87%). MP 214–216 °C; <sup>1</sup>H NMR (600 MHz, DMSO-*d*<sub>6</sub>) δ 10.36 (s, 1H), 10.30 (s, 1H), 8.37 (t, *J* = 1.7 Hz, 1H), 8.23 (dt, *J* = 7.9, 1.4 Hz, 1H), 8.04 (dt, *J* = 7.7, 1.4 Hz, 1H), 7.74 (t, *J* = 7.8 Hz, 1H), 7.66 (d, *J* = 2.1 Hz, 1H), 7.51 (dd, *J* = 8.4, 2.1 Hz, 1H), 6.81 (d, *J* = 8.3 Hz, 1H), 3.50 (s, 2H). <sup>13</sup>C NMR (150 MHz, DMSO-*d*<sub>6</sub>) δ 176.4, 163.2, 140.1, 136.0, 134.8, 132.7, 132.4, 131.2, 129.8, 126.1, 120.0, 118.4, 117.7, 111.5, 108.9, 36.1. HRMS *m/z* [M+H]<sup>+</sup> calcd for C<sub>16</sub>H<sub>12</sub>N<sub>3</sub>O<sub>2</sub>: 278.0929, found 278.0919, LC *t*<sub>R</sub> = 2.92 min, > 98% Purity.

**2-cyano-*N*-(2-oxoindolin-5-yl)benzamide (79):** Compound **79** was prepared by procedure F to afford a colourless solid (664 mg, 2.395 mmol, 71%). MP 218–220 °C; <sup>1</sup>H NMR (600 MHz, DMSO-*d*<sub>6</sub>) δ 10.53 (s, 1H), 10.18 (s, 1H), 8.23 (s, 1H), 7.91 (ddd, *J* = 33.5, 5.4, 3.1 Hz, 1H), 7.85 (q, *J* = 7.8 Hz, 2H), 7.77 (t, *J* = 7.5 Hz, 1H), 7.26 – 7.19 (m, 2H), 6.93 (d, *J* = 8.2 Hz, 1H), 3.55 (s, 2H). <sup>13</sup>C NMR (150 MHz, DMSO-*d*<sub>6</sub>) δ 176.5, 167.3, 143.7, 134.6, 133.6, 132.5, 131.6, 127.8, 127.2, 126.4, 124.7, 124.0, 123.3, 122.8, 109.1, 35.9. HRMS *m/z* [M+H]<sup>+</sup> calcd for C<sub>16</sub>H<sub>12</sub>N<sub>3</sub>O<sub>2</sub>: 278.0929, found 278.0921, LC *t*<sub>R</sub> = 3.08 min, > 98% Purity.

**4-methoxy-*N*-(2-oxoindolin-5-yl)benzamide (80):** Compound **80** was prepared by procedure F to afford a colourless solid (738 mg, 2.614 mmol, 77%). MP 125-127 °C; <sup>1</sup>H NMR (600 MHz, DMSO-*d*<sub>6</sub>) δ 10.33 (s, 1H), 9.96 (s, 1H), 7.97 – 7.91 (m, 2H), 7.68 – 7.64 (m, 1H), 7.51 (dd, *J* = 8.4, 2.2 Hz, 1H), 7.08 – 7.01 (m, 2H), 6.79 (d, *J* = 8.3 Hz, 1H), 3.83 (s, 3H), 3.49 (s, 2H). <sup>13</sup>C NMR (100 MHz, DMSO-*d*<sub>6</sub>) δ 176.4, 164.6, 161.8, 139.6, 133.3, 129.5 (s, 2C), 127.1, 125.9, 120.0, 117.9, 113.6 (s, 2C), 108.8, 55.4, 36.1. HRMS *m/z* [M+H]<sup>+</sup> calcd for C<sub>16</sub>H<sub>15</sub>N<sub>2</sub>O<sub>3</sub>: 283.1083, found 283.1072, LC *t*<sub>R</sub> = 3.01 min, > 98% Purity.

**3-methoxy-*N*-(2-oxoindolin-5-yl)benzamide (81):** Compound **81** was prepared by procedure F to afford a colourless solid (820 mg, 2.905 mmol, 86%). MP 125-127 °C; <sup>1</sup>H NMR (600 MHz, DMSO-*d*<sub>6</sub>) δ 10.34 (s, 1H), 10.08 (s, 1H), 7.65 (s, 1H), 7.52 (dq, *J* = 7.8, 1.8, 1.2 Hz, 2H), 7.48 – 7.46 (m, 1H), 7.43 (t, *J* = 7.9 Hz, 1H), 7.14 (ddd, *J* = 8.2, 2.6, 1.0 Hz, 1H), 6.79 (d, *J* = 8.3 Hz, 1H), 3.83 (s, 3H), 3.50 (s, 2H). <sup>13</sup>C NMR (150 MHz, DMSO-*d*<sub>6</sub>) δ 176.4, 164.9, 159.2, 139.8, 136.5, 133.1, 129.5, 125.9, 120.0, 119.8, 117.9, 117.1, 112.8, 108.8, 55.3, 36.1. HRMS *m/z* [M+H]<sup>+</sup> calcd for C<sub>16</sub>H<sub>15</sub>N<sub>2</sub>O<sub>3</sub>: 283.1083, found 283.1073, LC *t*<sub>R</sub> = 3.08 min, > 98% Purity.

**2-methoxy-*N*-(2-oxoindolin-5-yl)benzamide (82):** Compound **82** was prepared by procedure F to afford a colourless oil (676 mg, 2.395 mmol, 71%). <sup>1</sup>H NMR (600 MHz, DMSO-*d*<sub>6</sub>) δ 10.33 (s, 1H), 9.98 (s, 1H), 7.65 (d, *J* = 2.0 Hz, 1H), 7.63 (dd, *J* = 7.5, 1.8 Hz, 1H), 7.49 (tdd, *J* = 8.8, 6.9, 2.0 Hz, 2H), 7.17 (d, *J* = 8.4 Hz, 1H), 7.06 (td, *J* = 7.5, 0.9 Hz, 1H), 6.77 (d, *J* = 8.3 Hz, 1H), 3.89 (s, 3H), 3.49 (s, 2H). <sup>13</sup>C NMR (150 MHz, DMSO-*d*<sub>6</sub>) δ 176.4, 164.1, 156.5, 139.6, 133.2, 132.0, 129.7, 126.1, 125.0, 120.5, 119.2, 117.0, 112.0, 108.9, 55.9, 36.1. HRMS *m/z* [M+H]<sup>+</sup> calcd for C<sub>16</sub>H<sub>15</sub>N<sub>2</sub>O<sub>3</sub>: 283.1083, found 283.1072, LC *t*<sub>R</sub> = 3.21 min, > 98% Purity.

**4-fluoro-*N*-(2-oxoindolin-5-yl)benzamide (83):** Compound **83** was prepared by procedure F to afford a colourless solid (812 mg, 3.005 mmol, 89%). MP 150-152 °C; <sup>1</sup>H NMR (600 MHz, DMSO-*d*<sub>6</sub>) δ 10.38 (s, 1H), 10.17 (s, 1H), 8.04 – 7.99 (m, 2H), 7.65 (d, *J* = 2.0 Hz, 1H), 7.50 (dd, *J* = 8.4, 2.1 Hz, 1H), 7.35 (t, *J* = 8.8 Hz, 2H), 6.80 (d, *J* = 8.3 Hz, 1H), 3.49 (s, 2H). <sup>13</sup>C NMR (150 MHz, DMSO-*d*<sub>6</sub>) δ 176.4, 164.1, 164.0 (d, *J* = 248.8 Hz), 139.9, 133.1, 131.5 (d, *J* = 3.0 Hz), 130.3 (d, *J* = 9.0 Hz, 2C), 126.0, 120.1, 117.9, 115.3 (d, *J* = 21.8 Hz, 2C), 108.8, 36.1. HRMS *m/z* [M+H]<sup>+</sup> calcd for C<sub>15</sub>H<sub>12</sub>FN<sub>2</sub>O<sub>2</sub>: 271.0883, found 271.0872, LC *t*<sub>R</sub> = 3.09 min, > 98% Purity.

**3-fluoro-*N*-(2-oxoindolin-5-yl)benzamide (84):** Compound **84** was prepared by procedure F to afford a colourless solid (830 mg, 3.071 mmol, 91%). MP 89-91 °C; <sup>1</sup>H NMR (600 MHz, DMSO-*d*<sub>6</sub>) δ 10.40 (s, 1H), 10.23 (s, 1H), 7.80 (dd, *J* = 7.8, 1.3 Hz, 1H), 7.75 (dt, *J* = 9.8, 2.1 Hz, 1H), 7.66 (d, *J* = 2.0 Hz, 1H), 7.57 (td, *J* = 8.0, 5.8 Hz, 1H), 7.52 (dd, *J* = 8.4, 2.1 Hz, 1H), 7.43 (td, *J* = 8.5, 2.6 Hz, 1H), 6.80 (d, *J* = 8.3 Hz, 1H), 3.50 (s, 2H). <sup>13</sup>C NMR (150 MHz, DMSO-*d*<sub>6</sub>) δ 176.4, 163.7 (d, *J* = 2.3 Hz), 161.9 (d, *J* = 244.2 Hz), 140.0, 137.4 (d, *J* = 6.8 Hz), 132.9, 130.6 (d, *J* = 8.1 Hz), 126.0, 123.8 (d, *J* = 2.7 Hz), 120.1, 118.3 (d, *J* = 21.2 Hz), 117.9, 114.4 (d, *J* = 22.9 Hz), 108.8, 36.1. HRMS *m/z* [M+H]<sup>+</sup> calcd for C<sub>15</sub>H<sub>12</sub>FN<sub>2</sub>O<sub>2</sub>: 271.0883, found 271.0873, LC *t*<sub>R</sub> = 3.12 min, > 98% Purity.

**2-fluoro-*N*-(2-oxoindolin-5-yl)benzamide (85):** Compound **85** was prepared by procedure F to afford a colourless solid (438 mg, 1.621 mmol, 48%). MP 85-87 °C; <sup>1</sup>H NMR (600 MHz,

DMSO-*d*<sub>6</sub>) δ 10.36 (s, 1H), 10.26 (s, 1H), 7.74 – 7.59 (m, 2H), 7.56 (d, *J* = 9.0 Hz, 1H), 7.48 (d, *J* = 8.2 Hz, 1H), 7.33 (t, *J* = 9.8 Hz, 2H), 6.79 (t, *J* = 6.5 Hz, 1H), 3.49 (s, 2H). <sup>13</sup>C NMR (150 MHz, DMSO-*d*<sub>6</sub>) δ 176.4, 162.4, 158.9 (d, *J* = 248.2 Hz), 139.9, 133.0, 132.3 (d, *J* = 8.2 Hz), 129.9 (d, *J* = 2.8 Hz), 126.1, 125.21 (d, *J* = 15.3 Hz), 124.6 (d, *J* = 3.1 Hz), 119.2, 117.0, 116.2 (d, *J* = 21.8 Hz), 108.9, 36.1. HRMS *m/z* [M+H]<sup>+</sup> calcd for C<sub>15</sub>H<sub>12</sub>FN<sub>2</sub>O<sub>2</sub>: 271.0883, found 271.0866, LC *t*<sub>R</sub> = 3.14 min, > 98% Purity.

***N*-(2-oxoindolin-5-yl)-4-(trifluoromethyl)benzamide (86):** Compound **86** was prepared by procedure F to afford a colourless solid (897 mg, 2.801 mmol, 83%). MP 140-142 °C; <sup>1</sup>H NMR (400 MHz, DMSO-*d*<sub>6</sub>) δ 10.39 (s, 1H), 10.34 (s, 1H), 7.84 (dd, *J* = 8.0, 1.3 Hz, 1H), 7.78 (t, *J* = 7.5 Hz, 1H), 7.75 – 7.63 (m, 2H), 7.60 (d, *J* = 2.0 Hz, 1H), 7.43 (dd, *J* = 8.4, 2.1 Hz, 1H), 6.79 (d, *J* = 8.3 Hz, 1H). <sup>13</sup>C NMR (100 MHz, DMSO-*d*<sub>6</sub>) δ 176.4, 165.2, 139.9, 136.4 (q, *J* = 2.2 Hz), 133.0, 131.2 (d, *J* = 272.0 Hz), 128.5, 126.3 (m, 1C), 126.2, 125.8 (d, *J* = 31.3 Hz), 125.2, 122.5, 119.1, 116.9, 108.9, 36.1. HRMS *m/z* [M+H]<sup>+</sup> calcd for C<sub>16</sub>H<sub>12</sub>F<sub>3</sub>N<sub>2</sub>O<sub>2</sub>: 321.0851, found 321.0841, LC *t*<sub>R</sub> = 3.69 min, > 98% Purity.

***N*-(2-oxoindolin-5-yl)-2-(trifluoromethyl)benzamide (87):** Compound **87** was prepared by procedure F to afford a colourless solid (778 mg, 2.429 mmol, 72%). MP >240 °C (decomp.); <sup>1</sup>H NMR (400 MHz, DMSO-*d*<sub>6</sub>) δ 10.39 (s, 1H), 10.34 (s, 1H), 7.84 (dd, *J* = 7.9, 1.2 Hz, 1H), 7.81 – 7.75 (m, 1H), 7.73 – 7.64 (m, 2H), 7.60 (d, *J* = 2.0 Hz, 1H), 7.44 (dd, *J* = 8.4, 2.1 Hz, 1H), 6.79 (d, *J* = 8.3 Hz, 1H), 3.50 (s, 2H). <sup>13</sup>C NMR (100 MHz, DMSO-*d*<sub>6</sub>) δ 176.4, 165.2, 139.9, 136.5 (q, *J* = 2.4 Hz), 133.0, 132.6, 129.9, 128.5, 126.3 (q, *J* = 4.5 Hz), 126.2, 125.8 (d, *J* = 31.3 Hz), 123.8 (d, *J* = 273.9 Hz), 119.1, 116.9, 108.9, 36.1. HRMS *m/z* [M+H]<sup>+</sup> calcd for C<sub>16</sub>H<sub>12</sub>F<sub>3</sub>N<sub>2</sub>O<sub>2</sub>: 321.0851, found 321.0839, LC *t*<sub>R</sub> = 3.23 min, > 98% Purity.

**4-cyano-*N*-[(3*Z*)-3-(1*H*-imidazol-5-yl)methylidene]-2-oxo-2,3-dihydro-1*H*-indol-5-yl]benzamide (88):** Compound **88** was prepared by procedure A to afford a red/orange solid (68 mg, 0.191 mmol, 53%, *E:Z* ratio 50:50 - not able to distinguish *E/Z* isomers). MP >300 °C; Diastereoisomer 1. *N*-(3-((1*H*-imidazol-5-yl)methylene)-2-oxoindolin-5-yl)-4-cyanobenzamide. <sup>1</sup>H NMR (600 MHz, DMSO-*d*<sub>6</sub>) δ 10.50 (s, 1H), 9.48 (d, *J* = 2.2 Hz, 1H), 8.14 – 8.12 (m, 2H), 8.05 – 8.02 (m, 2H), 7.60 (s, 1H), 7.58 (s, 1H), 7.35 (bs, 1H), 6.94 (d, *J* = 8.3 Hz, 1H). Diastereoisomer 2. *N*-(3-((1*H*-imidazol-5-yl)methylene)-2-oxoindolin-5-yl)-4-cyanobenzamide. <sup>1</sup>H NMR (600 MHz, DMSO-*d*<sub>6</sub>) δ 10.55 (s, 1H), 10.46 (s, 1H), 8.14 – 8.12 (m, 2H), 8.12 – 8.10 (m, 1H), 8.05 – 8.02 (m, 2H), 7.56 (s, 2H), 7.52 (bs, 1H), 7.41 (s, 1H), 7.39 (bs, 1H), 6.86 (d, *J* = 8.3 Hz, 1H). HRMS *m/z* [M+H]<sup>+</sup> calcd for C<sub>20</sub>H<sub>14</sub>N<sub>5</sub>O<sub>2</sub>: 356.1148, found 356.1138, LC *t*<sub>R</sub> = 3.13 min, > 98% Purity.

**3-cyano-*N*-[(3*Z*)-3-(1*H*-imidazol-5-yl)methylidene]-2-oxo-2,3-dihydro-1*H*-indol-5-yl]benzamide (89):** Compound **89** was prepared by procedure A to afford a red/orange solid (73 mg, 0.205 mmol, 73%, *E:Z* ratio 43:57 - not able to distinguish *E/Z* isomers). MP >250 °C (decomp.); Major diastereoisomer. *N*-(3-((1*H*-imidazol-5-yl)methylene)-2-oxoindolin-5-yl)-3-cyanobenzamide. <sup>1</sup>H NMR (600 MHz, DMSO-*d*<sub>6</sub>) δ 12.94 (bs, 1H), 10.55 (s, 1H), 9.48 (d, *J* = 2.2 Hz, 1H), 8.43 (s, 1H), 8.29 – 8.26 (m, 1H), 8.07 (tt, *J* = 7.9, 1.4 Hz, 2H), 7.78 – 7.74 (m, 1H), 7.58 (m, 1H), 7.58 – 7.56 (m, 1H), 7.41 (s, 1H), 6.86 (d, *J* = 8.3 Hz, 1H). Minor diastereoisomer. *N*-(3-((1*H*-imidazol-5-yl)methylene)-2-oxoindolin-5-yl)-3-cyanobenzamide. <sup>1</sup>H NMR (600 MHz, DMSO-*d*<sub>6</sub>) δ 14.06 (bs, 1H), 11.18 (bs, 1H), 10.45 (s, 1H), 8.43 – 8.42 (m, 1H), 8.29 – 8.26 (m, 1H), 8.10 (d, *J* = 2.1 Hz, 1H), 8.06



– 7.98 (m, 1H), 7.78 – 7.74 (m, 1H), 7.60 (s, 1H), 7.57 – 7.56 (m, 1H), 7.41 (s, 1H), 7.36 (s, 1H), 6.95 (d,  $J = 8.3$  Hz, 1H). HRMS  $m/z$   $[M+H]^+$  calcd for  $C_{20}H_{14}N_5O_2$ : 356.1148, found 356.1142, LC  $t_R = 3.13$  min, > 98% Purity.

**3-cyano-*N*-[(3*Z*)-3-(1*H*-imidazol-2-ylmethylidene)-2-oxo-2,3-dihydro-1*H*-indol-5-yl]benzamide (90):** Compound **90** was prepared by procedure A to afford a yellow/mustard solid (69 mg, 0.194 mmol, 54%). MP >250 °C (decomp.);  $^1H$  NMR (600 MHz, DMSO- $d_6$ )  $\delta$  13.70 (s, 1H), 11.02 (s, 1H), 10.40 (s, 1H), 8.42 (t,  $J = 1.7$  Hz, 1H), 8.27 (dt,  $J = 8.0, 1.5$  Hz, 1H), 8.13 (d,  $J = 2.0$  Hz, 1H), 8.07 (dt,  $J = 7.7, 1.4$  Hz, 1H), 8.03 (s, 1H), 7.79 (d,  $J = 3.7$  Hz, 1H), 7.76 (d,  $J = 7.8$  Hz, 1H), 7.73 (s, 1H), 7.43 (dd,  $J = 8.4, 2.0$  Hz, 1H), 6.91 (d,  $J = 8.3$  Hz, 1H).  $^{13}C$  NMR (150 MHz, DMSO- $d_6$ )  $\delta$  169.1, 163.3, 139.7, 138.9, 136.4, 135.9, 134.9, 133.0, 132.4, 131.2, 129.9, 128.1, 124.4, 123.0, 121.2, 120.0, 118.4, 112.6, 111.5, 109.8. HRMS  $m/z$   $[M+H]^+$  calcd for  $C_{20}H_{14}N_5O_2$ : 356.1148, found 356.1140, LC  $t_R = 3.18$  min, > 98% Purity.

**2-cyano-*N*-[(3*Z*)-3-(1*H*-imidazol-2-ylmethylidene)-2-oxo-2,3-dihydro-1*H*-indol-5-yl]benzamide (91):** Compound **91** was prepared by procedure A to afford an orange solid (76 mg, 0.214 mmol, 59%, *E/Z* ratio 25:75 - not able to distinguish *E/Z* isomers). MP >300 °C; (*Z*)-*N*-(3-((1*H*-imidazol-2-yl)methylene)-2-oxoindolin-5-yl)-2-cyanobenzamide.  $^1H$  NMR (600 MHz, DMSO- $d_6$ )  $\delta$  13.28 (bs, 1H), 11.07 (bs, 1H), 8.18 (s, 1H), 7.78 – 7.77 (m, 1H), 7.77 (s, 1H), 7.33 (s, 1H), 6.87 (s, 1H), 6.82 (d,  $J = 8.0$  Hz, 1H), 6.35 – 6.34 (m, 1H). (*E*)-*N*-(3-((1*H*-imidazol-2-yl)methylene)-2-oxoindolin-5-yl)-2-cyanobenzamide.  $^1H$  NMR (600 MHz, DMSO- $d_6$ )  $\delta$  11.91 (bs, 1H), 10.59 (bs, 1H), 8.59 (s, 1H), 7.81 (dd,  $J = 8.0, 1.4$  Hz, 1H), 7.52 (s, 1H), 7.20 (s, 1H), 7.10 (s, 1H), 6.80 (d,  $J = 8.0$  Hz, 1H), 6.41 (s, 1H). HRMS  $m/z$   $[M+H]^+$  calcd for  $C_{20}H_{14}N_5O_2$ : 356.1148, found 356.1135, LC  $t_R = 2.45$  min, > 98% Purity.

***N*-[(3*Z*)-3-(1*H*-imidazol-5-ylmethylidene)-2-oxo-2,3-dihydro-1*H*-indol-5-yl]-4-methoxybenzamide (92):** Compound **92** was prepared by procedure A to afford a yellow solid (70 mg, 0.194 mmol, 55%). MP 275-277 °C;  $^1H$  NMR (600 MHz, DMSO- $d_6$ )  $\delta$  13.69 (s, 1H), 10.91 (s, 1H), 10.04 (s, 1H), 8.10 (s, 1H), 8.00 (s, 1H), 7.99 – 7.95 (m, 2H), 7.74 (s, 2H), 7.43 (dd,  $J = 8.3, 2.0$  Hz, 1H), 7.09 – 7.05 (m, 2H), 6.87 (d,  $J = 8.3$  Hz, 1H), 3.84 (s, 3H).  $^{13}C$  NMR (150 MHz, DMSO- $d_6$ )  $\delta$  176.3, 168.9, 164.6, 161.8, 136.0, 133.5, 129.4 (s, 2C), 127.0, 124.4, 121.3, 120.4, 119.9, 117.8, 113.6 (s, 2C), 112.7, 109.6, 108.7, 55.4. HRMS  $m/z$   $[M+H]^+$  calcd for  $C_{20}H_{17}N_4O_3$ : 361.1301, found 361.1291, LC  $t_R = 2.74$  min, > 98% Purity.

***N*-[(3*Z*)-3-(1*H*-imidazol-2-ylmethylidene)-2-oxo-2,3-dihydro-1*H*-indol-5-yl]-4-methoxybenzamide (93):** Compound **93** was prepared by procedure A to afford a bright orange solid (91 mg, 0.253 mmol, 71%). MP >300 °C;  $^1H$  NMR (400 MHz, DMSO- $d_6$ )  $\delta$  11.14 (s, 1H), 10.06 (s, 1H), 8.10 (d,  $J = 2.0$  Hz, 1H), 8.02 – 7.94 (m, 2H), 7.66 – 7.49 (m, 3H), 7.36 (s, 1H), 7.12 – 7.04 (m, 2H), 6.95 – 6.87 (m, 1H), 3.84 (s, 3H).  $^{13}C$  NMR (100 MHz, DMSO- $d_6$ )  $\delta$  169.0, 164.7, 161.8, 143.4, 136.2, 133.8, 132.6, 129.5 (2C, s), 126.9, 123.9, 123.8, 123.8, 122.3, 120.9, 113.6 (2C, s), 113.2, 109.9, 55.4. HRMS  $m/z$   $[M+H]^+$  calcd for  $C_{20}H_{17}N_4O_3$ : 361.1301, found 361.1292, LC  $t_R = 3.25$  min, > 98% Purity.

***N*-[(3*Z*)-3-(1*H*-imidazol-5-ylmethylidene)-2-oxo-2,3-dihydro-1*H*-indol-5-yl]-3-methoxybenzamide (94):** Compound **94** was prepared by procedure A to afford a yellow solid (98 mg, 0.272 mmol, 70%). MP 138-140 °C;  $^1H$  NMR (400 MHz, DMSO- $d_6$ )  $\delta$  13.71 (s, 1H), 10.99 (s, 1H), 10.18 (s, 1H), 8.12 (d,  $J = 2.0$  Hz, 1H), 8.03 (s, 1H), 7.78 (s, 1H), 7.72 (s, 1H), 7.58 – 7.55 (m, 1H),

7.52 (dd,  $J = 2.7, 1.5$  Hz, 1H), 7.48 – 7.44 (m, 1H), 7.44 – 7.41 (m, 1H), 7.16 (ddd,  $J = 8.2, 2.6, 1.0$  Hz, 1H), 6.89 (d,  $J = 8.4$  Hz, 1H), 3.85 (s, 3H).  $^{13}C$  NMR (100 MHz, DMSO- $d_6$ )  $\delta$  169.1, 164.9, 159.2, 139.7, 138.8, 136.3, 136.2, 133.3, 129.6, 128.1, 124.3, 122.9, 121.4, 120.1, 119.8, 117.2, 112.8, 109.7, 55.3. HRMS  $m/z$   $[M+H]^+$  calcd for  $C_{20}H_{17}N_4O_3$ : 361.1301, found 361.1288, LC  $t_R = 2.78$  min, > 98% Purity.

***N*-[(3*Z*)-3-(1*H*-imidazol-2-ylmethylidene)-2-oxo-2,3-dihydro-1*H*-indol-5-yl]-3-methoxybenzamide (95):** Compound **95** was prepared by procedure A to afford a red solid (55 mg, 0.153 mmol, 43%, *E/Z* ratio 37:63 - not able to distinguish *E/Z* isomers). MP >300 °C; Major diastereoisomer. *N*-(3-((1*H*-imidazol-2-yl)methylene)-2-oxoindolin-5-yl)-3-methoxybenzamide.  $^1H$  NMR (600 MHz, DMSO- $d_6$ )  $\delta$  12.90 (bs, 1H), 11.15 (bs, 1H), 10.53 (s, 1H), 10.21 (s, 1H), 9.44 (d,  $J = 2.2$  Hz, 1H), 7.58 – 7.40 (m, 5H), 7.40 (s, 1H), 7.15 (tdd,  $J = 8.2, 2.7, 0.9$  Hz, 1H), 6.85 (d,  $J = 8.2$  Hz, 1H), 3.85 (s, 3H). Minor diastereoisomer. *N*-(3-((1*H*-imidazol-2-yl)methylene)-2-oxoindolin-5-yl)-3-methoxybenzamide.  $^1H$  NMR (600 MHz, DMSO- $d_6$ )  $\delta$  14.07 (s, 1H), 10.19 (s, 1H), 8.10 (d,  $J = 2.0$  Hz, 1H), 7.60 (s, 1H), 7.58 – 7.40 (m, 5H), 7.35 (d,  $J = 1.2$  Hz, 1H), 7.17 – 7.14 (m, 1H), 6.93 (d,  $J = 8.3$  Hz, 1H), 3.84 (s, 3H). HRMS  $m/z$   $[M+H]^+$  calcd for  $C_{20}H_{17}N_4O_3$ : 361.1301, found 361.1291, LC  $t_R = 3.28$  min, > 98% Purity.

***N*-[(3*Z*)-3-(1*H*-imidazol-5-ylmethylidene)-2-oxo-2,3-dihydro-1*H*-indol-5-yl]-2-methoxybenzamide (96):** Compound **96** was prepared by procedure A to afford a mustard/yellow solid (59 mg, 0.164 mmol, 46%). MP >250 °C (decomp.);  $^1H$  NMR (600 MHz, DMSO- $d_6$ )  $\delta$  13.70 (s, 1H), 10.94 (d,  $J = 74.7$  Hz, 1H), 10.44 (s, 1H), 8.21 – 7.99 (m, 6H), 7.76 (s, 2H), 7.52 – 7.39 (m, 1H), 6.90 (d,  $J = 8.3$  Hz, 1H), 3.34 (s, 3H).  $^{13}C$  NMR (150 MHz, DMSO- $d_6$ )  $\delta$  206.5, 169.0, 163.8, 139.7, 139.0, 136.5, 132.9, 132.5 (s, 2C), 128.4 (s, 2C), 124.5, 123.0, 121.3, 120.1, 118.4, 113.8, 112.6, 109.7, 30.7. HRMS  $m/z$   $[M+H]^+$  calcd for  $C_{20}H_{17}N_4O_3$ : 361.1301, found 361.1290, LC  $t_R = 2.96$  min, > 98% Purity.

***N*-[(3*Z*)-3-(1*H*-imidazol-2-ylmethylidene)-2-oxo-2,3-dihydro-1*H*-indol-5-yl]-2-methoxybenzamide (97):** Compound **97** was prepared by procedure A to afford a bright red solid (49 mg, 0.136 mmol, 38%). MP >300 °C;  $^1H$  NMR (600 MHz, DMSO- $d_6$ )  $\delta$  14.08 (s, 1H), 11.13 (s, 1H), 10.08 (s, 1H), 8.07 (d,  $J = 2.0$  Hz, 1H), 7.74 (dd,  $J = 7.6, 1.8$  Hz, 1H), 7.68 (dd,  $J = 8.4, 2.0$  Hz, 1H), 7.65 (s, 1H), 7.57 (d,  $J = 2.2$  Hz, 1H), 7.53 – 7.51 (m, 1H), 7.36 (t,  $J = 1.2$  Hz, 1H), 7.20 (dd,  $J = 8.5, 0.9$  Hz, 1H), 7.09 (td,  $J = 7.5, 1.0$  Hz, 1H), 6.91 (d,  $J = 8.4$  Hz, 1H), 3.96 (s, 3H).  $^{13}C$  NMR (150 MHz, DMSO- $d_6$ )  $\delta$  169.0, 163.9, 156.6, 143.5, 136.2, 133.7, 132.6, 132.3, 130.0, 124.2, 124.2, 124.0, 123.7, 121.3, 120.9, 120.6, 112.3, 112.1, 110.0, 56.0. HRMS  $m/z$   $[M+H]^+$  calcd for  $C_{20}H_{17}N_4O_3$ : 361.1301, found 361.1290, LC  $t_R = 2.84$  min, > 98% Purity.

**4-fluoro-*N*-[(3*Z*)-3-[(1*H*-imidazol-5-yl)methylidene]-2-oxo-2,3-dihydro-1*H*-indol-5-yl]benzamide (98):** Compound **98** was prepared by procedure A to afford a yellow/orange solid (57 mg, 0.164 mmol, 44%). MP >250 °C (decomp.);  $^1H$  NMR (600 MHz, DMSO- $d_6$ )  $\delta$  13.72 (s, 1H), 11.00 (s, 1H), 10.22 (s, 1H), 8.12 (s, 1H), 8.07 – 8.04 (m, 2H), 8.03 (s, 1H), 7.75 (d,  $J = 32.5$  Hz, 2H), 7.48 – 7.39 (m, 1H), 7.39 – 7.36 (m, 2H), 6.89 (d,  $J = 8.3$  Hz, 1H).  $^{13}C$  NMR (150 MHz, DMSO- $d_6$ )  $\delta$  169.1, 164.1, 164.0 (d,  $J = 250.0$  Hz), 139.7, 138.8, 136.3, 133.3, 131.4 (d,  $J = 2.8$  Hz), 130.3 (d,  $J = 8.9$  Hz, 2C), 128.1, 124.4, 122.9, 121.4, 120.2, 115.4 (d,  $J = 21.8$  Hz, 2C), 112.8, 109.7. HRMS  $m/z$   $[M+H]^+$  calcd for  $C_{19}H_{14}FN_4O_2$ : 349.1101, found 349.1092, LC  $t_R = 2.80$  min, > 98% Purity.



**4-fluoro-*N*-[(3*Z*)-3-[(1*H*-imidazol-2-yl)methylidene]-2-oxo-2,3-dihydro-1*H*-indol-5-yl]benzamide (99):** Compound **99** was prepared by procedure A to afford an orange solid (87 mg, 0.250 mmol, 68%). MP >300 °C (decomp.); <sup>1</sup>H NMR (400 MHz, DMSO-*d*<sub>6</sub>) δ 11.15 (s, 1H), 10.23 (s, 1H), 8.14 – 8.01 (m, 3H), 7.59 (s, 1H), 7.56 (dd, *J* = 8.4, 2.0 Hz, 1H), 7.45 – 7.27 (m, 3H), 6.93 (d, *J* = 8.3 Hz, 1H). <sup>13</sup>C NMR (100 MHz, DMSO-*d*<sub>6</sub>) δ 169.0, 164.2, 164.0 (d, *J* = 249.0 Hz), 143.4, 136.4, 133.5, 132.6, 131.3 (d, *J* = 3.0 Hz), 130.3, 130.2, 124.0, 123.8 (2C, d, *J* = 19.9 Hz), 122.3, 121.0, 115.3 (2C, d, *J* = 21.8 Hz), 113.3, 109.9. HRMS *m/z* [M+H]<sup>+</sup> calcd for C<sub>19</sub>H<sub>14</sub>FN<sub>4</sub>O<sub>2</sub>: 349.1101, found 349.1091, LC *t*<sub>R</sub> = 2.74 min, > 98% Purity.

**3-fluoro-*N*-[(3*Z*)-3-[(1*H*-imidazol-5-yl)methylidene]-2-oxo-2,3-dihydro-1*H*-indol-5-yl]benzamide (100):** Compound **100** was prepared by procedure A to afford an orange solid (67 mg, 0.192 mmol, 52%). MP >300 °C; <sup>1</sup>H NMR (600 MHz, DMSO-*d*<sub>6</sub>) δ 13.71 (s, 1H), 11.00 (s, 1H), 10.28 (s, 1H), 8.12 (s, 1H), 8.03 (s, 1H), 7.84 (dt, *J* = 7.8, 1.2 Hz, 1H), 7.83 – 7.75 (m, 2H), 7.73 (s, 1H), 7.60 (td, *J* = 8.0, 5.8 Hz, 1H), 7.50 – 7.38 (m, 2H), 6.90 (d, *J* = 8.3 Hz, 1H). <sup>13</sup>C NMR (150 MHz, DMSO-*d*<sub>6</sub>) δ 169.1, 163.8 (d, *J* = 2.7 Hz), 162.0 (d, *J* = 244.4 Hz), 139.7, 138.9, 137.2 (d, *J* = 6.8 Hz), 136.4, 133.1, 130.6 (d, *J* = 8.1 Hz), 128.1, 124.4, 123.8 (d, *J* = 2.6 Hz), 123.0, 121.4, 120.1, 118.4 (d, *J* = 21.1 Hz), 114.4 (d, *J* = 22.8 Hz), 112.8, 109.8. HRMS *m/z* [M+H]<sup>+</sup> calcd for C<sub>19</sub>H<sub>14</sub>FN<sub>4</sub>O<sub>2</sub>: 349.1101, found 349.1090, LC *t*<sub>R</sub> = 2.80 min, > 98% Purity.

**3-fluoro-*N*-[(3*Z*)-3-[(1*H*-imidazol-2-yl)methylidene]-2-oxo-2,3-dihydro-1*H*-indol-5-yl]benzamide (101):** Compound **101** was prepared by procedure A to afford a yellow solid (75 mg, 0.215 mmol, 58%, *E/Z* ratio 35:65), MP >210 °C (decomp.); (*Z*)-*N*-(3-((1*H*-imidazol-2-yl)methylene)-2-oxoindolin-5-yl)-3-fluorobenzamide. <sup>1</sup>H NMR (600 MHz, DMSO-*d*<sub>6</sub>) δ 10.54 (s, 1H), 10.32 (s, 1H), 9.46 (d, *J* = 2.2 Hz, 1H), 7.86 – 7.83 (m, 1H), 7.81 – 7.77 (m, 1H), 7.59 – 7.56 (m, 1H), 7.53 (dd, *J* = 8.3, 2.2 Hz, 1H), 7.47 – 7.42 (m, 2H), 7.41 (s, 1H), 6.85 (d, *J* = 8.3 Hz, 1H). (*E*)-*N*-(3-((1*H*-imidazol-2-yl)methylene)-2-oxoindolin-5-yl)-3-fluorobenzamide. <sup>1</sup>H NMR (600 MHz, DMSO-*d*<sub>6</sub>) δ 14.06 (s, 1H), 10.29 (s, 1H), 8.10 (d, *J* = 2.0 Hz, 1H), 7.86 – 7.83 (m, 1H), 7.81 – 7.77 (m, 1H), 7.60 (s, 1H), 7.59 – 7.56 (m, 1H), 7.47 – 7.42 (m, 2H), 7.35 (s, 1H), 6.94 (d, *J* = 8.3 Hz, 1H). HRMS *m/z* [M+H]<sup>+</sup> calcd for C<sub>19</sub>H<sub>14</sub>FN<sub>4</sub>O<sub>2</sub>: 349.1101, found 349.1088, LC *t*<sub>R</sub> = 3.33 min, > 98% Purity.

**2-fluoro-*N*-[(3*Z*)-3-[(1*H*-imidazol-2-yl)methylidene]-2-oxo-2,3-dihydro-1*H*-indol-5-yl]benzamide (102):** Compound **102** was prepared by procedure A to afford an orange solid (48 mg, 0.138 mmol, 37%). MP >300 °C; <sup>1</sup>H NMR (400 MHz, DMSO-*d*<sub>6</sub>) δ 11.15 (s, 1H), 10.33 (s, 1H), 8.09 (d, *J* = 2.0 Hz, 1H), 7.69 (td, *J* = 7.4, 1.8 Hz, 1H), 7.62 – 7.57 (m, 2H), 7.54 (dd, *J* = 8.4, 2.0 Hz, 1H), 7.45 – 7.22 (m, 3H), 6.92 (d, *J* = 8.3 Hz, 1H). <sup>13</sup>C NMR (100 MHz, DMSO-*d*<sub>6</sub>) δ 169.0, 162.5, 158.9 (d, *J* = 248.8 Hz), 143.4, 136.4, 133.4, 132.5 (d, *J* = 8.4 Hz), 129.9 (d, *J* = 3.0 Hz), 125.0, 124.9, 124.6 (d, *J* = 3.4 Hz), 124.1, 123.9, 123.6, 121.5, 121.1–120.9 (m), 116.2 (d, *J* = 22.0 Hz), 112.4, 110.1. HRMS *m/z* [M+H]<sup>+</sup> calcd for C<sub>19</sub>H<sub>14</sub>FN<sub>4</sub>O<sub>2</sub>: 349.1101, found 349.1084, LC *t*<sub>R</sub> = 2.83 min, > 98% Purity.

***N*-[(3*Z*)-3-[(1*H*-imidazol-5-yl)methylidene]-2-oxo-2,3-dihydro-1*H*-indol-5-yl]-4-(trifluoromethyl)benzamide (103):** Compound **100** was prepared by procedure A to afford a yellow solid (58 mg, 0.146 mmol, 47%). MP >300 °C; <sup>1</sup>H NMR (600 MHz, DMSO-*d*<sub>6</sub>) δ 13.71 (s, 1H), 11.01 (s, 1H), 10.44 (s, 1H), 8.17 (d, *J* = 8.0 Hz, 2H), 8.14 (d, *J* = 2.0 Hz, 1H), 8.03 – 8.02 (m, 1H),

7.93 (d, *J* = 8.2 Hz, 2H), 7.80 (s, 1H), 7.73 (s, 1H), 7.43 (dd, *J* = 8.3, 2.0 Hz, 1H), 6.91 (d, *J* = 8.3 Hz, 1H). <sup>13</sup>C NMR (150 MHz, DMSO-*d*<sub>6</sub>) δ 169.1, 164.0, 139.7, 138.9, 138.7, 136.4, 133.0, 131.3 (q, *J* = 32.8, 31.9 Hz), 128.5 (s, 2C), 128.1, 125.5 (dd, *J* = 4.9, 2.2 Hz, 2C), 124.9, 124.4, 123.0 (d, *J* = 6.1 Hz), 121.4, 120.1, 112.8, 109.8. HRMS *m/z* [M+H]<sup>+</sup> calcd for C<sub>20</sub>H<sub>14</sub>F<sub>3</sub>N<sub>4</sub>O<sub>2</sub>: 399.1069, found 399.1058, LC *t*<sub>R</sub> = 3.25 min, > 98% Purity.

**(*Z*)-*N*-(3-((1*H*-imidazol-2-yl)methylene)-2-oxoindolin-5-yl)-4-(trifluoromethyl)benzamide (104):** Compound **104** was prepared by procedure A to afford a yellow solid (51 mg, 0.128 mmol, 41%, *E/Z* ratio 34:66 - not able to distinguish *E/Z* isomers). MP >210 °C (decomp.); Major diastereoisomer. *N*-(3-((1*H*-imidazol-2-yl)methylene)-2-oxoindolin-5-yl)-4-(trifluoromethyl)benzamide. <sup>1</sup>H NMR (600 MHz, DMSO-*d*<sub>6</sub>) δ 12.87 (bs, 1H), 10.55 (bs, 1H), 10.48 (s, 1H), 9.48 (d, *J* = 2.2 Hz, 1H), 8.18 – 8.17 (m, 2H), 7.92 – 7.91 (m, 2H), 7.61 – 7.56 (m, 2H), 7.41 (s, 1H), 6.86 (d, *J* = 8.3 Hz, 1H). Minor diastereoisomer. *N*-(3-((1*H*-imidazol-2-yl)methylene)-2-oxoindolin-5-yl)-4-(trifluoromethyl)benzamide. <sup>1</sup>H NMR (600 MHz, DMSO-*d*<sub>6</sub>) δ 14.06 (bs, 1H), 11.16 (bs, 1H), 10.45 (s, 1H), 8.18 – 8.17 (m, 2H), 7.97 – 7.92 (m, 2H), 7.61 (s, 1H), 7.46 (bs, 2H), 7.35 (s, 1H), 6.95 (d, *J* = 8.3 Hz, 1H). HRMS *m/z* [M+H]<sup>+</sup> calcd for C<sub>20</sub>H<sub>14</sub>F<sub>3</sub>N<sub>4</sub>O<sub>2</sub>: 399.1069, found 399.1058, LC *t*<sub>R</sub> = 3.20 min, > 98% Purity.

***N*-[(3*Z*)-3-[(1*H*-imidazol-5-yl)methylidene]-2-oxo-2,3-dihydro-1*H*-indol-5-yl]-2-(trifluoromethyl)benzamide (105):** Compound **105** was prepared by procedure A to afford a yellow solid (46 mg, 0.116 mmol, 37%, *E/Z* ratio 38:62 - not able to distinguish *E/Z* isomers). MP 225–227 °C; Major Diastereoisomer. *N*-(3-((1*H*-imidazol-5-yl)methylene)-2-oxoindolin-5-yl)-2-(trifluoromethyl)benzamide. <sup>1</sup>H NMR (600 MHz, DMSO-*d*<sub>6</sub>) δ 10.47 (bs, 1H), 10.42 (bs, 1H), 9.29 (d, *J* = 2.1 Hz, 1H), 7.88 (s, 2H), 7.86 – 7.68 (m, 4H), 7.60 (dd, *J* = 8.3, 2.2 Hz, 1H), 7.50 (s, 1H), 6.82 (d, *J* = 8.3 Hz, 1H). Minor Diastereoisomer. *N*-(3-((1*H*-imidazol-5-yl)methylene)-2-oxoindolin-5-yl)-2-(trifluoromethyl)benzamide. <sup>1</sup>H NMR (600 MHz, DMSO-*d*<sub>6</sub>) δ 10.53 (bs, 1H), 8.09 (d, *J* = 2.0 Hz, 1H), 8.00 (s, 1H), 7.95 (s, 1H), 7.86 – 7.68 (m, 5H), 7.34 (dd, *J* = 8.3, 2.0 Hz, 1H), 6.89 (d, *J* = 8.3 Hz, 1H). HRMS *m/z* [M+H]<sup>+</sup> calcd for C<sub>20</sub>H<sub>14</sub>F<sub>3</sub>N<sub>4</sub>O<sub>2</sub>: 399.1069, found 399.1058, LC *t*<sub>R</sub> = 2.89 min, > 98% Purity.

***N*-[(3*Z*)-3-[(1*H*-imidazol-2-yl)methylidene]-2-oxo-2,3-dihydro-1*H*-indol-5-yl]-2-(trifluoromethyl)benzamide (106):** Compound **106** was prepared by procedure A to afford a yellow solid (56 mg, 0.141 mmol, 45%, *E/Z* ratio 34:66 - not able to distinguish *E/Z* isomers). MP >300 °C; Major diastereoisomer. *N*-(3-((1*H*-imidazol-2-yl)methylene)-2-oxoindolin-5-yl)-2-(trifluoromethyl)benzamide. <sup>1</sup>H NMR (600 MHz, DMSO-*d*<sub>6</sub>) δ 12.93 (bs, 1H), 10.54 (bs, 1H), 10.50 (bs, 1H), 9.45 (d, *J* = 2.1 Hz, 1H), 7.87 – 7.83 (m, 1H), 7.81 – 7.77 (m, 1H), 7.73 – 7.68 (m, 3H), 7.50 (s, 1H), 7.41 (s, 1H), 7.36 (s, 1H), 6.85 (d, *J* = 8.3 Hz, 1H). Minor diastereoisomer. *N*-(3-((1*H*-imidazol-2-yl)methylene)-2-oxoindolin-5-yl)-2-(trifluoromethyl)benzamide. <sup>1</sup>H NMR (600 MHz, DMSO-*d*<sub>6</sub>) δ 14.07 (bs, 1H), 11.17 (bs, 1H), 10.51 (bs, 1H), 8.04 (d, *J* = 2.0 Hz, 1H), 7.81 – 7.77 (m, 1H), 7.70 – 7.68 (m, 3H), 7.58 – 7.57 (m, 2H), 7.52 (d, *J* = 2.0 Hz, 1H), 7.37 – 7.34 (m, 1H), 6.93 (d, *J* = 8.3 Hz, 1H). HRMS *m/z* [M+H]<sup>+</sup> calcd for C<sub>20</sub>H<sub>14</sub>F<sub>3</sub>N<sub>4</sub>O<sub>2</sub>: 399.1069, found 399.1057, LC *t*<sub>R</sub> = 2.86 min, > 98% Purity.

***N*-(2-oxoindolin-5-yl)thiophene-2-carboxamide (107):** Compound **107** was prepared by procedure F to afford a red solid (514 mg, 1.991 mmol, 59%). MP 105–107 °C; <sup>1</sup>H NMR (600 MHz, DMSO-*d*<sub>6</sub>) δ 10.34 (s, 1H), 10.10 (s, 1H), 7.97 (dd, *J* = 3.7, 1.1 Hz,

1H), 7.82 (dd,  $J = 5.0, 1.1$  Hz, 1H), 7.63 – 7.57 (m, 1H), 7.46 (dd,  $J = 8.4, 2.1$  Hz, 1H), 7.21 (dd,  $J = 5.0, 3.7$  Hz, 1H), 6.79 (d,  $J = 8.3$  Hz, 1H), 3.50 (s, 2H).  $^{13}\text{C}$  NMR (150 MHz, DMSO- $d_6$ )  $\delta$  176.3, 159.6, 140.3, 139.9, 132.6, 131.5, 128.7, 128.0, 126.1, 120.1, 117.9, 108.9, 36.1. HRMS  $m/z$   $[\text{M}+\text{H}]^+$  calcd for  $\text{C}_{13}\text{H}_{11}\text{N}_2\text{O}_2\text{S}$ : 259.0541, found 259.0532, LC  $t_{\text{R}} = 2.84$  min, > 98% Purity.

### 3-methoxy-*N*-(2-oxoindolin-5-yl)thiophene-2-carboxamide

(108): Compound 108 was prepared by procedure F to afford a beige solid (662 mg, 2.296 mmol, 68%). MP 75-77 °C;  $^1\text{H}$  NMR (600 MHz, DMSO- $d_6$ )  $\delta$  10.37 (s, 1H), 9.14 (s, 1H), 7.80 (d,  $J = 5.5$  Hz, 1H), 7.59 – 7.55 (m, 1H), 7.43 (dd,  $J = 8.3, 2.2$  Hz, 1H), 7.18 (d,  $J = 5.6$  Hz, 1H), 6.77 (d,  $J = 8.3$  Hz, 1H), 4.06 (s, 3H), 3.48 (s, 2H).  $^{13}\text{C}$  NMR (150 MHz, DMSO- $d_6$ )  $\delta$  176.3, 159.1, 156.7, 139.8, 132.2, 130.4, 126.2, 119.6, 117.4, 117.1, 115.6, 108.9, 59.5, 36.0. HRMS  $m/z$   $[\text{M}+\text{H}]^+$  calcd for  $\text{C}_{14}\text{H}_{13}\text{N}_2\text{O}_3\text{S}$ : 289.0647, found 289.0637, LC  $t_{\text{R}} = 3.05$  min, > 98% Purity.

### 3-ethoxy-*N*-(2-oxoindolin-5-yl)thiophene-2-carboxamide

(109): Compound 109 was prepared by procedure F to afford a beige solid (796 mg, 2.633 mmol, 78%). MP 98-100 °C;  $^1\text{H}$  NMR (600 MHz, DMSO- $d_6$ )  $\delta$  10.33 (s, 1H), 9.20 (s, 1H), 7.78 (d,  $J = 5.5$  Hz, 1H), 7.56 – 7.51 (m, 1H), 7.39 (dd,  $J = 8.4, 2.1$  Hz, 1H), 7.16 (d,  $J = 5.5$  Hz, 1H), 6.78 (d,  $J = 8.3$  Hz, 1H), 4.33 (q,  $J = 7.0$  Hz, 2H), 3.49 (s, 2H), 1.45 (t,  $J = 7.0$  Hz, 3H).  $^{13}\text{C}$  NMR (150 MHz, DMSO- $d_6$ )  $\delta$  176.3, 159.0, 155.8, 139.8, 132.3, 130.4, 126.4, 119.0, 117.5, 116.9, 115.9, 109.1, 68.0, 36.1, 14.8. HRMS  $m/z$   $[\text{M}+\text{H}]^+$  calcd for  $\text{C}_{15}\text{H}_{15}\text{N}_2\text{O}_3\text{S}$ : 303.0803, found 303.0795, LC  $t_{\text{R}} = 3.56$  min, > 98% Purity.

### 3-fluoro-*N*-(2-oxoindolin-5-yl)thiophene-2-carboxamide (110):

Compound 110 was prepared by procedure F to afford a beige solid (532 mg, 1.926 mmol, 57%). MP 101-103 °C; HRMS  $m/z$   $[\text{M}+\text{H}]^+$  calcd for  $\text{C}_{13}\text{H}_{10}\text{FN}_2\text{O}_2\text{S}$ : 277.0447, found 277.0438, LC  $t_{\text{R}} = 3.35$  min, > 98% Purity.

### *N*-(2-oxoindolin-5-yl)thieno[3,2-*b*]thiophene-2-carboxamide

(111): Compound 111 was prepared by procedure F to afford a beige solid (366 mg, 1.164 mmol, 69%). MP 125-127 °C; HRMS  $m/z$   $[\text{M}+\text{H}]^+$  calcd for  $\text{C}_{15}\text{H}_{11}\text{N}_2\text{O}_2\text{S}_2$ : 315.0262, found 315.0251, LC  $t_{\text{R}} = 3.45$  min, > 98% Purity.

### 2-fluoro-*N*-(2-oxoindolin-5-yl)-5-(trifluoromethyl)benzamide

(112): Compound 112 was prepared by procedure F to afford a beige solid (651 mg, 1.925 mmol, 57%). MP 96-97 °C;  $^1\text{H}$  NMR (600 MHz, DMSO- $d_6$ )  $\delta$  10.46 (s, 1H), 10.38 (s, 1H), 8.03 (dd,  $J = 6.2, 2.5$  Hz, 1H), 7.97 (dt,  $J = 7.7, 3.2$  Hz, 1H), 7.65 – 7.54 (m, 2H), 7.46 (dd,  $J = 8.3, 2.1$  Hz, 1H), 6.81 (d,  $J = 8.3$  Hz, 1H), 3.50 (s, 2H).  $^{13}\text{C}$  NMR (150 MHz, DMSO- $d_6$ )  $\delta$  176.4, 162.0-160.0 (m, 1C), 140.1, 132.6, 129.6 (dd,  $J = 9.6, 3.9$  Hz), 127.3 (p,  $J = 3.9$  Hz), 126.2, 126.1 (d,  $J = 17.0$  Hz), 125.4 (qd,  $J = 32.8, 3.2$  Hz), 124.5, 122.7, 119.4, 117.7 (d,  $J = 23.5$  Hz), 117.2, 109.0, 36.1. HRMS  $m/z$   $[\text{M}+\text{H}]^+$  calcd for  $\text{C}_{16}\text{H}_{11}\text{F}_4\text{N}_2\text{O}_2$ : 339.0757, found 339.0740, LC  $t_{\text{R}} = 3.80$  min, > 98% Purity.

### *N*-(2-oxoindolin-5-yl)benzo[*d*][1,3]dioxole-4-carboxamide

(113): Compound 113 was prepared by procedure F to afford a beige solid (750 mg, 2.531 mmol, 75%). MP 105-107 °C;  $^1\text{H}$  NMR (600 MHz, DMSO- $d_6$ )  $\delta$  10.38 (s, 1H), 9.70 (s, 1H), 7.60 (d,  $J = 2.0$  Hz, 1H), 7.47 (dd,  $J = 8.4, 2.0$  Hz, 1H), 7.22 (d,  $J = 8.1$  Hz, 1H), 7.10 (d,  $J = 7.7$  Hz, 1H), 6.96 (t,  $J = 7.9$  Hz, 1H), 6.78 (d,  $J = 8.3$  Hz, 1H), 6.15 (s, 2H), 3.49 (s, 2H).  $^{13}\text{C}$  NMR (150 MHz, DMSO- $d_6$ )  $\delta$  176.3, 161.8, 147.8, 145.2, 139.9, 132.7, 126.1, 121.7, 121.1, 119.4, 117.7, 117.2, 110.9, 108.90, 101.7, 36.1. HRMS  $m/z$   $[\text{M}+\text{H}]^+$  calcd for  $\text{C}_{16}\text{H}_{13}\text{N}_2\text{O}_4$ : 297.0875, found 297.0865, LC  $t_{\text{R}} = 3.18$  min, > 98% Purity.

*N*-(2-oxoindolin-5-yl)thiazole-2-carboxamide (114): Compound 114 was prepared by procedure F to afford a beige solid (735 mg, 2.835 mmol, 84%). MP 108-110 °C;  $^1\text{H}$  NMR (600 MHz, DMSO- $d_6$ )  $\delta$  10.71 (s, 1H), 10.39 (s, 1H), 8.38 (s, 1H), 7.68 (d,  $J = 2.0$  Hz, 1H), 7.57 (dd,  $J = 8.4, 2.1$  Hz, 1H), 7.53 (s, 1H), 6.79 (d,  $J = 8.4$  Hz, 1H), 3.50 (s, 2H).  $^{13}\text{C}$  NMR (150 MHz, DMSO- $d_6$ )  $\delta$  176.4, 155.1, 152.9, 142.5, 140.4, 131.8, 128.3, 126.1, 120.3, 117.8, 108.9, 36.0. HRMS  $m/z$   $[\text{M}+\text{H}]^+$  calcd for  $\text{C}_{12}\text{H}_{10}\text{N}_3\text{O}_2\text{S}$ : 260.0494, found 260.0484, LC  $t_{\text{R}} = 2.72$  min, > 98% Purity.

### *N*-(2-oxoindolin-5-yl)oxazole-2-carboxamide (115):

Compound 115 was prepared by procedure F to afford a beige solid (345 mg, 1.418 mmol, 70%). MP 87-89 °C;  $^1\text{H}$  NMR (600 MHz, DMSO- $d_6$ )  $\delta$  10.65 (s, 1H), 10.39 (s, 1H), 8.13 – 8.07 (m, 2H), 7.72 (d,  $J = 2.0$  Hz, 1H), 7.63 (dd,  $J = 8.4, 2.1$  Hz, 1H), 6.80 (d,  $J = 8.4$  Hz, 1H), 3.49 (s, 2H).  $^{13}\text{C}$  NMR (150 MHz, DMSO- $d_6$ )  $\delta$  176.8, 164.6, 157.9, 144.4, 140.7, 132.4, 126.7, 126.5, 120.7, 118.3, 109.3, 36.5. HRMS  $m/z$   $[\text{M}+\text{H}]^+$  calcd for  $\text{C}_{12}\text{H}_{10}\text{N}_3\text{O}_3$ : 244.0722, found 244.0709, LC  $t_{\text{R}} = 2.25$  min, > 98% Purity.

### *N*-(2-oxoindolin-5-yl)isothiazole-5-carboxamide (116):

Compound 116 was prepared by procedure A to afford a beige solid (328 mg, 1.265 mmol, 75%). MP 178-180 °C;  $^1\text{H}$  NMR (400 MHz, DMSO- $d_6$ )  $\delta$  10.47 (s, 1H), 10.38 (s, 1H), 8.71 (d,  $J = 1.8$  Hz, 1H), 8.09 (d,  $J = 1.8$  Hz, 1H), 7.61 (d,  $J = 2.0$  Hz, 1H), 7.47 (dd,  $J = 8.4, 2.1$  Hz, 1H), 6.82 (d,  $J = 8.3$  Hz, 1H), 3.51 (s, 2H).  $^{13}\text{C}$  NMR (100 MHz, DMSO- $d_6$ )  $\delta$  176.33, 163.32, 159.18, 157.40, 140.49, 131.77, 126.22, 123.87, 120.32, 117.97, 108.97, 36.03. HRMS  $m/z$   $[\text{M}+\text{H}]^+$  calcd for  $\text{C}_{12}\text{H}_{10}\text{N}_3\text{O}_2\text{S}$ : 260.0494, found 260.0485, LC  $t_{\text{R}} = 2.57$  min, > 98% Purity.

### *N*-[(3*Z*)-3-[(1*H*-imidazol-5-yl)methylidene]-2-oxo-2,3-dihydro-1*H*-indol-5-yl]thiophene-2-carboxamide (117):

Compound 117 was prepared by procedure A to afford an orange solid (89 mg, 0.265 mmol, 68%). MP > 300 °C;  $^1\text{H}$  NMR (600 MHz, DMSO- $d_6$ )  $\delta$  13.71 (s, 1H), 11.00 (s, 1H), 10.22 (s, 1H), 8.06 (d,  $J = 2.0$  Hz, 1H), 8.03 (s, 1H), 8.01 – 8.00 (m, 1H), 7.84 (dd,  $J = 5.0, 1.1$  Hz, 1H), 7.80 (s, 1H), 7.71 (s, 1H), 7.39 (dd,  $J = 8.3, 2.0$  Hz, 1H), 7.23 (dd,  $J = 5.0, 3.7$  Hz, 1H), 6.90 (d,  $J = 8.3$  Hz, 1H).  $^{13}\text{C}$  NMR (150 MHz, DMSO- $d_6$ )  $\delta$  169.1, 159.7, 140.2, 139.7, 138.8, 136.3, 132.8, 131.6, 128.8, 128.1 (s, 2C), 124.5, 123.0, 121.4, 120.1, 112.9, 109.8. HRMS  $m/z$   $[\text{M}+\text{H}]^+$  calcd for  $\text{C}_{17}\text{H}_{13}\text{N}_4\text{O}_2\text{S}$ : 337.0759, found 327.0721, LC  $t_{\text{R}} = 2.78$  min, > 98% Purity.

### *N*-[(3*Z*)-3-[(1*H*-imidazol-2-yl)methylidene]-2-oxo-2,3-dihydro-1*H*-indol-5-yl]thiophene-2-carboxamide (118):

Compound 118 was prepared by procedure A to afford an orange solid (92 mg, 0.274 mmol, 71%, *E*:*Z* ratio 34:66 - not able to distinguish *E*/*Z* isomers). MP > 300 °C; Major diastereoisomer. *N*-(3-((1*H*-imidazol-2-yl)methylene)-2-oxoindolin-5-yl)thiophene-2-carboxamide.  $^1\text{H}$  NMR (600 MHz, DMSO- $d_6$ )  $\delta$  12.94 (bs, 1H), 10.55 (bs, 1H), 10.26 (bs, 1H), 9.42 (d,  $J = 2.2$  Hz, 1H), 8.05 (d,  $J = 3.9$  Hz, 1H), 7.83 (dd,  $J = 5.0, 1.1$  Hz, 1H), 7.49 (dd,  $J = 8.3, 2.2$  Hz, 1H), 7.50 – 7.44 (bs, 2H), 7.41 (s, 1H), 7.22 (dd,  $J = 5.0, 3.7$  Hz, 1H), 6.85 (d,  $J = 8.3$  Hz, 1H). Minor diastereoisomer. *N*-(3-((1*H*-imidazol-2-yl)methylene)-2-oxoindolin-5-yl)thiophene-2-carboxamide.  $^1\text{H}$  NMR (600 MHz, DMSO- $d_6$ )  $\delta$  14.07 (bs, 1H), 11.16 (bs, 1H), 10.22 (bs, 1H), 8.06 (d,  $J = 2.0$  Hz, 1H), 8.01 (dd,  $J = 3.8, 1.2$  Hz, 1H), 7.85 (dd,  $J = 5.0, 1.1$  Hz, 1H), 7.62 (s, 1H), 7.57 (d,  $J = 2.1$  Hz, 1H), 7.52 (dd,  $J = 8.4, 2.1$  Hz, 1H), 7.36 (bt,  $J = 1.2$  Hz, 1H), 7.23 (dd,  $J = 5.0, 3.7$  Hz, 1H), 6.93 (d,  $J = 8.3$  Hz, 1H). HRMS  $m/z$   $[\text{M}+\text{H}]^+$  calcd for  $\text{C}_{17}\text{H}_{13}\text{N}_4\text{O}_2\text{S}$ : 337.0759, found 337.0753, LC  $t_{\text{R}} = 3.07$  min, > 98% Purity.

**(Z)-N-(3-((1H-imidazol-5-yl)methylene)-2-oxoindolin-5-yl)-3-methoxythiophene-2-carboxamide (119):** Compound **119** was prepared by procedure A to afford an orange solid (45 mg, 0.123 mmol, 35%). MP 268-270 °C; <sup>1</sup>H NMR (400 MHz, DMSO-*d*<sub>6</sub>) δ 13.72 (s, 1H), 10.99 (s, 1H), 9.20 (s, 1H), 8.03 (s, 1H), 7.96 (d, *J* = 2.0 Hz, 1H), 7.84 – 7.80 (m, 2H), 7.69 (s, 1H), 7.50 – 7.47 (m, 1H), 7.20 (d, *J* = 5.6 Hz, 1H), 6.87 (d, *J* = 8.3 Hz, 1H), 4.09 (s, 3H). <sup>13</sup>C NMR (100 MHz, DMSO-*d*<sub>6</sub>) δ 169.1, 159.2, 156.8, 139.7, 138.7, 136.2, 132.5, 130.5, 128.1, 124.6, 123.1, 120.7, 120.0, 117.1, 115.5, 112.3, 109.7, 59.6. HRMS *m/z* [M+H]<sup>+</sup> calcd for C<sub>18</sub>H<sub>15</sub>N<sub>4</sub>O<sub>3</sub>S: 367.0865, found 367.0854, LC *t*<sub>R</sub> = 2.78 min, > 98% Purity.

**3-ethoxy-N-[(3Z)-3-[(1H-imidazol-5-yl)methylidene]-2-oxo-2,3-dihydro-1H-indol-5-yl]thiophene-2-carboxamide (120):**

Compound **120** was prepared by procedure A to afford an orange solid (52 mg, 0.137 mmol, 41%, *E*:*Z* ratio 28:72 - not able to distinguish *E/Z* isomers). MP Decomp. >250 °C; Major diastereoisomer. *N*-(3-((1*H*-imidazol-5-yl)methylene)-2-oxoindolin-5-yl)-3-ethoxythiophene-2-carboxamide. <sup>1</sup>H NMR (600 MHz, DMSO-*d*<sub>6</sub>) δ 12.74 (bs, 1H), 10.39 (bs, 1H), 9.32 (s, 1H), 9.23 (bs, 1H), 7.96 – 7.95 (m, 2H), 7.87 (dd, *J* = 8.3, 2.2 Hz, 1H), 7.81 (d, *J* = 5.5 Hz, 1H), 7.51 (s, 1H), 7.21 (d, *J* = 5.5 Hz, 1H), 6.81 (d, *J* = 8.3 Hz, 1H), 4.41 – 4.37 (m, 2H), 1.59 (t, *J* = 6.9 Hz, 3H). Minor diastereoisomer. *N*-(3-((1*H*-imidazol-5-yl)methylene)-2-oxoindolin-5-yl)-3-ethoxythiophene-2-carboxamide. <sup>1</sup>H NMR (600 MHz, DMSO-*d*<sub>6</sub>) δ 13.73 (bs, 1H), 10.99 (bs, 1H), 9.25 (s, 1H), 8.02 (d, *J* = 14.3 Hz, 2H), 7.83 (s, 1H), 7.81 – 7.79 (m, 1H), 7.71 (s, 1H), 7.37 (dd, *J* = 8.4, 2.1 Hz, 1H), 7.19 (d, *J* = 5.5 Hz, 1H), 6.89 (d, *J* = 8.3 Hz, 1H), 4.39 – 4.35 (m, 2H), 1.47 (t, *J* = 7.0 Hz, 3H). HRMS *m/z* [M+H]<sup>+</sup> calcd for C<sub>19</sub>H<sub>17</sub>N<sub>4</sub>O<sub>3</sub>S: 381.1021, found 381.1007, LC *t*<sub>R</sub> = 3.03 min, > 98% Purity.

**3-fluoro-N-[(3Z)-3-[(1H-imidazol-5-yl)methylidene]-2-oxo-2,3-dihydro-1H-indol-5-yl]thiophene-2-carboxamide (121):**

Compound **121** was prepared by procedure A to afford an orange solid (37 mg, 0.104 mmol, 29%). MP >300 °C; <sup>1</sup>H NMR (400 MHz, DMSO-*d*<sub>6</sub>) δ 13.69 (s, 1H), 11.00 (s, 1H), 9.83 – 9.72 (m, 1H), 8.03 (s, 1H), 7.98 (d, *J* = 2.0 Hz, 1H), 7.86 (dd, *J* = 5.5, 4.0 Hz, 1H), 7.81 (s, 1H), 7.70 (s, 1H), 7.38 (dd, *J* = 8.3, 2.0 Hz, 1H), 7.16 (d, *J* = 5.5 Hz, 1H), 6.88 (d, *J* = 8.3 Hz, 1H). <sup>13</sup>C NMR (100 MHz, DMSO-*d*<sub>6</sub>) δ 169.10, 157.67, 156.86, 154.22, 139.70, 138.82, 136.49, 132.43, 129.77 (d, *J* = 9.9 Hz), 128.08, 124.46, 123.10, 121.51, 119.97, 118.30 (d, *J* = 26.4 Hz), 113.03, 109.72. HRMS *m/z* [M+H]<sup>+</sup> calcd for C<sub>17</sub>H<sub>12</sub>FN<sub>4</sub>O<sub>2</sub>S: 355.0665, found 355.0652, LC *t*<sub>R</sub> = 2.68 min, > 98% Purity.

**(Z)-N-(3-((1H-imidazol-5-yl)methylene)-2-oxoindolin-5-yl)thieno[3,2-*b*]thiophene-2-carboxamide (122):**

Compound **122** was prepared by procedure A to afford a light orange solid (45 mg, 0.110 mmol, 36%). MP >250 °C (decomp.); <sup>1</sup>H NMR (600 MHz, DMSO-*d*<sub>6</sub>) δ 13.68 (s, 1H), 10.95 (s, 1H), 10.34 (s, 1H), 8.34 (s, 1H), 8.09 (d, *J* = 2.0 Hz, 1H), 8.01 (s, 1H), 7.89 (d, *J* = 5.2 Hz, 1H), 7.78 (s, 1H), 7.54 (d, *J* = 5.2 Hz, 1H), 7.40 (dd, *J* = 8.2, 2.0 Hz, 1H), 6.90 (d, *J* = 8.3 Hz, 1H). <sup>13</sup>C NMR (150 MHz, DMSO-*d*<sub>6</sub>) δ 169.0, 160.1, 142.0, 141.6, 139.4, 138.5, 136.3, 132.7, 131.8, 124.5, 121.4 (s, 2C), 121.2, 120.6, 120.4 (s, 2C), 120.3, 112.7, 109.7. HRMS *m/z* [M+H]<sup>+</sup> calcd for C<sub>19</sub>H<sub>13</sub>N<sub>4</sub>O<sub>2</sub>S<sub>2</sub>: 393.0480, found 393.0468, LC *t*<sub>R</sub> = 3.08 min, > 98% Purity.

**2-fluoro-N-[(3Z)-3-[(1H-imidazol-5-yl)methylidene]-2-oxo-2,3-dihydro-1H-indol-5-yl]-5-(trifluoromethyl)benzamide (123):**

Compound **123** was prepared by procedure A to afford an orange solid (21 mg, 0.062 mmol, 21%). MP 202-204 °C; <sup>1</sup>H NMR

(600 MHz, DMSO-*d*<sub>6</sub>) δ 13.73 (s, 1H), 10.99 (s, 1H), 10.75 (s, 1H), 8.22 (s, 1H), 8.03 (s, 1H), 7.85 (d, *J* = 2.3 Hz, 1H), 7.79 – 7.75 (m, 2H), 7.35 (dd, *J* = 9.4, 5.8 Hz, 2H), 6.91 (d, *J* = 8.4 Hz, 1H). <sup>13</sup>C NMR (150 MHz, DMSO) δ 169.1, 164.6, 154.3, 139.7, 139.0, 136.1, 133.3, 128.9, 128.1, 126.7, 125.3, 124.6, 123.5, 123.0, 121.7, 121.4, 120.1, 119.8, 111.4, 110.1. HRMS *m/z* [M+H]<sup>+</sup> calcd for C<sub>20</sub>H<sub>13</sub>F<sub>4</sub>N<sub>4</sub>O<sub>2</sub>: 417.0975, found 417.0962, LC *t*<sub>R</sub> = 3.22 min, > 98% Purity.

**(Z)-N-(3-((1H-imidazol-5-yl)methylene)-2-oxoindolin-5-yl)benzo[d][1,3]dioxole-4-carboxamide (124):**

Compound **124** was prepared by procedure A to afford a brown/red solid (47 mg, 0.126 mmol, 37%). MP 189-191 °C; <sup>1</sup>H NMR (600 MHz, DMSO-*d*<sub>6</sub>) δ 13.71 (s, 1H), 10.96 (s, 1H), 9.72 (s, 1H), 8.30 (s, 1H), 8.06 – 8.03 (m, 1H), 8.00 (d, *J* = 4.2 Hz, 1H), 7.85 – 7.66 (m, 2H), 7.45 (dt, *J* = 8.3, 3.1 Hz, 1H), 7.27 (dd, *J* = 8.1, 1.1 Hz, 1H), 7.12 (dd, *J* = 7.7, 1.1 Hz, 1H), 6.98 (t, *J* = 7.9 Hz, 1H), 6.88 (d, *J* = 8.3 Hz, 1H), 6.18 (s, 2H). <sup>13</sup>C NMR (150 MHz, DMSO-*d*<sub>6</sub>) δ 169.0, 161.9, 147.8, 145.3, 139.5, 136.3, 134.6, 132.9, 128.5, 124.6, 121.7, 121.1, 120.6, 120.3, 117.5, 112.0, 111.0, 109.7, 101.7, 43.8. HRMS *m/z* [M+H]<sup>+</sup> calcd for C<sub>20</sub>H<sub>15</sub>N<sub>4</sub>O<sub>4</sub>: 375.1093, found 375.1081, LC *t*<sub>R</sub> = 2.85 min, > 98% Purity.

**N-[(3Z)-3-[(1H-imidazol-5-yl)methylidene]-2-oxo-2,3-dihydro-1H-indol-5-yl]-1,3-thiazole-2-carboxamide (125):**

Compound **125** was prepared by procedure A to afford a mustard green solid (60 mg, 0.178 mmol, 46%). MP 271-273 °C; <sup>1</sup>H NMR (600 MHz, DMSO-*d*<sub>6</sub>) δ 13.70 (s, 1H), 11.01 (s, 1H), 10.70 (s, 1H), 8.17 (s, 1H), 8.13 – 8.10 (m, 2H), 8.03 (s, 1H), 7.74 (d, *J* = 24.9 Hz, 2H), 7.55 (d, *J* = 8.0 Hz, 1H), 6.89 (d, *J* = 8.3 Hz, 1H). <sup>13</sup>C NMR (150 MHz, DMSO-*d*<sub>6</sub>) δ 169.1, 164.1, 157.6, 157.6, 144.0, 139.7, 138.9, 136.6, 132.2, 126.4, 124.5, 123.0, 121.5, 120.1, 112.7, 109.8. HRMS *m/z* [M+H]<sup>+</sup> calcd for C<sub>16</sub>H<sub>12</sub>N<sub>5</sub>O<sub>2</sub>S: 338.0712, found 338.0700, LC *t*<sub>R</sub> = 2.52 min, > 98% Purity.

**N-[(3Z)-3-[(1H-imidazol-5-yl)methylidene]-2-oxo-2,3-dihydro-1H-indol-5-yl]-1,3-oxazole-2-carboxamide (126):**

Compound **126** was prepared by procedure A to afford a dark orange solid (57 mg, 0.177 mmol, 43%). MP >300 °C; <sup>1</sup>H NMR (400 MHz, DMSO-*d*<sub>6</sub>) δ 13.68 (s, 1H), 10.99 (s, 1H), 10.73 (s, 1H), 8.38 (dd, *J* = 6.0, 0.8 Hz, 1H), 8.15 – 7.96 (m, 2H), 7.73 (d, *J* = 14.6 Hz, 2H), 7.52 (dd, *J* = 4.0, 0.8 Hz, 1H), 7.47 (d, *J* = 7.7 Hz, 1H), 6.83 (dd, *J* = 29.0, 8.3 Hz, 1H). <sup>13</sup>C NMR (100 MHz, DMSO-*d*<sub>6</sub>) δ 169.1, 155.1, 153.0, 142.6, 139.7, 138.9, 136.7, 132.0, 128.4, 128.0, 124.4, 123.1, 121.5, 119.9, 112.7, 109.8. HRMS *m/z* [M+H]<sup>+</sup> calcd for C<sub>16</sub>H<sub>12</sub>N<sub>5</sub>O<sub>3</sub>: 322.0940, found 322.0930, LC *t*<sub>R</sub> = 2.21 min, > 98% Purity.

**N-[(3Z/E)-3-[(1H-imidazol-5-yl)methylidene]-2-oxo-2,3-dihydro-1H-indol-5-yl]-1,2-thiazole-5-carboxamide (127):**

Compound **127** was prepared by procedure A to afford an orange solid (48 mg, 0.142 mmol, 37%, *E*:*Z* ratio 30:70). MP >300 °C; (Z)-*N*-(3-((1*H*-imidazol-5-yl)methylene)-2-oxoindolin-5-yl)isothiazole-5-carboxamide. <sup>1</sup>H NMR (600 MHz, DMSO-*d*<sub>6</sub>) δ 12.74 (s, 1H), 10.60 (s, 1H), 10.46 (s, 1H), 9.41 (d, *J* = 2.1 Hz, 1H), 8.72 (dd, *J* = 3.5, 1.7 Hz, 1H), 8.16 (d, *J* = 1.8 Hz, 1H), 8.03 (s, 1H), 7.95 (s, 1H), 7.54 (s, 1H), 7.50 – 7.44 (m, 1H), 6.86 (d, *J* = 8.2 Hz, 1H). (E)-*N*-(3-((1*H*-imidazol-5-yl)methylene)-2-oxoindolin-5-yl)isothiazole-5-carboxamide. <sup>1</sup>H NMR (600 MHz, DMSO-*d*<sub>6</sub>) δ 13.71 (s, 1H), 11.05 (s, 1H), 10.59 (s, 1H), 8.12 (s, 0H), 8.07 (s, 1H), 8.04 (s, 1H), 7.82 (s, 1H), 7.73 (s, 1H), 7.42 (d, *J* = 7.5 Hz, 1H), 6.93 (d, *J* = 8.3 Hz, 1H). HRMS *m/z* [M+H]<sup>+</sup> calcd for C<sub>16</sub>H<sub>12</sub>N<sub>5</sub>O<sub>2</sub>S: 338.0712, found 338.0699, LC *t*<sub>R</sub> = 2.41 min, > 98% Purity.



**N-[(3Z)-3-[(4-methyl-1H-imidazol-5-yl)methylidene]-2-oxo-2,3-dihydro-1H-indol-5-yl]benzamide (128):** Compound **128** was prepared by procedure A to afford a light orange solid (59 mg, 0.171 mmol, 43%). MP >270 °C (decomp.); <sup>1</sup>H NMR (400 MHz, DMSO-*d*<sub>6</sub>) δ 13.91 (s, 1H), 11.02 (s, 1H), 10.23 (s, 1H), 8.15 (d, *J* = 2.0 Hz, 1H), 8.07 – 8.02 (m, 2H), 7.99 (s, 1H), 7.71 (d, *J* = 0.7 Hz, 1H), 7.67 – 7.62 (m, 1H), 7.62 – 7.56 (m, 2H), 7.51 (dd, *J* = 8.4, 2.0 Hz, 1H), 6.94 (d, *J* = 8.3 Hz, 1H), 2.50 (s, 3H). <sup>13</sup>C NMR (100 MHz, DMSO-*d*<sub>6</sub>) δ 169.5, 165.2, 147.6, 138.2, 135.9, 134.8, 133.1, 131.5, 128.4 (s, 2C), 127.5 (s, 2C), 124.8, 124.4, 122.3, 121.4, 118.1, 113.4, 109.5, 13.1. HRMS *m/z* [M+H]<sup>+</sup> calcd for C<sub>20</sub>H<sub>17</sub>N<sub>4</sub>O<sub>2</sub>: 345.1352, found 345.1342, LC *t*<sub>R</sub> = 2.76 min, > 98% Purity.

**N-[(3Z)-2-oxo-3-(1H-pyrazol-5-yl)methylidene]-2,3-dihydro-1H-indol-5-yl]benzamide (129):** Compound **129** was prepared by procedure A to afford a dark red/purple solid (87 mg, 0.263 mmol, 66%). MP 218–220 °C; <sup>1</sup>H NMR (600 MHz, DMSO-*d*<sub>6</sub>) δ 13.54 (s, 1H), 10.53 (s, 1H), 10.21 (s, 1H), 7.99 – 7.97 (m, 2H), 7.91 (d, *J* = 2.2 Hz, 1H), 7.72 – 7.44 (m, 6H), 6.88 (s, 1H), 6.86 (d, *J* = 8.3 Hz, 1H). <sup>13</sup>C NMR (150 MHz, DMSO-*d*<sub>6</sub>) δ 169.6, 165.3, 165.2, 139.2, 136.8, 135.0, 134.9, 132.5, 131.5, 131.4, 128.42, 128.36, 127.59, 127.55, 125.3, 123.9, 121.7, 109.8, 109.1. HRMS *m/z* [M+H]<sup>+</sup> calcd for C<sub>19</sub>H<sub>15</sub>N<sub>4</sub>O<sub>2</sub>: 331.1195, found 331.1185, LC *t*<sub>R</sub> = 3.56 min, > 98% Purity.

## Notes

The authors declare no competing financial interests.

## Acknowledgement

The SGC is a registered charity (number 1097737) that receives funds from AbbVie, Bayer Pharma AG, Boehringer Ingelheim, Canada Foundation for Innovation, Eshelman Institute for Innovation, Genome Canada, Innovative Medicines Initiative (EU/EFPIA) [ULTRA-DD grant no. 115766], Janssen, Merck KGaA Darmstadt Germany, MSD, Novartis Pharma AG, Ontario Ministry of Economic Development and Innovation, Pfizer, São Paulo Research Foundation-FAPESP, Takeda, and Wellcome [106169/ZZ14/Z]. The US National Institutes of Health (NIH) is acknowledged for support (1U24DK11604-01). We thank Biocenter Finland/DDCB for financial support and the CSC-IT Center for Science Ltd. (Finland) for allocation of computational resources. We also thank Dr. Brandie Ehrmann and Ms. Diane E. Wallace for LC-MS/HRMS support provided by in the Mass Spectrometry Core Laboratory at the University of North Carolina at Chapel Hill. The core is supported by the National Science Foundation under Grant No. (CHE-1726291). In addition, we thank the University of North Carolina's Department of Chemistry NMR Core Laboratory for the use of their NMR spectrometers, along with Dr. Marc ter Horst and Dr. Andrew Camp for their assistance with NMR spectroscopy. The core is supported by the National Science Foundation under Grant No. (CHE-1828183).

## Appendix A. Supplementary data

Supplementary data to this article can be found online at <https://doi.org/10.1016/j.ejmech.xxxxxx>

## References

1. Klimovskaia, I. M.; Young, C.; Strømme, C. B.; Menard, P.; Jasencakova, Z.; Mejlvang, J.; Ask, K.; Ploug, M.; Nielsen, M. L.; Jensen, O. L.; Groth, A. Tousled-like kinases phosphorylate

- Asf1 to promote histone supply during DNA replication. *Nat Commun.* **2014**, *5*, 3394. doi: 10.1038/ncomms4394.
2. Silljé, H. H.; Takahashi, K.; Tanaka, K.; Van Houwe, G.; Nigg, E. A. Mammalian homologues of the plant Tousled gene code for cell-cycle-regulated kinases with maximal activities linked to ongoing DNA replication. *EMBO J.* **1999**, *18*, 5691–5702. doi: 10.1093/emboj/18.20.5691.
3. Hammond, C. M.; Strømme, C. B.; Huang, H.; Patel, D. J.; Groth, A. Histone Chaperones as Cardinal Players in Development. *Nat Rev Mol Cell Biol.* **2017**, *18*, 141–158. doi: 10.3389/fcell.2022.767773.
4. Pilyugin, M.; Demmers, J.; Verrijzer, C. P.; Karch, F.; Moshkin, Y. M. Phosphorylation-mediated control of histone chaperone ASF1 levels by Tousled-like kinases *PLoS One.* **2009**, *4*, e8328. doi: 10.1371/journal.pone.0008328.
5. Bruinsma, W.; van den Berg, J.; Aprelia, M.; Medema, R. H. Tousled-like kinase 2 regulates recovery from a DNA damage-induced G2 arrest *EMBO Rep.* **2016**, *17*, 659–670. doi: 10.15252/embr.201540767.
6. Lee, S.; Segura-Bayona, S.; Villamor-Payà, M.; Saredi, G.; Todd, M. A. M.; Attolini, C. S.; Chang, T. Y.; Stracker, T. H.; Groth, A. Tousled-like kinases stabilize replication forks and show synthetic lethality with checkpoint and PARP inhibitors. *Sci Adv.* **2018**, *4*, eaat4985. doi: 10.1126/sciadv.aat4985.
7. Segura-Bayona, S.; Villamor-Payà, M.; Attolini, C. S.; Koenig, L. M.; Sanchiz-Calvo, M.; Boulton, S. J.; Stracker, T. H. Tousled-Like Kinases Suppress Innate Immune Signaling Triggered by Alternative Lengthening of Telomeres. *Cell Rep.* **2020**, *32*, 107983. doi: 10.1016/j.celrep.2020.107983.
8. Lelieveld, S. H.; Reijnders, M. R.; Pfundt, R.; Yntema, H. G.; Kamsteeg, E. J.; de Vries, P.; de Vries, B. B.; Willemsen, M. H.; Kleefstra, T.; Löhner, K.; Vreeburg, M.; Stevens, S. J.; van der Burgt, I.; Bongers, E. M.; Stegmann, A. P.; Rump, P.; Rinne, T.; Nelen, M. R.; Veltman, J. A.; Vissers, L. E.; Brunner, H. G.; Gilissen, C. Meta-analysis of 2,104 trios provides support for 10 new genes for intellectual disability. *Nat Neurosci.* **2016**, *19*, 1194–1196. doi: 10.1038/nn.4352.
9. Töpf, A.; Oktay, Y.; Balaraju, S.; Yilmaz, E.; Sonmezler, E.; Yis, U.; Laurie, S.; Thompson, R.; Roos, A.; MacArthur, D. G.; Yaramis, A.; Güngör, S.; Lochmüller, H.; Hiz, S.; Horvath, R. Severe neurodevelopmental disease caused by a homozygous TLK2 variant. *Eur J Hum Genet.* **2020**, *28*, 383–387. doi: 10.1038/s41431-019-0519-x.
10. Reijnders, M. R. F.; Miller, K. A.; Alvi, M.; Goos, J. A. C.; Lees, M. M.; de Burca, A.; Henderson, A.; Kraus, A.; Mikat, B.; de Vries, B. B. A.; Isidor, B.; Kerr, B.; Marcelis, C.; Schluth-Bolard, C.; Deshpande, C.; Ruivenkamp, C. A. L.; Wiczorek, D.; Deciphering Developmental Disorders Study, Baralle, D.; Blair, E. M.; Engels, H.; Lüdecke, H. J.; Eason, J.; Santen, G. W. E.; Clayton-Smith, J.; Chandler, K.; Tatton-Brown, K.; Payne, K.; Helbig, K.; Radtke, K.; Nugent, K. M.; Cremer, K.; Strom, T. M.; Bird, L. M.; Sinnema, M.; Bitner-Glindzicz, M.; van Dooren, M. F.; Alders, M.; Koopmans, M.; Brick, L.; Kozenko, M.; Harline, M. L.; Klaassens, M.; Steinraths, M.; Cooper, N. S.; Edery, P.; Yap, P.; Terhal, P. A.; van der Spek, P. J.; Lakeman, P.; Taylor, R. L.; Littlejohn, R. O.; Pfundt, R.; Mercimek-Andrews, S.; Stegmann, A. P. A.; Kant, S. G.; McLean, S.; Joss, S.; Swagemakers, S. M. A.; Douzgou, S.; Wall, S. A.; Küry, S.; Calpena, E.; Koelling, N.; McGowan, S. J.; Twigg, S. R. F.; Mathijssen, I. M. J.; Nellaker, C.; Brunner, H. G.; Wilkie, A. O. M. De Novo and Inherited Loss-of-Function Variants in TLK2: Clinical and Genotype-Phenotype Evaluation of a Distinct Neurodevelopmental Disorder. *Am J Hum Genet.* **2018**, *102*, 1195–1203. doi: 10.1016/j.ajhg.2018.04.014.
11. Mortuza, G. B.; Hermida, D.; Pedersen, A. K.; Segura-Bayona, S.; López-Méndez, B.; Redondo, P.; Rüther, P.;

- Pozdnyakova, I.; Garrote, A. M.; Muñoz, I. G.; Villamor-Payà, M.; Jauset, C.; Olsen, J. V.; Stracker, T. H.; Montoya, G. Molecular basis of Toslud-Like Kinase 2 activation. *Nat Commun.* **2018**, *9*, 2535. doi: 10.1038/s41467-018-04941-y.
12. Dillon, P. J.; Gregory, S. M.; Tamburro, K.; Sanders, M. K.; Johnson, G. L.; Raab-Traub, N.; Dittmer, D. P.; Damania, B. Toslud-like kinases modulate reactivation of gammaherpesviruses from latency. *Cell Host Microbe.* **2013**, *13*, 204-214. doi: 10.1016/j.chom.2012.12.005.
13. Kim, Y.; Anderson, J. L.; Lewin, S. R. Getting the “kill” into “shock and kill”: strategies to eliminate latent HIV. *Cell Host Microbe.* **2018**, *23*, 14-26. doi: 10.1016/j.chom.2017.12.004.
14. Lin, M.; Yao, Z.; Zhao, N.; Zhang, C. TLK2 enhances aggressive phenotypes of glioblastoma cells through the activation of SRC signaling pathway. *Cancer Biol Ther.* **2019**, *20*, 101-108. doi: 10.1080/15384047.2018.1507257.
15. Kim, J. A.; Anurag, M.; Veeraraghavan, J.; Schiff, R.; Li, K.; Wang, X. S. Amplification of TLK2 Induces Genomic Instability via Impairing the G2-M Checkpoint. *Mol Cancer Res.* **2016**, *14*, 920-927. doi: 10.1158/1541-7786.MCR-16-0161
16. Kim, J. A.; Tan, Y.; Wang, X.; Cao, X.; Veeraraghavan, J.; Liang, Y.; Edwards, D. P.; Huang, S.; Pan, X.; Li, K.; Schiff, R.; Wang, X. S. Comprehensive functional analysis of the toslud-like kinase 2 frequently amplified in aggressive luminal breast cancers. *Nat Commun.* **2016**, *7*, 12991. doi: 10.1038/ncomms12991.
17. Segura-Bayona, S.; Knobel, P. A.; González-Burón, H.; Youssef, S. A.; Peña-Blanco, A.; Coyaudo, É.; López-Rovira, T.; Rein, K.; Palenzuela, L.; Colombelli, J.; Forrow, S.; Raught, B.; Groth, A.; de Bruin, A.; Stracker, T. H. Differential requirements for Toslud-like kinases 1 and 2 in mammalian development. *Cell Death Differ.* **2017**, *24*, 1872-1885. doi: 10.1038/cdd.2017.108.
18. Lee, S. B.; Chang, T. Y.; Lee, N. Z.; Yu, Z. Y.; Liu, C. Y.; Lee, H. Y. Design, synthesis and biological evaluation of bisindole derivatives as anticancer agents against Toslud-like kinases. *Eur J Med Chem.* **2022**, *227*, 113904. doi: 10.1016/j.ejmech.2021.113904.
19. Arrowsmith, C. H.; Audia, J. E.; Austin, C.; Baell, J.; Bennett, J.; Blagg, J.; Bountra, C.; Brennan, P. E.; Brown, P. J.; Bunnage, M. E.; Buser-Doepner, C.; Campbell, R. M.; Carter, A. J.; Cohen, P.; Copeland, R. A.; Cravatt, B.; Dahlin, J. L.; Dhanak, D.; Edwards, A. M.; Frederiksen, M.; Frye, S. V.; Gray, N.; Grimshaw, C. E.; Hepworth, D.; Howe, T.; Huber, K. V.; Jin, J.; Knapp, S.; Kotz, J. D.; Kruger, R. G.; Lowe, D.; Mader, M. M.; Marsden, B.; Mueller-Fahrnow, A.; Müller, S.; O'Hagan, R. C.; Overington, J. P.; Owen, D. R.; Rosenberg, S. H.; Roth, B.; Ross, R.; Schapira, M.; Schreiber, S. L.; Shoichet, B.; Sundström, M.; Superti-Furga, G.; Taunton, J.; Toledo-Sherman, L.; Walpole, C.; Walters, M. A.; Willson, T. M.; Workman, P.; Young, R. N.; Zuercher, W. J. The promise and peril of chemical probes. *Nat Chem Biol.* **2015**, *11*, 536-541. doi: 10.1038/nchembio.1867.
20. Fabian, M. A.; Biggs, W. H., 3rd; Treiber, D. K.; Atteridge, C. E.; Azimioara, M. D.; Benedetti, M. G.; Carter, T. A.; Ciceri, P.; Edeen, P. T.; Floyd, M.; Ford, J. M.; Galvin, M.; Gerlach, J. L.; Grotzfeld, R. M.; Herrgard, S.; Insko, D. E.; Insko, M. A.; Lai, A. G.; Lelias, J. M.; Mehta, S. A.; Milanov, Z. V.; Velasco, A. M.; Wodicka, L. M.; Patel, H. K.; Zarrinkar, P. P.; Lockhart, D. J., A small molecule-kinase interaction map for clinical kinase inhibitors. *Nat Biotechnol.* **2005**, *23*, 329-336. doi: 10.1038/nbt1068.
21. Karaman, M. W.; Herrgard, S.; Treiber, D. K.; Gallant, P.; Atteridge, C. E.; Campbell, B. T.; Chan, K. W.; Ciceri, P.; Davis, M. I.; Edeen, P. T.; Faraoni, R.; Floyd, M.; Hunt, J. P.; Lockhart, D. J.; Milanov, Z. V.; Morrison, M. J.; Pallares, G.; Patel, H. K.; Pritchard, S.; Wodicka, L. M.; Zarrinkar, P. P. A quantitative analysis of kinase inhibitor selectivity. *Nat Biotechnol.* **2008**, *26*, 127-132. doi: 10.1038/nbt1358.
22. Davis, M. I.; Hunt, J. P.; Herrgard, S.; Ciceri, P.; Wodicka, L. M.; Pallares, G.; Hocker, M.; Treiber, D. K.; Zarrinkar, P. P. Comprehensive analysis of kinase inhibitor selectivity. *Nat Biotechnol.* **2011**, *29*, 1046-1051. doi: 10.1038/nbt.1990.
23. Anastasiadis, T.; Deacon, S. W.; Devarajan, K.; Ma, H.; Peterson, J. R. Comprehensive assay of kinase catalytic activity reveals features of kinase inhibitor selectivity. *Nat Biotechnol.* **2011**, *29*, 1039-1045. doi: 10.1038/nbt.2017.
24. Elkins, J. M.; Fedele, V.; Szklarz, M.; Abdul Azeed, K. R.; Salah, E.; Mikolajczyk, J.; Romanov, S.; Sepetov, N.; Huang, X. P.; Roth, B. L.; Al Haj Zen, A.; Fourches, D.; Muratov, E.; Tropsha, A.; Morris, J.; Teicher, B. A.; Kunkel, M.; Polley, E.; Lackey, K. E.; Atkinson, F. L.; Overington, J. P.; Bamborough, P.; Müller, S.; Price, D. J.; Willson, T. M.; Drewry, D. H.; Knapp, S.; Zuercher, W. J. Comprehensive characterization of the Published Kinase Inhibitor Set. *Nat Biotechnol.* **2016**, *34*, 95-103. doi: 10.1038/nbt.3374.
25. Drewry, D. H.; Wells, C. I.; Andrews, D. M.; Angell, R.; Al-Ali, H.; Axtman, A. D.; Capuzzi, S. J.; Elkins, J. M.; Ettmayer, P.; Frederiksen, M.; Gileadi, O.; Gray, N.; Hooper, A.; Knapp, S.; Laufer, S.; Luecking, U.; Michaelides, M.; Müller, S.; Muratov, E.; Denny, R. A.; Saikatendu, K. S.; Treiber, D. K.; Zuercher, W. J.; Willson, T. M. Progress towards a public chemogenomic set for protein kinases and a call for contributions. *PLoS One.* **2017**, *12*, e0181585. doi: 10.1371/journal.pone.0181585.
26. Wells, C. I.; Al-Ali, H.; Andrews, D. M.; Asquith, C. R. M.; Axtman, A. D.; Dikic, I.; Ebner, D.; Ettmayer, P.; Fischer, C.; Frederiksen, M.; Futrell, R. E.; Gray, N. S.; Hatch, S. B.; Knapp, S.; Lücking, U.; Michaelides, M.; Mills, C. E.; Müller, S.; Owen, D.; Picado, A.; Saikatendu, K. S.; Schröder, M.; Stolz, A.; Tellechea, M.; Turunen, B. J.; Vilar, S.; Wang, J.; Zuercher, W. J.; Willson, T. M.; Drewry, D. H. The Kinase Chemogenomic Set (KCGS): An Open Science Resource for Kinase Vulnerability Identification. *Int J Mol Sci.* **2021**, *22*, 566. doi: 10.3390/ijms22020566.
27. Klaeger, S.; Heinzlmeir, S.; Wilhelm, M.; Polzer, H.; Vick, B.; Koenig, P. A.; Reinecke, M.; Ruprecht, B.; Petzoldt, S.; Meng, C.; Zecha, J.; Reiter, K.; Qiao, H.; Helm, D.; Koch, H.; Schoof, M.; Canevari, G.; Casale, E.; Depaolini, S. R.; Feuchtinger, A.; Wu, Z.; Schmidt, T.; Rueckert, L.; Becker, W.; Huenges, J.; Garz, A. K.; Gohlke, B. O.; Zolg, D. P.; Kayser, G.; Voeder, T.; Preissner, R.; Hahne, H.; Tonisson, N.; Kramer, K.; Gotze, K.; Bassermann, F.; Schlegel, J.; Ehrlich, H. C.; Aiche, S.; Walch, A.; Greif, P. A.; Schneider, S.; Felder, E. R.; Ruland, J.; Medard, G.; Jeremias, I.; Spiekermann, K.; Kuster, B., The target landscape of clinical kinase drugs. *Science* **2017**, *358*, eaan4368. doi: 10.1126/science.aan4368.
28. Knapp, S.; Arruda, P.; Blagg, J.; Burley, S.; Drewry, D. H.; Edwards, A.; Fabbro, D.; Gillespie, P.; Gray, N. S.; Kuster, B.; Lackey, K. E.; Mazzafera, P.; Tomkinson, N. C.; Willson, T. M.; Workman, P.; Zuercher, W. J. A public-private partnership to unlock the untargeted kinome. *Nat Chem Biol.* **2013**, *9*, 3-6. doi: 10.1038/nchembio.1113.
29. Sun, L.; Liang, C.; Shirazian, S.; Zhou, Y.; Miller, T.; Cui, J.; Fukuda, J. Y.; Chu, J. Y.; Nematalla, A.; Wang, X.; Chen, H.; Sistla, A.; Luu, T. C.; Tang, F.; Wei, J.; Tang, C. Discovery of 5-[5-fluoro-2-oxo-1,2-dihydroindol-3(3Z)-ylidenemethyl]-2,4-dimethyl-1H-pyrrole-3-carboxylic acid (2-diethylaminoethyl)amide, a novel tyrosine kinase inhibitor targeting vascular endothelial and platelet-derived growth factor

- receptor tyrosine kinase. *J Med Chem.* **2003**, *46*, 1116-1119. doi: 10.1021/jm0204183.
30. Pryer, N. K.; Lee, L. B.; Zadovaskaya, R.; Yu, X.; Sukbuntherng, J.; Cherrington, J. M.; London, C. A. Proof of target for SU11654: inhibition of KIT phosphorylation in canine mast cell tumors. *Clin Cancer Res.* **2003**, *9*, 5729-5734.
31. Patyna, S.; Laird, A. D.; Mendel, D. B.; O'farrell, A. M.; Liang, C.; Guan, H.; Vojtkovsky, T.; Vasile, S.; Wang, X.; Chen, J.; Grazzini, M.; Yang, C. Y.; Haznedar, J. O.; Sukbuntherng, J.; Zhong, W. Z.; Cherrington, J. M.; Hu-Lowe, D. SU14813: a novel multiple receptor tyrosine kinase inhibitor with potent antiangiogenic and antitumor activity. *Mol Cancer Ther.* **2006**, *5*, 1774-1782. doi: 10.1158/1535-7163.MCT-05-0333.
32. Hoessel, R.; Leclerc, S.; Endicott, J. A.; Nobel, M. E.; Lawrie, A.; Tunnah, P.; Leost, M.; Damiens, E.; Marie, D.; Marko, D.; Niederberger, E.; Tang, W.; Eisenbrand, G.; Meijer, L. Indirubin, the active constituent of a Chinese antileukaemia medicine, inhibits cyclin-dependent kinases. *Nat Cell Biol.* **1999**, *1*, 60-67. doi: 10.1038/9035.
33. Leclerc, S.; Garnier, M.; Hoessel, R.; Marko, D.; Bibb, J. A.; Snyder, G. L.; Greengard, P.; Biernat, J.; Wu, Y. Z.; Mandelkow, E. M.; Eisenbrand, G.; Meijer, L. Indirubins inhibit glycogen synthase kinase-3 beta and CDK5/p25, two protein kinases involved in abnormal tau phosphorylation in Alzheimer's disease. A property common to most cyclin-dependent kinase inhibitors? *J Biol Chem.* **2001**, *276*, 251-260. doi: 10.1074/jbc.M002466200.
34. Bertrand, J. A.; Thieffine, S.; Vulpetti, A.; Cristiani, C.; Valsasina, B.; Knapp, S.; Kalisz, H. M.; Flocco, M. Structural characterization of the GSK-3beta active site using selective and non-selective ATP-mimetic inhibitors. *J Mol Biol.* **2003**, *333*, 393-407. doi: 10.1016/j.jmb.2003.08.031.
35. Mapelli, M.; Massimiliano, L.; Crovace, C.; Seeliger, M. A.; Tsai, L. H.; Meijer, L.; Musacchio, A. Mechanism of CDK5/p25 binding by CDK inhibitors. *J Med Chem.* **2005**, *48*, 671-679. doi: 10.1021/jm049323m.
36. Asquith, C. R. M.; Treiber, D. K.; Zuercher, W. J. Utilizing comprehensive and mini-kinome panels to optimize the selectivity of quinoline inhibitors for cyclin G associated kinase (GAK). *Bioorg. Med. Chem. Lett.* **2019**, *29*, 1727-1731. doi: 10.1016/j.bmcl.2019.05.025.
37. Bembek, S. D.; Hirst, G.; Mirzadegan, T. Determination of a Focused Mini Kinase Panel for Early Identification of Selective Kinase Inhibitors. *J Chem Inf Model.* **2018**, *58*, 1434-1440. doi: 10.1021/acs.jcim.8b00222.
38. Brandt, P.; Jensen, A. J.; Nilsson, J. Small kinase assay panels can provide a measure of selectivity. *Bioorg. Med. Chem. Lett.* **2009**, *19*, 5861-5863. doi: 10.1016/j.bmcl.2009.08.083.
39. Sun, L.; Tran, N.; Tang, F.; App, H.; Hirth, P.; McMahon, G.; Tang, C. Synthesis and biological evaluations of 3-substituted indolin-2-ones: a novel class of tyrosine kinase inhibitors that exhibit selectivity toward particular receptor tyrosine kinases. *J Med Chem.* **1998**, *41*, 2588-4603. doi: 10.1021/jm980123i.
40. Jones, G. The Knoevenagel Condensation. *Organic Reactions.* **2004**, 204-273. <https://doi.org/10.1002/0471264180.or015.02>
41. Knoevenagel E. Condensation von Malonsäure mit aromatischen Aldehyden durch Ammoniak und Amine [Condensation of malonic acid with aromatic aldehydes via ammonia and amines]. *Berichte der deutschen chemischen Gesellschaft.* **1898**, *31*, 2596-2619. doi: 10.1002/cber.18980310308
42. Rueping, R.; Nachtsheim, B. J. A Review of New Developments in the Friedel-Crafts Alkylation - From Green Chemistry to Asymmetric Catalysis. *Beilstein J. Org. Chem.* **2010**, *6*, No. 6. <https://doi.org/10.3762/bjoc.6.6>
43. Friedel, C.; Crafts, J. M. Sur une Méthode Générale Nouvelle de Synthèse d'Hydrocarbures, d'Acétones, etc., *Compt. Rend.* **1877**, *84*, 1392-1395.
44. Friedel, C.; Crafts, J. M., Sur une Méthode Générale Nouvelle de Synthèse d'Hydrocarbures, d'Acétones, etc., *Compt. Rend.* **1877**, *84*, 1450-1454.
45. Xiao, J.; Westbroek, W.; Motabar, O.; Lea, W. A.; Hu, X.; Velayati, A.; Zheng, W.; Southall, N.; Gustafson, A. M.; Goldin, E.; Sidransky, E.; Liu, K.; Simeonov, A.; Tamargo, R. J.; Ribes, A.; Matalonga, L.; Ferrer, M.; Marugan, J. J. Discovery of a novel noniminosugar acid  $\alpha$  glucosidase chaperone series. *J Med Chem.* **2012**, *55*, 7546-7559. doi: 10.1021/jm3005543.
46. Mitsunobu, O.; Yamada, Y. Preparation of Esters of Carboxylic and Phosphoric Acid via Quaternary Phosphonium Salts. *Bull. Chem. Soc. Jpn.* **1967**, *40*, 2380-2382. doi:10.1246/bcsj.40.2380
47. Mitsunobu, O. The Use of Diethyl Azodicarboxylate and Triphenylphosphine in Synthesis and Transformation of Natural Products. *Synthesis.* **1981**, (1), 1-28. doi: 10.1055/s-1981-29317
48. Lepore, S. D.; He, Y. Use of Sonication for the Coupling of Sterically Hindered Substrates in the Phenolic Mitsunobu Reaction. *J. Org. Chem.* **2003**, *68*, 8261-8263. doi: 10.1021/jo0345751.
49. Carpino, L. A.; Imazumi, H.; El-Faham, A.; Ferrer, F. J.; Zhang, C.; Lee, Y.; Foxman, B. M.; Henklein, P.; Hanay, C.; Mügge, C.; Wenschuh, H.; Klose, J.; Beyermann, M.; Bienert, M. The Uronium/Guanidinium Peptide Coupling Reagents: Finally the True Uronium Salts. *Angew. Chem. Int. Ed. Engl.* **2002**, *41*, 441-445. doi: 10.1002/1521-3773(20020201)41:3<441::aid-anie441>3.0.
50. Cavallo, G.; Metrangola, P.; Milani, R.; Pilati, T.; Priimagi, A.; Resnati, G.; Terraneo, G. The Halogen Bond. *Chem. Rev.* **2016**, *116*, 2478-2601 doi: 10.1021/acs.chemrev.5b00484.
49. Auffinger, P.; Hays, F. A.; Westhof, E.; Ho, P. S.; Halogen bonds in biological molecules. *Proc Natl Acad Sci USA.* **2004**, *101*, 16789-16794. doi: 10.1073/pnas.0407607101.
51. Stumpfe, D.; Bajorath, J. Exploring Activity Cliffs in Medicinal Chemistry. *J Med Chem.* **2012**, *55*, 2932-2942. doi: 10.1021/jm201706b.
52. Bemis, G. W.; Murcko, M. A. The Properties of Known Drugs. 1. Molecular Frameworks *J Med Chem.* **1996**, *39*, 2887-2893. doi: 10.1021/jm9602928.
53. Kohlmann, A.; Zhu, X.; Dalgarno, D. Application of MM-GB/SA and WaterMap to SRC Kinase Inhibitor Potency Prediction. *ACS Med Chem Lett.* **2012**, *3*, 94-99. doi: 10.1021/ml200222u.
54. Higgs, C.; Beuming, T.; Sherman, W. Hydration Site Thermodynamics Explain SARs for Triazolympurines Analogues Binding to the A2A Receptor. *ACS Med Chem Lett.* **2010**, *1*, 160-164. doi: 10.1021/ml100008s.
55. Asquith, C. R. M.; Tizzard, G. J.; Bennett, J. M.; Wells, C. I.; Elkins, J. M.; Willson, T. M.; Poso, A.; Laitinen, T. Targeting the Water Network in Cyclin G-Associated Kinase (GAK) with 4-Anilino-quin(az)oline Inhibitors. *ChemMedChem.* **2020**, *15*, 1200-1215. doi: 10.1002/cmdc.202000150
56. Asquith, C. R. M.; Maffuid, K. A.; Laitinen, T.; Torrice, C. D.; Tizzard, G. J.; Crona, D. J.; Zuercher, W. J. Targeting an EGFR Water Network with 4-Anilinoquin(az)oline Inhibitors for Chordoma. *ChemMedChem.* **2019**, *14*, 1693-1700. doi: 10.1002/cmdc.201900428.
57. Fang, Z.; Song, Y.; Zhan, P.; Zhang, Q.; Liu, X. Conformational Restriction: An Effective Tactic in 'Follow-On'-Based Drug Discovery *Future Med. Chem.* **2014**, *8*, 885-901. doi: 10.4155/fmc.14.50.
58. Asquith, C. R. M.; Laitinen, T.; Bennett, J. M.; Wells, C. I.; Elkins, J. M.; Zuercher, W. J.; Tizzard, G. J.; Poso, A. Design



and analysis of the 4-anilino-quin(az)oline kinase inhibition profiles of GAK/SLK/STK10 using quantitative structure activity relationships. *ChemMedChem*. **2020**, *15*, 26-49. doi: 10.1002/cmdc.201900521.

59. Kleman-Leyer, K. M.; Klink, T. A.; Kopp, A. L.; Westermeyer, T. A.; Koeff, M. D.; Larson, B. R.; Worzella, T. J.; Pinchard, C. A.; van de Kar, S. A.; Zaman, G. J.; Hornberg, J. J.; Lowery, R. G. Characterization and optimization of a red-shifted fluorescence polarization ADP detection assay. *Assay Drug Dev Technol*. **2009**, *7*, 56-67. doi: 10.1089/adt.2008.175.

60. Zegzouti, H.; Zdanovskaia, M.; Hsiao, K.; Goueli, S. A. ADP-Glo: A Bioluminescent and Homogeneous ADP Monitoring Assay for Kinases. *Assay Drug Dev Technol*. **2009**, *7*, 560-572. doi: 10.1089/adt.2009.0222.

61. Li, H.; Totoritis, R. D.; Lor, L. A.; Schwartz, B.; Caprioli, P.; Jurewicz, A. J.; Zhang, G. Evaluation of an antibody-free ADP detection assay: ADP-Glo. *Assay Drug Dev Technol*. **2009**, *7*, 598-605. doi: 10.1089/adt.2009.0221.

62. Johnson, D.; Hussain, J.; Bhoir, S.; Chandrasekaran, V.; Sahrawat, P.; Hans, T.; Khalil, M. I.; De Benedetti, A.; Thiruvengadam, V.; Kirubakaran, S. Synthesis, kinetics and cellular studies of new phenothiazine analogs as potent human-TLK inhibitors. *Org Biomol Chem*. **2023**, *21*, 1980-1991. doi: 10.1039/d2ob02191a.

63. Ronald, S.; Awate, S.; Rath, A.; Carroll, J.; Galiano, F.; Dwyer, D.; Kleiner-Hancock, H.; Mathis, J. M.; Vigod, S.; De Benedetti, A. Phenothiazine Inhibitors of TLKs Affect Double-Strand Break Repair and DNA Damage Response Recovery and Potentiate Tumor Killing with Radiomimetic Therapy. *Genes Cancer*. **2013**, *4*, 39-53. doi: 10.1177/1947601913479020.

64. Uitdehaag, J. C.; Verkaar, F.; Alwan, H.; de Man, J.; Buijsman, R. C.; Zaman, G. J. A guide to picking the most selective kinase inhibitor tool compounds for pharmacological validation of drug targets. *Br J Pharmacol*. **2012**, *166*, (3), 858-876. doi: 10.1111/j.1476-5381.2012.01859.x.

65. Rokosz, L. L.; Beasley, J. R.; Carroll, C. D.; Lin, T.; Zhao, J.; Appell, K. C.; Webb, M. L. Kinase inhibitors as drugs for chronic inflammatory and immunological diseases: progress and challenges *Expert Opin. Ther. Targets* **2008**, *12*, 883-903. doi: 10.1517/14728222.12.7.883.

66. Sun, L.; Tran, N.; Liang, C.; Tang, F.; Rice, A.; Schreck, R.; Waltz, K.; Shawver, L. K.; McMahon, G.; Tang, C. Design, synthesis, and evaluations of substituted 3-[(3- or 4-carboxyethylpyrrol-2-yl)methylidene]indolin-2-ones as inhibitors of VEGF, FGF, and PDGF receptor tyrosine kinases. *J Med Chem*. **1999**, *42*, 5120-5130. doi: 10.1021/jm9904295.

67. Wood, E. R.; Kuyper, L.; Petrov, K. G.; Hunter, R. N 3rd.; Harris, P. A.; Lackey, K. Discovery and in vitro evaluation of potent TrkA kinase inhibitors: oxindole and aza-oxindoles. *Bioorg Med Chem Lett*. **2004**, *14*, 953-957. doi: 10.1016/j.bmcl.2003.12.002.

68. Bramson, H. N.; Corona, J.; Davis, S. T.; Dickerson, S. H.; Edelstein, M.; Frye, S. V.; Gampe, R. T Jr.; Harris, P. A.; Hassell, A.; Holmes, W. D.; Hunter, R. N.; Lackey, K. E.; Lovejoy, B.; Luzzio, M. J.; Montana, V.; Rocque, W. J.; Rusnak, D.; Shewchuk, L.; Veal, J. M.; Walker, D. H.; Kuyper, L. F. Oxindole-based inhibitors of cyclin-dependent kinase 2 (CDK2): design, synthesis, enzymatic activities, and X-ray crystallographic analysis. *J Med Chem*. **2001**, *44*, 4339-4358. doi: 10.1021/jm010117d.

69. Luk, K. C.; Simcox, M. E.; Schutt, A.; Rowan, K.; Thompson, T.; Chen, Y.; Kammlott, U.; DePinto, W.; Dunten, P.; Dermatakis, A. A new series of potent oxindole inhibitors of CDK2. *Bioorg Med Chem Lett*. **2004**, *14*, 913-917. doi: 10.1016/j.bmcl.2003.12.009.

70. Dermatakis, A.; Luk, K. C.; DePinto, W. Synthesis of potent oxindole CDK2 inhibitors. *Bioorg Med Chem*. **2003**, *11*, 1873-1881. doi: 10.1016/s0968-0896(03)00036-1.

71. Islam, I.; Brown, G.; Bryant, J.; Hrvatin, P.; Kochanny, M. J.; Phillips, G. B.; Yuan, S.; Adler, M.; Whitlow, M.; Lentz, D.; Polokoff, M. A.; Wu, J.; Shen, J.; Walters, J.; Ho, E.; Subramanyam, B.; Zhu, D.; Feldman, R. I.; Arnaiz, D. O. Indolinone based phosphoinositide-dependent kinase-1 (PDK1) inhibitors. Part 2: optimization of BX-517. *Bioorg Med Chem Lett*. **2007**, *17*, 3819-3825. doi: 10.1016/j.bmcl.2007.05.060.

72. Guan, H.; Laird, A. D.; Blake, R. A.; Tang, C.; Liang, C. Design and synthesis of aminopropyl tetrahydroindole-based indolin-2-ones as selective and potent inhibitors of Src and Yes tyrosine kinase. *Bioorg Med Chem Lett*. **2004**, *14*, 187-190. doi: 10.1016/j.bmcl.2003.09.069.

73. Kaur, M.; Singh, M.; Chadha, N.; Silakari, O. Oxindole: A chemical prism carrying plethora of therapeutic benefits. *Eur J Med Chem*. **2016**, *123*, 858-894. doi: 10.1016/j.ejmech.2016.08.011.

74. Troxler, T.; Greenidge, P.; Zimmermann, K.; Desrayaud, S.; Drückes, P.; Schweizer, T.; Stauffer, D.; Rovelli, G.; Shimshek, D. R. Discovery of novel indolinone-based, potent, selective and brain penetrant inhibitors of LRRK2. *Bioorg Med Chem Lett*. **2013**, *23*, 4085-4090. doi: 10.1016/j.bmcl.2013.05.054.

75. Fang, Z.; Song, Y.; Zhan, P.; Zhang, Q.; Liu, X. Conformational restriction: an effective tactic in 'follow-on'-based drug discovery. *Future Med Chem*. **2014**, *6*, 885-901. doi: 10.4155/fmc.14.50.

76. Asquith, C. R. M.; Laitinen, T.; Bennett, J. M.; Godoi, P. H.; East, M. P.; Tizzard, G. J.; Graves, L. M.; Johnson, G. L.; Dornsife, R. E.; Wells, C. I.; Elkins, J. M.; Willson, T. M.; Zuercher, W. J. Identification and Optimization of 4-Anilinoquinolines as Inhibitors of Cyclin G Associated Kinase. *ChemMedChem* **2018**, *13*, 48-66. doi: 10.1002/cmdc.201700663.

77. Ellis, J. M.; Altman, M. D.; Bass, A.; Butcher, J. W.; Byford, A. J.; Donofrio, A.; Galloway, S.; Haidle, A. M.; Jewell, J.; Kelly, N.; Leccese, E. K.; Lee, S.; Maddess, M.; Miller, J. R.; Moy, L. Y.; Osimboni, E.; Otte, R. D.; Reddy, M. V.; Spencer, K.; Sun, B.; Vincent, S. H.; Ward, G. J.; Woo, G. H.; Yang, C.; Houshyar, H.; Northrup, A. B. Overcoming mutagenicity and ion channel activity: optimization of selective spleen tyrosine kinase inhibitors. *J Med Chem*. **2015**, *58*, 1929-1939. doi: 10.1021/jm5018169.

78. Lawhorn, B. G.; Philp, J.; Zhao, Y.; Louer, C.; Hammond, M.; Cheung, M.; Fries, H.; Graves, A. P.; Shewchuk, L.; Wang, L.; Cottom, J. E.; Qi, H.; Zhao, H.; Totoritis, R.; Zhang, G.; Schwartz, B.; Li, H.; Sweitzer, S.; Holt, D. A.; Gatto, G. J. Jr.; Kallander, L. S. Identification of Purines and 7-Deazapurines as Potent and Selective Type I Inhibitors of Troponin I-Interacting Kinase (TNNI3K). *J Med Chem*. **2015**, *58*, 7431-7448. doi: 10.1021/acs.jmedchem.5b00931.

79. Asquith, C. R. M.; Laitinen, T.; Wells, C. I.; Tizzard, G. J.; Zuercher, W. J. New Insights into 4-Anilinoquinazolines as Inhibitors of Cardiac Troponin I-Interacting Kinase (TNNI3K). *Molecules*. **2020**, *25*, 1697. doi: 10.3390/molecules25071697.

80. Azuaje, J.; Jespers, W.; Yaziji, V.; Mallo, A.; Majellaro, M.; Caamaño, O.; Loza, M. I.; Cadavid, M. I.; Brea, J.; Åqvist, J.; Sotelo, E.; Gutiérrez-de-Terán, H. Effect of Nitrogen Atom Substitution in A3 Adenosine Receptor Binding: *N*-(4,6-Diarylpyridin-2-yl)acetamides as Potent and Selective Antagonists. *J Med Chem*. **2017**, *60*, 7502-7511. doi: 10.1021/acs.jmedchem.7b00860.

81. Geyer, R.; Nordemann, U.; Strasser, A.; Wittmann, H. J.; Buschauer, A. Conformational Restriction and Enantioseparation Increase Potency and Selectivity of Cyanoguanidine-Type

- Histamine H4 Receptor Agonists. *J Med Chem.* **2016**, *59*, 3452-3470. doi: 10.1021/acs.jmedchem.6b00120.
82. El Bakali, J.; Muccioli, G. G.; Body-Malapel, M.; Djouina, M.; Klupsch, F.; Ghinet, A.; Barczyk, A.; Renault, N.; Chavatte, P.; Desreumaux, P.; Lambert, D. M.; Millet, R. Conformational Restriction Leading to a Selective CB2 Cannabinoid Receptor Agonist Orally Active Against Colitis. *ACS Med Chem Lett.* **2014**, *6*, 198-203. doi: 10.1021/ml500439x.
83. Pennington, L. D.; Moustakas, D. T. The Necessary Nitrogen Atom: A Versatile High-Impact Design Element for Multiparameter Optimization. *J. Med. Chem.* **2017**, *60*, 3552-3579. doi: 10.1021/acs.jmedchem.6b01807.
84. Robinson, D. D.; Sherman, W.; Farid, R. Understanding kinase selectivity through energetic analysis of binding site waters. *ChemMedChem.* **2010**, *5*, 618-627. doi: 10.1002/cmdc.200900501.
85. Robinson, D.; Bertrand, T.; Carry, J. C.; Halley, F.; Karlsson, A.; Mathieu, M.; Minoux, H.; Perrin, M. A.; Robert, B.; Schio, L.; Sherman, W. Differential Water Thermodynamics Determine PI3K-Beta/Delta Selectivity for Solvent-Exposed Ligand Modifications. *J Chem Inf Model.* **2016**, *56*, 886-894. doi: 10.1021/acs.jcim.5b00641.
86. Hu, Y.; Kunimoto, R.; Bajorath, J. Mapping of inhibitors and activity data to the human kinome and exploring promiscuity from a ligand and target perspective. *Chem Biol Drug Des.* **2017**, *89*, 834-845. doi: 10.1111/cbdd.12919.
87. CrysAlisPro Software System, Rigaku Oxford Diffraction, (2018)
88. Sheldrick, G. M. Crystal structure refinement with SHELXL. *Acta Crystallogr. Sect. A*, **2015**, *71*, 3-8. doi: 10.1107/S2053229614024218.
89. Dolomanov, O. V.; Bourhis, L. J.; Gildea, R. J.; Howard, J. A. K.; Puschmann, H. OLEX2: a complete structure solution, refinement and analysis program. *J. Appl. Crystallogr.* **2009**, *42*, 339-341. doi: 10.1107/S0021889808042726
90. Fong, T. A.; Shawver, L. K.; Sun, L.; Tang, C.; App, H.; Powell, T. J.; Kim, Y. H.; Schreck, R.; Wang, X.; Risau, W.; Ullrich, A.; Hirth, K. P.; McMahon, G. SU5416 is a potent and selective inhibitor of the vascular endothelial growth factor receptor (Flk-1/KDR) that inhibits tyrosine kinase catalysis, tumor vascularization, and growth of multiple tumor types. *Cancer Res.* **1999**, *59*, 99-106.
91. Lane, M. E.; Yu, B.; Rice, A.; Lipson, K. E.; Liang, C.; Sun, L.; Tang, C.; McMahon, G.; Pestell, R. G.; Wadler, S. A novel cdk2-selective inhibitor, SU9516, induces apoptosis in colon carcinoma cells. *Cancer Res.* **2001**, *61*, 6170-6177.
92. Dumas, M. E.; Chen, G. Y.; Kendrick, N. D.; Xu, G.; Larsen, S. D.; Jana, S.; Waterson, A. G.; Bauer, J. A.; Hancock, W.; Sulikowski, G. A.; Ohi, R. Dual inhibition of Kif15 by oxindole and quinazolinone chemical probes. *Bioorg Med Chem Lett.* **2019**, *29*, 148-154. doi: 10.1016/j.bmcl.2018.12.008.
93. Kim, M. H.; Tshako, A. L.; Co, E. W.; Aftab, D. T.; Bentzien, F.; Chen, J.; Cheng, W.; Engst, S.; Goon, L.; Klein, R.; Le, D. T.; Mac, M.; Parks, J. J.; Qian, F.; Rodriguez, M.; Stout, T. J.; Till, J. H.; Won, K. A.; Wu, X.; Yakes, F. M.; Yu, P.; Zhang, W.; Zhao, Y.; Lamb, P.; Nuss, J. M.; Xu, W. The design, synthesis, and biological evaluation of potent receptor tyrosine kinase inhibitors. *Bioorg Med Chem Lett.* **2012**, *22*, 4979-4985. doi: 10.1016/j.bmcl.2012.06.029.